FORCE BALANCING DESIGN AND TRAJECTORY TRACKING CONTROL OF REAL-TIME CONTROLLABLE MECHANISMS

A Thesis Submitted to the

College of Graduate Studies and Research

in Partial Fulfillment of the Requirements

for the Degree of Master of Science

in the Department of Mechanical Engineering

University of Saskatchewan

Saskatoon, Saskatchewan

Canada

By

Puren Ouyang

Spring 2002

PERMISSION TO USE

In presenting this thesis in partial fulfillment of the requirements for a Postgraduate degree from the University of Saskatchewan, I agree that the Libraries of this University may make it freely available for inspection. I further agree that permission for copying of this thesis in any manner, in whole or in part, for scholarly purposes may be granted by the professor or professors who supervised my thesis work or, in their absence, by the Head of the Department or the Dean of the College in which my thesis work was done. It is understood that any copying or publication or use of this thesis or parts thereof for financial gain shall not be allowed without my written permission. It is also understood that due recognition shall be given to me and to the University of Saskatchewan in any scholarly use which may be made of any material in my thesis.

Requests for permission to copy or to make other use of material in this thesis in whole or part should be addressed to:

Head of the Department of Mechanical Engineering

University of Saskatchewan

Saskatoon, Saskatchewan

CANADA S7N 5A9

ABSTRACT

Real-time controllable (RTC) mechanisms refer to those mechanisms driven by RTC actuators or servomotors. There are many benefits to an RTC mechanism that is force balanced. A novel method called the *Adjusting Kinematic Parameters* method for force balancing of RTC mechanisms is more promising than the *Counterweights* method. The motivation of the research described in this thesis is to overcome the problems with the present Adjusting Kinematic Parameters method and further extend it to be more general and robust.

The extended Adjusting Kinematic Parameters method is presented in this thesis. This method can work for any general mass distribution of a closed-loop RTC mechanism, and is extended to incorporate the masses of adjusting sliding blocks. The extended Adjusting Kinematic Parameters method has been verified to be consistently better than the Counterweights method for closed-loop RTC mechanisms.

The generic task of an RTC mechanism is trajectory tracking. Trajectory planning is needed for trajectory tracking. A new method for trajectory planning that can achieve C^3 continuity is developed in this thesis. The new method, based on quintic polynomials for trajectory planning, can insure that the trajectory has a smooth acceleration curve and a continuous jerk on the trajectory.

The dynamics of an RTC mechanism is important for developing a better controller to achieve optimal trajectory tracking performance. To study the extended AKP method, the dynamic model of a 2 degree of freedom RTC mechanism is developed with consideration of the off-line mass center of a link using the reduced order method. Stability analysis for the *Proportional Derivative* (PD) control applied to the closed-loop RTC mechanism is discussed.

Dynamic control is an essential part of an RTC mechanism. Based on the analysis of the existing *Nonlinear PD* control method and the *Computed Torque Control* method, a novel PD-based control method, namely, the *Evolutionary PD control* method, is proposed. The Evolutionary PD method incorporates plant dynamics into the control law in such a way that the control law is the result of the superposition of a series of runs of a controlled plant system.

Case studies are carried out for force balanced mechanisms using the extended Adjusting Kinematic Parameters method, the Counterweights method, and the unbalanced mechanism in terms of the joint forces, trajectory tracking performance, and fluctuation of the torques in the actuators. Three control laws (i.e., PD control, Nonlinear PD control, and Evolutionary PD control) are used to perform the feedback control for several case studies. All the simulation results show that the extended Adjusting Kinematic Parameters method is better than the Counterweights method with respect to the reduction of joint forces and trajectory tracking errors. It is also shown that the

Evolutionary PD control law is a promising control law when compared with the PD/Nonlinear PD control laws in terms of the selection of control gain and high trajectory tracking performance.

ACKNOWLEDGMENTS

I would like to take this opportunity to express my sincere thanks to my supervisor, Professor C. Zhang, for his invaluable guidance, stimulating discussion and continuous encouragement in the whole research as well as the critical review of the manuscript.

I would like to extend special thanks to other members of my advisory committee: Professor M. M. Gupta, Professor A.T. Dolovich, and Professor R. L. Kushwaha (the external examiner). Their valuable support and constructive suggestions have greatly improved the present work.

I acknowledge Dr. Q. Li from Nanyang Technological University (Singapore), Mr. D. C. Handley, and Mr. F. X. Wu for reviewing a part of the draft version of this thesis and giving valuable suggestions for the thesis. I would like to thank Mr. K. D. Backstrom for making the LEGO model for testing the AKP method developed in this thesis.

My research was made possible by the generous support of the Natural Sciences and Engineering Research Council (NSERC) and Atomic Energy of Canada Limited (AECL).

Dedicated to my family

Yanhua & Lu

TABLE OF CONTENTS

LIST OF TABLES

LIST OF FIGURES

ACRONYMS

AEDL	Advanced engineering design laboratory
AKP	Adjusting kinematic parameters
CTC	Computed torque control
CW	Counterweights
DOF	Degree of freedom
EPD	Evolutionary PD
LIV	Linearly independent vector
MC	Mass center
NPD	Nonlinear PD
PD	Proportional derivative
RTC	Real-time controllable

CHAPTER 1

INTRODUCTION

1.1 From traditional mechanism to mechatronic mechanism

A *mechanism* is defined as a set of connected components to perform a definite motion transfer and force transfer (IFToMM, 1991). *Traditional mechanisms* are driven by constant velocity motors that are not real-time controllable or adjustable. Mechanisms driven by real-time controllable (RTC) motors, or servomotors, are called RTC mechanisms. In general, RTC mechanisms are multi-degrees of freedom systems. RTC mechanisms are also called *mechatronic mechanisms*. A generic task of an RTC mechanism is to generate trajectory tracking motion. *Trajectory tracking* can be defined as follows:

> *Given a trajectory of the end-effector of a mechanism, which is expressed by a mathematic function, i.e., $x(t)$, $y(t)$, $\theta(t)$, t represents time, to control the mechanism such that the end-effector follows the given trajectory in the time domain.*

There is another generic task of RTC mechanisms, namely, *point-set* tracking. In tracking of a set of discrete points, motions between any two points are not of interest. Therefore, the *point-set tracking* problem can be viewed as a simple version of the trajectory tracking problem. Tracking of a trajectory is more difficult than tracking of a set of points. This thesis focuses on trajectory tracking.

Throughout the thesis, the traditional mechanism is referred to as the *non-RTC* mechanism. It should be noted that in the design of a non-RTC mechanism, one of the generic design problems is called path generation (Klein, 1987). However, the *path generation* problem usually does not involve the time factor, and nor is the feedback control involved.

RTC mechanisms are fundamental building blocks in many machine tools and advanced robots due to their flexibility in terms of adapting to different applications without the need of redesign of their physical structures. Since there is no well-developed guidance available to design an RTC mechanism system with consideration of both control structures and mechanical structure designs, it is therefore significant to develop methodologies for this purpose.

1.2 One challenging issue in RTC mechanism design

For an RTC mechanism, the mechanical properties, such as shaking force balancing, shaking moment balancing, machine cooling, and vibration are highly coupled with the

characteristics of the controller. One challenging issue in the RTC mechanism design is that in order to achieve the optimal performance from the overall system viewpoint, both the controller design and the mechanical structure design need to be considered simultaneously. This thesis only takes the property of force balancing into consideration in addressing this issue. The definitions of force balancing and moment balancing are given below:

Definition 1.1 ***Force balancing***: Force balancing is defined as a set of conditions under which the weight of the links of a mechanism dose not produce any torque or force at the actuators under static conditions for any configuration of the manipulator or mechanism (Wang and Gosselin, 2000). The force balancing defined as such is also called the *static balancing* or *shaking force cancellation.*

Definition 1.2 ***Moment balancing***: Moment balancing is defined as a set of conditions under which the angular momentum of a mechanism is constant at all configurations of the mechanism (Bagic, 1983).

1.3 State of the art of the methods for RTC mechanism design

There were some ad-hoc design methods for RTC mechanisms developed at MIT during 1980s. The main objective of the design methods was to improve the positioning accuracy of a manipulator that runs at high speeds. The basic idea of the design methods is to design the mechanical structure with a parallel structure so that it results in a

simple and decoupled dynamic model. When this idea is implemented in the structure design, an independent joint control strategy can readily be applied for a multi-input-multi-output system. As a positive side effect of these design methods, the shaking force of a manipulator system happens to be cancelled.

Many studies on force balancing of spatial mechanisms, i.e., robots, are performed at Laval University. These studies are limited within the scope of mechanical structure design only. When attached with a controller and programmed to follow different trajectories, however, mechanisms designed with complete force balancing property in this manner may not generate satisfactory dynamic performance. This consequence was revealed by the recent studies carried out at the Advanced Engineering Design Laboratory (AEDL) of the University of Saskatchewan (Wang, 2000) and other research (Xi and Sinatra, 1997).

At AEDL, a novel method called the Adjusting Kinematic Parameters (AKP) method for force balancing of RTC mechanisms was developed (Wang, 2000). This method suggests that adjusting the kinematic parameters can achieve force balancing of RTC mechanisms. Although showing advantages, there are some problems with this method. *First*, the initial development assumed that the center of mass of each link in a mechanism was in line with its axis, see Figure 1.1(a). However, in general, the center of mass of a link is likely off-line with its axis, see Figure 1.1b. In mechanisms, a link may also take the ternary form instead of the binary form, see Figure 1.1c. *Second*, the physical implementation was not considered in Wang's study. It should be noted that

when adjusting the kinematic parameters of a link, extra masses are included in the system, and adjustment of kinematic parameters related to these masses may involve a change of the mass distribution of the system. *Third*, the exploration of how control methods affect trajectory tracking performance with respect to different force balancing methods was not well addressed. In particular, the control method used was a simple PD law with gains selected in a trial and error manner. *Finally*, trajectory planning was not well studied in spite of its importance in the AKP method. In fact, whenever the kinematic parameters are adjusted, the geometry of the mechanism may be varied, hence the trajectory must be replanned to achieve the desired motion task.

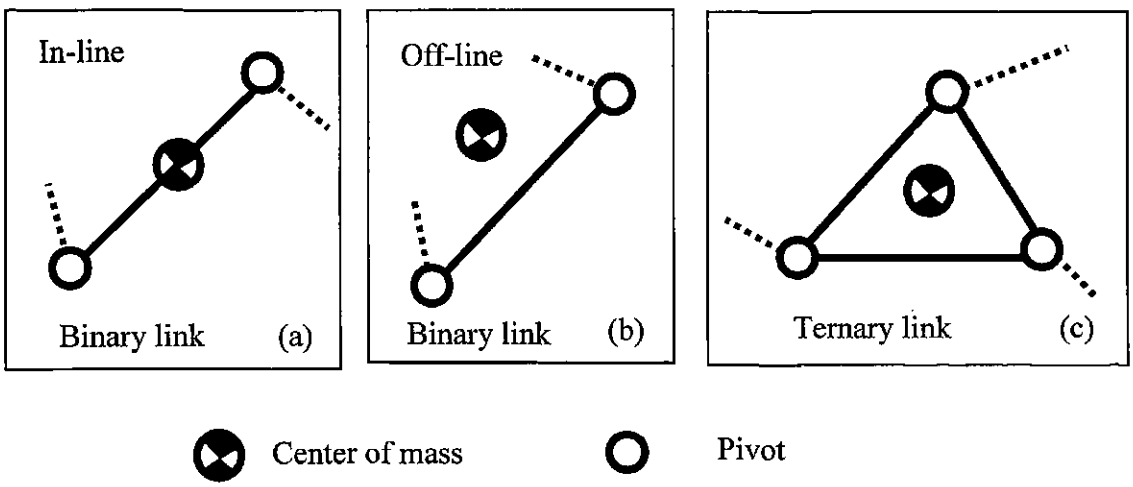

Figure 1.1 Different situations of mass centers and different forms of links

1.4 Research objectives and scopes

The research presented in this thesis aims to improve and extend the AKP method previously developed at AEDL. In particular, the following research objectives were pursued.

Objective 1: To develop a more general AKP method to take into account (i) the situation where the mass center of a link was off-line with its axes, and (ii) the effect of sliding blocks when adjusting the kinematic parameters.

Objective 2: To develop a trajectory planning method to achieve a smoother trajectory, in particular, to avoid trajectories with infinitive jerks.

It is remarked that in the present AKP method, the trajectory planning only ensures the continuity of acceleration on the trajectory, which may introduce infinitive jerks.

Objective 3: To develop a dynamic model of a five-bar closed-loop RTC mechanism with consideration of the off-line mass center of a link using the reduced order method.

It is remarked that the reduced order method developed by Ghorbel (1994,1995) only considers the mechanism with the in-line mass center. It is important to extend this method to the mechanism with the off-line mass center in order to study the extended AKP method.

Objective 4: To develop a more comprehensive understanding of how control methods could affect trajectory tracking with respect to different force balancing methods.

It is remarked that when designing an RTC mechanism for force balancing, trajectory tracking should be taken into consideration simultaneously, as the latter is the generic task of the RTC mechanism. A force balancing method without taking control aspects into consideration might degrade the trajectory tracking performance.

1.5 General research methods

With respect to objective 1, a general thought is that the masses of sliding blocks need to be separately represented in the expression of the total mass center of an RTC mechanism. Another thought is that when the off-line mass center is considered, adjusting of only one pivot along a link, which is the case in the present AKP method, may not be sufficient. It may be needed to consider the adjusting of two pivots of a link. With respect to objective 2, a quintic function will be used, as it contains six coefficients that allow specifying the acceleration at two ends of a segment. Thus, it is possible to achieve at least the bounded jerk on a trajectory. With respect to objective 3, the reduced order method will be extended for the mechanism with the off-line mass center design. Finally, with respect to objective 4, both the PD control and the non-linear PD (NPD) control methods will be used due to their low computational cost. A novel PD-based control method, namely, Evolutionary PD (EPD) control, is proposed. The EPD control method incorporates plant dynamics into the PD control law.

1.6 Organization of the thesis

Chapter 2 presents a literature review, focusing on the objectives discussed above. The goal is to further analyze and justify the objectives of the thesis by discussing the state of the art of the current researches related to the objectives. Chapter 3 will present an extended AKP method with the goal to overcome the problems associated with the present version of the AKP method. Chapter 4 discusses kinematics of a five-bar closed-loop RTC mechanism, and presents a new method for trajectory planning aiming to achieve a trajectory with bounded jerks. Chapter 5 extends the reduced order method to a five-bar closed-loop RTC mechanism with the mass center of a link off line with its axis, develops the PD and NPD control methods, and proposes an EPD control method for comprehensive studies of how control methods affect the performance of trajectory tracking with respect to different force balancing methods. Chapter 6 presents results and discussion. Chapter 7 contains a conclusion with discussion of future work.

CHAPTER 2

LITERATURE REVIEW

2.1 Introduction

The purpose of this chapter is to provide further justification regarding the significance of the research objectives listed in Chapter 1. The commonly used methods and technologies will also be presented to form a common basis for subsequent discussions. Methods for force balancing of mechanisms, dynamic modeling and controlling of mechanisms, and trajectory planning are reviewed to show the state of the art in the relevant research areas. Section 2.2 discusses the commonly used force balancing principles, methods, applications, and their problems. The commonly used methods for trajectory planning are discussed in Section 2.3. Section 2.4 introduces methods for developing dynamic models of closed-loop mechanisms. Control laws that are applied to closed-loop mechanisms are discussed in Section 2.5. Section 2.6 gives a summary, highlighting the significance of the research in this thesis.

2.2 Force balancing principles and methods

2.2.1 Principles for complete force balancing

There are two principles for complete force balancing: (i) making the total mass center of a mechanism stationary (Berkof and Lowen, 1969; Bagic, 1979), and (ii) making the total potential energy of a mechanism stationary (Gosselin, 1999; Wang and Gosselin, 2000). *Principle* (i) is explained as follows.

Consider a mechanism that transmits forces to its base at point O. Let $\mathbf{f}_0$ stand for the sum of the reacting forces the mechanism imposes on the base. The application of the Newton's second law leads to

$$\mathbf{f}_0 = -\frac{d}{dt}\{M\dot{\mathbf{r}}_c\} + M\mathbf{g} \tag{2.1}$$

where M is the total mass of a mechanism, $\mathbf{g}$ the gravitational acceleration, and $\dot{\mathbf{r}}_c$ the velocity of the *Mass Center* (MC) of the mechanism. It can be seen from Eq. (2.1) that the undesired shaking force results from changes in the system's linear momentum. This dynamic component becomes zero if the system MC does not change in any configuration, i.e., $\mathbf{r}_c = \mathbf{constant}$, during a period of motion. Therefore, *Principle (i)* can be stated as: to transmit zero shaking force, the mechanism's MC has to be stationary or configuration invariant. The property of configuration invariance of MC

can be obtained in several ways, depending on the types of the mechanisms. For instance, for any mechanism containing only revolute kinematic pairs, the mass distribution of the mechanism to achieve the force balance can be obtained by using the *linearly independent vector* (LIV) approach (Berkof and Lowen, 1969).

The LIV approach is explained by taking a 2 DOF closed-loop mechanism as an example, see Figure 2.1. This mechanism consists of two kinematic chains connecting the fixed base and the end-effector of the mechanism. The two kinematic chains are $O_1O_2O_3P$ and $O_5O_4O_3P$, respectively. Two revolute actuators are mounted at joints O_1 and O_5 and described by joint variables q_1 and q_4, respectively. Joints O_2, O_3 and O_4 are passive revolute joints. Point P (overlapping with O_3) is the position of the end-effector of the mechanism.

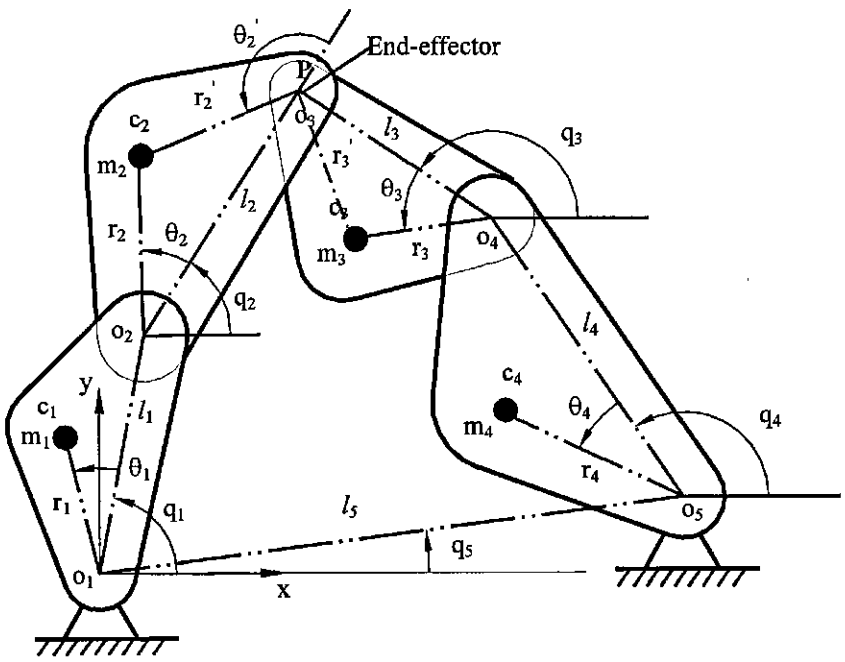

Figure 2.1 A 2 DOF closed-loop mechanism with arbitrary mass distribution

The stationary total mass center condition can be expressed by the following equation.

$$\mathbf{r}_c = \frac{1}{M}\sum_{i=1}^{4} m_i \mathbf{r}_i = \textbf{constant} \tag{2.2}$$

where m_i and $\mathbf{r}_i$ are the mass and the position vector of mass center of link I, respectively, and $M = \sum_{i=1}^{4} m_i$. According to the LIV approach, position vector $\mathbf{r}_i$ in Eq. (2.2) can be expressed as:

$$\begin{cases} \mathbf{r}_1 = r_1 e^{\mathrm{i}(q_1+\theta_1)} \\ \mathbf{r}_2 = l_1 e^{\mathrm{i}q_1} + r_2 e^{\mathrm{i}(q_2+\theta_2)} \\ \mathbf{r}_3 = l_5 e^{\mathrm{i}q_5} + l_4 e^{\mathrm{i}q_4} + r_3 e^{\mathrm{i}(q_3+\theta_3)} \\ \mathbf{r}_4 = l_5 e^{\mathrm{i}q_5} + r_4 e^{\mathrm{i}(q_4+\theta_4)} \end{cases} \tag{2.3}$$

Substituting Eq. (2.3) into Eq. (2.2) leads to:

$$\begin{aligned} M\mathbf{r}_c = {} & (m_3 l_5 e^{\mathrm{i}q_5} + m_4 l_5 e^{\mathrm{i}q_5}) + (m_1 r_1 e^{\mathrm{i}\theta_1} + m_2 l_1) e^{\mathrm{i}q_1} + (m_2 r_2 e^{\mathrm{i}\theta_2}) e^{\mathrm{i}q_2} + \\ & (m_3 r_3 e^{\mathrm{i}\theta_3}) e^{\mathrm{i}q_3} + (m_4 r_4 e^{\mathrm{i}\theta_4} + m_3 l_4) e^{\mathrm{i}q_4} \end{aligned} \tag{2.4}$$

The unit vectors $e^{\mathrm{i}q_1}$, $e^{\mathrm{i}q_2}$, $e^{\mathrm{i}q_3}$, and $e^{\mathrm{i}q_4}$ are constrained by the kinematic closed-loop equation, i.e., $l_1 e^{\mathrm{i}q_1} + l_2 e^{\mathrm{i}q_2} - l_3 e^{\mathrm{i}q_3} - l_4 e^{\mathrm{i}q_4} - l_5 e^{\mathrm{i}q_5} = 0$. Substituting this constraint equation into Eq. (2.4) leads to:

$$
\begin{aligned}
M\mathbf{r}_c = & (m_3 l_5 e^{iq_5} + m_4 l_5 e^{iq_5} + \lambda_{25} m_2 r_2 e^{i\theta_2} e^{iq_5}) \\
& + (m_1 r_1 e^{i\theta_1} + m_2 l_1 - \lambda_{21} m_2 r_2 e^{i\theta_2}) e^{iq_1} + (m_3 r_3 e^{i\theta_3} + \lambda_{23} m_2 r_2 e^{i\theta_2}) e^{iq_3} \\
& + (m_4 r_4 e^{i\theta_4} + m_3 l_4 + \lambda_{24} m_2 r_2 e^{i\theta_2}) e^{iq_4}
\end{aligned} \tag{2.5}
$$

where $\lambda_{ij} = {}^{l_j}\!/_{l_i}$, $i, j = 1,...,5$. In order to make the total mass center stationary, all the terms with the time-varying quantities in Eq. (2.5) should vanish. This will result in the following equations:

$$
m_1 r_1 e^{i\theta_1} + m_2 l_1 - \lambda_{21} m_2 r_2 e^{i\theta_2} = 0 \tag{2.6}
$$

$$
m_3 r_3 e^{i\theta_3} + \lambda_{23} m_2 r_2 e^{i\theta_2} = 0 \tag{2.7}
$$

$$
m_4 r_4 e^{i\theta_4} + m_3 l_4 + \lambda_{24} m_2 r_2 e^{i\theta_2} = 0 \tag{2.8}
$$

As long as Eqs. (2.6) to (2.8) are satisfied during design, the shaking force of the mechanism is cancelled. Such a mechanism is called a force balanced mechanism.

Principle (ii) is that if the total potential energy of a mechanism in any configuration is kept constant (i.e., the weight of the mechanism has no effect on the actuators), then the mechanism is force balanced. The expression of the total potential energy of the mechanism can be written as:

$$
V = V_w + V_s \tag{2.9}
$$

where V_w and V_s are, respectively, the gravitational potential energy and the elastic potential energy stored in the springs. The way of implementing this principle is to eliminate the effect of the potential energy through properly adding springs into the original mechanism (Wang and Gosselin, 2000).

2.2.2 Counterweights method

Suppose that a mechanism is not force-balanced. Redesign of the mass distribution of the mechanism to achieve the force balance can be accomplished by adding masses or counterweights into the original mechanism. This method is called the *counterweights* (CW) method (Berkof, 1973). For the example shown in Figure 2.1, the equations for the redesign of the mass can be derived as follows.

As shown in Figure 2.1, two relationships $r_2 e^{i\theta_2} = l_2 + r_2' e^{i\theta_2'}$ and $r_3 e^{i\theta_3} = l_3 + r_3' e^{i\theta_3'}$ can be readily obtained. By using these relationships, Eqs. (2.6)-(2.8) can be rewritten as:

$$m_1 r_1 l_2 = l_1 m_2 r_2' \text{ and } \theta_1 = \theta_2' \tag{2.10}$$

$$m_3 r_3 l_2 = l_3 m_2 r_2 \text{ and } \theta_3 = \pi + \theta_2 \tag{2.11}$$

$$m_4 r_4 l_3 = l_4 m_3 r_3' \text{ and } \theta_4 = \theta_3' \tag{2.12}$$

From the above three equations, it can be seen that whenever the mass distribution of one of the links is given, the mass distributions of the remaining three links can be

determined. The equations to calculate the additional masses can be derived as (assume that link 2 is unchanged):

$$m_i^* r_i^* e^{i\theta_i^*} = m_i r_i e^{i\theta_i} - m_i^0 r_i^0 e^{i\theta_i^0} \quad (i=1,3,4) \tag{2.13}$$

where m_i^0, r_i^0, and θ_i^0 are the parameters of the original link, m_i^*, r_i^*, and θ_i^* are the parameters of the counterweights, and m_i, r_i, and θ_i are the parameters after adding or deducting the counterweights to the original mechanism.

Apparently, in general, either m_i^* or r_i^* is arbitrarily selected, then the other one is computed from Eq. (2.13).

There are several problems associated with the CW method. The first problem is that both joint forces and actuator output torques might increase. The second problem is that the vibration behavior of the mechanism may be degraded (Xi and Sinatra, 1997). The third problem is that the balanced mechanism may have a poor trajectory tracking performance, and consume more energy when running at high speeds (Ouyang et al., 2001). Although a careful design of the mass redistribution may help in solving these problems to some degree, new methods are needed for further improvement. It should be further noted that the CW method is only applicable to pivot joint mechanisms.

2.2.3 Add-spring method

The add-spring method for the force balancing of planar mechanisms was presented by Streit and Shin (1990). Force balancing of some special types of parallel manipulators with this method was studied by Wang and Gosselin (1999), Ebert-Uphoff et al. (2000). They showed that the total mass of the mechanism could be significantly reduced by using this method compared with the CW method. However, it remains to be examined whether this benefit will lead to the reduction of joint forces, and a positive effect on trajectory tracking performance. In general, the add-spring method is suitable to both pivot mechanisms and mechanisms containing prismatic joints.

There are several problems with the add-spring method. First, the contracted length of springs must be zero, which is not practical. Second, a mechanism using this method can only be force balanced in one direction, i.e., the gravity direction, which may be unsuitable for some applications. Third, the spring can be easily fatigued, especially when machines run at high speeds. Fourth, the effects of the masses of springs are very difficult to be considered in the design procedure, which may introduce errors to the system.

2.2.4 Other methods

For the force balancing of a crank-slider mechanism, there is an efficient method called the "duplicating mechanism" method (Davies, 1968). In this method, an identical

mechanism is added to the structure to form a revolved mirror reflection of the original mechanism. In general, this method cannot be used in designing complex types of mechanisms containing prismatic joints. Bagci (1982) presented a complete force balancing method by adding "balancing idler loops" which form a parallelogram with links in the original mechanism. The balancing equations, similar to Eqs. (2.10 – 2.11), were also derived by means of the LIV approach. Feng (1991) utilized the geared inertia counterweights and planetary-gear-train-inertia counterweights to completely balance the shaking force and shaking moment for some specific linkages. Hilpert (1968) successfully used the pantograph mechanism for complete shaking force balancing of four-bar linkages. The same idea was developed by Arakelian (1998) for complete shaking force and shaking moment balancing of an in-line crank-slider mechanism.

2.2.5 AKP method

As mentioned in Chapter 1, the AKP method was developed at the AEDL of the University of Saskatchewan (Wang, 2000). By using this method, the reaction forces in joints can be successfully reduced and the trajectory tracking performance can be improved (Wang, 2000). The initial version of this method, however, has the following problems: First, the study presented by Wang only considered the situation where the mass center of a link lies in its kinematic axis. Second, only the adjustment of a pivot on a link was considered. Thus, this design does not suit the situation where the mass center of a link lies off its kinematic axis. Third, the limitations of the physical implementation were not considered. For example, the mass of a sliding block will

affect the adjustment (detailed discussions will be presented in Chapter 3). To overcome these problems is the main basis of this thesis, as referred to in objective 1, in Chapter 1. Details on the extension and improvement of the AKP method will be discussed in Chapter 3.

2.2.6 Integrated design and control method

A zero reaction manipulator designed based on the redundant actuator method was presented in a recent paper (Papadopoulos and Abu-Abed, 1996). In their method, an additional actuator that has no contribution to the degree of freedom of the system is employed. Though this method is effective in eliminating both the shaking force and the shaking moment, there are several problems with this method. First, extra actuators will create challenges in trajectory tracking control, and will increase the cost of the system. Second, the parallelogram structure, being introduced by the extra actuators, restricts the workspace considerably.

Using the CW method, Diken (1997) discussed a study that simultaneously considered the force balancing and trajectory tracking performance for a serial robot manipulator. Zhang et al. (1999) and Li et al. (1999) comparatively studied how to integrate both force balancing and trajectory tracking for closed-loop mechanisms. They argued that the performance of a mechatronic system not only relies on the design of its control schemes, but also hinges on the design of its mechanical structure. However, the conventional design of the mechanical structure in a mechatronic system is concerned

only with kinematics and statics. Even though that design may be claimed as "optimal", it is not always true from the viewpoint of dynamics. Therefore, a perfect control performance may be hardly achieved due to the hardware limitation. To avoid this situation, an approach called *concurrent design approach* was proposed (Li et. al., 2001). This approach suggests creating an integrated design procedure can be used. This approach has the potential to obtain an optimal system performance from the viewpoints of both kinematics and dynamics. The study in this thesis will further explore the couplings of mechanical structure design and control system design.

2.3 Trajectory planning methods

Trajectory planning is concerned with the development of time schedules for either the end-effector or the joint position, velocity, and acceleration of a mechanism, based on initial, intermediate, and final path specifications (Paul, 1979). Cartesian space trajectory planning is a straightforward concept, since it is easy to perceive desired end-effector configurations in the Cartesian space. However, to execute a trajectory planning algorithm in the Cartesian space, the transformation from Cartesian to joint coordinates in real-time is required, as the control of mechanism motion is done at the joint level. The highly computational complexities involved in trajectory planning and coordinate transformation have hindered the actual implementations of on-line Cartesian-based path planning algorithms. An alternative for planning Cartesian space trajectories is to approximate Cartesian paths using trajectories in the joint space. In this

thesis, the term "trajectory planning" is referring to the joint or actuator trajectory planning.

Much work has been done in the area of smooth trajectory generation. For smooth trajectory generation, it is required that there are small jerks at points through which the end-effector passes. It is important to note that jerks are especially harmful to systems in leading to excessive vibration. Cubic splines are often used in smooth trajectory generation. Lin et al. (1983) discussed the trajectory planning algorithm that was executed off-line. In their paper, the trajectory planning was done at the joint level. Piecewise cubic polynomials were used to fit the sequence of joint displacements for each actuator. Although the jerk constraints were included for each segment in their method, the jerks at the intermediate points were not considered. Therefore, their algorithm cannot assure the jerks to be in the acceptable ranges during the entire motion. Constantinescu and Croft (2000) presented a method for the determination of smooth and time-optimal path constrained trajectories under the constraints on the actuator torques and torque rates. The main concern in their paper was the point-to-point trajectory with special boundary conditions. Piazzi and Visioli (2000) discussed the global minimum-jerk trajectory planning problem. The cubic splines were employed to assure the overall continuity of velocities and accelerations. It should be noted that in their study two extra points should be determined by the algorithm. It is possible that these extra points are beyond the range of the two neighboring points. In such a case, overshoot displacements are unavoidable. Tondu and Bazaz (1999) developed a three-cubic method to generate a joint trajectory by interpolating intermediate positions and

velocities based on a combination of cubic splines ensuring the acceleration continuity. The jerks of the actuators in their paper were not continuous, and also were very large.

High order polynomials are sometimes used for the trajectory generation. Macfarlane and Croft (2001) used a concatenation of quintics to provide a controlled description of point-to-point trajectory. The trajectory is determined based on approximating a linear segment with a parabolic blend trajectory. They showed that the acceleration and jerk with their proposed method were much larger than those with a quintic trajectory planning method. This will lead to difficulty for the real-time control of the system. Egerstedt and Martin (2001) presented the development of optimal trajectory planning and smoothing splines where the trajectory passes closely (may not exactly pass through specific points at the specific times) to a prescribed point at a prescribed time. Such a problem is not the concern of the present study.

In fact, the traveling time from point to point for a mechanism is determined by the operative context in most cases. The problem of trajectory planning in this case can be stated as: generating a smooth connection from segment to segment to achieve a small overall jerk. This problem is unsolved in current literature. Investigation on the solutions of this problem is part of the objective of the thesis; see objective 2, Chapter 1.

2.4 Dynamics of multi-DOF closed-loop mechanisms

In RTC mechanisms, the mechanisms are driven by servomotors, which apply torques

(or forces in the case of linear motors or actuators) at the joints of the mechanisms. The dynamics of a mechanism describes how the mechanism moves in response to the driving torques or forces generated by motors or actuators.

There are many methods for deriving the dynamic equations of a mechanism. Whether a method is superior to others depends on its accuracy and computational efficiency. One method is to apply the Newton and Euler laws for the derivation of dynamics. Generating the Newton's and Euler's equations for each link of the mechanism results in a series of equations that contain both the driving forces and the forces due to constraints. The constrained forces may be eliminated by substituting the geometric and kinematic equations describing the nature of these constraints. Another method for the dynamic modeling is the Lagrangian analysis method. This method has the advantage of requiring only the kinetic and potential energies of the system for computation, and hence tends to be less prone to error. However, the dynamic equations of a closed-loop mechanism developed with this method may not be computationally efficient. Computational efficiency is very important in closed-loop mechanisms from a viewpoint of control (Codourey, 1998).

There are several studies on the dynamic modeling of serial mechanisms, but few on closed-loop mechanisms, especially the multi-DOF closed-loop mechanisms. Nguyen and Cipra (1999) proposed an approach to model the dynamics of closed-loop systems. Their procedure involves finding the first and the second order kinematic coefficients. For a closed-loop mechanism, some dependent joints are highly coupled with the

independent joint variables. These dependent variables need to be replaced by the independent variables in dynamics. Using the Lagrangian analysis, Wang (2000) presented the dynamic model of a 2 DOF closed-loop mechanism by following the approach described in Nguyen and Cipra (1999).

Another approach used for dynamic modeling of the closed-loop mechanisms is the so-called reduced order model analysis method (Ghorbel, 1994, 1997). In Ghorbel's study, however, only a special case for closed-loop mechanisms, where the mass center was in-line for each link, was considered. Therefore, it is necessary to extend this method to a more general situation, where the mass center of each link in the mechanism is arbitrarily distributed with respect to the link reference coordinate system. The extended version is thus more suitable to be used to model the mechanism of interests to this thesis. Objective 3 focuses on the extension of this method. The details will be presented in Chapter 5.

2.5 Control algorithms

Control components form an important part of an RTC mechanism, without which an RTC mechanism is not able to generate flexible trajectory. In this thesis, the term "control" refers to "feedback control". There are three types of control algorithms of interests to this thesis, namely, (i) *Proportional Derivative* (PD) based control methods, (ii) model-based control methods, and (iii) integrated structural design and control methods.

2.5.1 PD based control methods

To control a nonlinear system, one of the practical methods is to design a linear controller based on the linearization of the system about an operating point. An example of applying this method is a PD control law for a robot manipulator. In its simplest form, a PD control law can be expressed as:

$$T = K_p e + K_d \dot{e} \tag{2.14}$$

where K_p and K_d are positive definite matrices, e is the error between the desired trajectory and the actual one, and T is the torque.

It is well known that when position and velocity measurements are available, a PD control is the simplest control law and can be implemented using commercial control modules. In Craig (1988,1989), and Kelly (1997), the PD control with desired gravity compensation was shown to guarantee global and asymptotic stability for a point-set tracking problem. More works on the global stability of trajectory tracking with the manipulators under PD control were given by Qu (1994), and Chen et al. (2001). To improve the trajectory tracking performance of robot manipulators, significant effort has been made to seek advanced control strategies. In spite of the presence of many advanced control laws, the majority of the industrial robots are still controlled by the decentralized (independent joint) PD law in favor of its simple computation and low-

cost set-up. This is because the PD controllers, despite their simple structures, assure acceptable performances for a wide range of industrial plants. Furthermore, their usages are well known among industrial operators. Hence, the PD controllers provide a cost effective mean in industrial environments.

One of the refinements for a fixed-gain PD controller is the NPD controller (Rugh, 1987; Shahruz and Schwartz, 1994; Xu et al, 1995; Seraji, 1998; Armstrong and Wade, 2000). Design procedures for NPD control systems based on heuristic rules or fuzzy rules were reported by Shinskey (1988), and Tao and Taur (2000). Rugh (1987) designed a NPID control by the extended linearization technique in which the three gains of the controller are functions of the error state. Xu et al (1995) proposed a NPD control for the force control tasks, and also–pointed out that the method is also applicable to position control. Seraji (1998) introduced a new class of simple NPD controllers and provided a formal treatment of their stability analysis. It should be noted that a lot of previous studies on NPD control were applied to the point-set control of linear systems. There are only a few papers describing the NPD control for trajectory tracking of nonlinear systems such as parallel manipulators. Objective 4 of this thesis is to extend the NPD control to the trajectory tracking of a mechanism. The details will be given in Chapter 5 and Chapter 6, along with a more comprehensive study of PD and NPD controllers to the mechanism that is force balanced using the CW method and the AKP method.

2.5.2 Model based control methods

In this thesis, *model based control* refers to those methods that employ the plant dynamic models in their control laws. For a closed-loop mechanism, the dynamic model can be generally represented as follows:

$$D(q)\ddot{q} + C(q,\dot{q})\dot{q} + G(q,\dot{q}) = T \tag{2.15}$$

where $q \in R^n$ is a set of configuration variables for the mechanism, and $T \in R^n$ denotes the torques applied at the joints. Model-based control methods incorporate these quantities: D, C and G in Eq. (2.15), into the mathematical expressions of their control laws.

The prominent model-based control method for robot control was proposed by Craig (1986). This method is also called the *Computed Torque Control* (CTC) method. The computed torque can be written as:

$$T = \underbrace{D(q)\ddot{q}_d + C\dot{q} + G}_{T_1} + \underbrace{D(q)(K_p e + K_d \dot{e})}_{T_2} \tag{2.16}$$

where e is the position error, $e = q_d - q$, and K_p and K_d are constant gain matrices. The CTC law consists of two components. The first component T_1 is the feedforward item. It provides the amount of torque necessary to drive the system along its nominal

path. The second component T_2 is the feedback component and provides correction torques to reduce any errors in the trajectory tracking. The power of the CTC law is that it converts a nonlinear dynamical system into a linear one for the error dynamics, allowing the use of any of a number of linear control synthesis tools. There are some problems with the CTC law, especially for the control of closed-loop mechanisms, e.g., parallel robots. First, the CTC law strongly depends on the dynamic model of a plant system. The more accurate the dynamic model, the better the trajectory tracking performance. However, It is usually very difficult to obtain an accurate dynamic model of a closed-loop mechanical system due to such factors as frictions, backlash, and assembly clearance. Second, the CTC law requires considerable computational resources that lead to the difficulty in practical implementations, in particular when the mechanism is required to run at high speeds.

For a closed-loop mechanism, due to the high nonlinearity and complexity of the dynamics, it renders difficulties for control engineers to control such mechanisms to follow a trajectory precisely and quickly. Several methods reported in the literature were proposed to handle this problem. Lin and Chen (1996) proposed a very sophisticated control structure that composes of several sub-control algorithms such as *model reference adaptive control* (MRAC), a disturbance compensation loop, a modified switching control and some feedback loops to control a closed-loop pivot four-bar linkage. It is easy to imagine that such a control method will require considerable computation time. As a consequence, the linkage can only run at low speeds (30 rpm).

2.5.3 Integrated structural design and control methods

For the control of high speed mechanisms with the character of high accurate tracking of a trajectory, one effective approach is to design the mechanical structure in such a way that it results in a simple dynamic model, and then apply a simple PD control. There are several different ways to design a mechanical structure for a simple dynamic model. Asada and Youcef-Toumi (1987) suggested adding a parallelogram structure to an existing series chain structure to form a special configuration of a 2 DOF five-bar mechanism. This method leads to completely decoupled dynamic equations of the modified system, which makes the use of the independent PD control method possible. Another method to achieve a simple dynamic model is through mass redistribution (Diken, 1997; Zhang et al., 1999, Li et al., 2000). It is easy to see from Eq. (2.1) that the design condition for force balancing can also lead to the cancellation of gravitational term in the dynamic model, see Eq. (2.15). On the top of cancellation of the gravitational term, Wu et al. (2001) showed the possibility of designing the mechanical structure for the same mechanism (Figure 2.1) such that the inertia matrix $\boldsymbol{D}$ in Eq. (2.15) becomes partially configuration-invariant. This integrated design can further improve trajectory tracking performance.

2.6 Conclusion

With reference to the research objectives defined in Chapter 1, the literature review presented in this chapter shows that none of these objectives has been fully achieved.

With respect to objective 1, the commonly used force balancing methods were developed from the viewpoint of mechanical structure design only. The motion generation tasks such as trajectory tracking are not considered in the design. The AKP method developed at the AEDL of the University of Saskatchewan is the only one considered both force balancing and trajectory tracking. However, the present version of the AKP method has some problems that need to be overcome. With respect to objective 2, there was considerable amount of studies on trajectory planning without considering the continuity of the jerks. However, to achieve a smooth trajectory and reduce machine wear, the continuity of the jerk during the overall motion must be considered. With respect to objective 3, only dynamic models of closed-loop mechanisms with special structures are developed. It is necessary to find a general approach to develop dynamic models for general purpose closed-loop mechanisms. Finally, with respect to objective 4, the use of PD/NPD control laws for complex mechanical systems with incorporation of mechanical structure design is a new direction. More studies need to be carried out in order to understand how different control laws would affect trajectory tracking performance by different force balancing methods.

CHAPTER 3

THE EXTENDED AKP METHOD

3.1 Introduction

In the previous chapter, the force balancing issue in mechanism design was addressed. Amongst all the force balancing methods, the AKP method is of direct interest to this thesis. The limitations of the AKP method were detailed earlier. The objective of this chapter is to improve this method and extend it to general applications. As discussed in Chapter 1 and Chapter 2, the present AKP method did not consider the masses of sliding blocks while adjusting the kinematic parameters. When this factor is taken into consideration, the force balancing condition equations have to be changed. The details are discussed in Section 3.2. The principle and the design equations for the extended AKP method are described in Section 3.3. Section 3.4 presents the comparison of the extended AKP method and the CW method in terms of the joint forces under different operating conditions. Finally, a conclusion is given in Section 3.5.

3.2 New force balancing condition equations

When implementing the extended AKP method, the masses of sliding blocks, which are used to adjust the pivots, must be taken into account in the force balancing condition equations. The implementation of the pivot adjustment is illustrated in Figure 3.1. When sliding block 3 is adjusted along link 1 or sliding block 4 adjusted along link 2, the mass distribution of this group of links will vary.

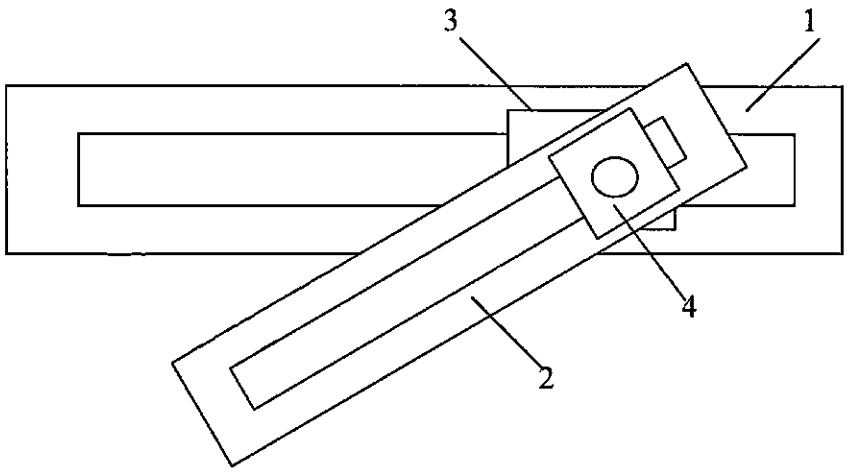

Figure 3.1 Illustration of pivot adjustment

Assume that the sliding block is a point mass acting on the pivot, denoting m_{ij} as the mass of the sliding block between link i and link j. The schematic diagram of a mechanism with consideration of these point masses, m_{ij}, is shown in Figure 3.2.

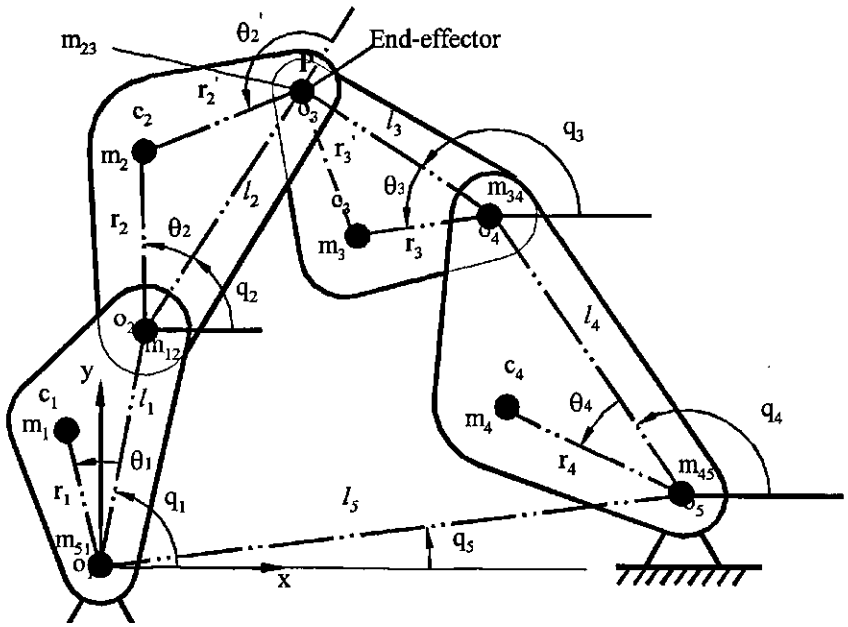

Figure 3.2 Scheme of mechanism with the point mass at the pivot

The new force balancing condition equations can be derived by following the LIV approach outlined in Chapter 2, namely

$$m_1 r_1 e^{i\theta_1} + (m_2 + m_{12}) l_1 - l_1 m_2 r_2 e^{i\theta_2} / l_2 = 0 \tag{3.1}$$

$$m_3 r_3 e^{i\theta_3} + m_{23} l_3 + l_3 m_2 r_2 e^{i\theta_2} / l_2 = 0 \tag{3.2}$$

$$m_4 r_4 e^{i\theta_4} + (m_3 + m_{23} + m_{34}) l_4 + l_4 m_2 r_2 e^{i\theta_2} / l_2 = 0 \tag{3.3}$$

Using the relationship $r_2 e^{i\theta_2} = l_2 + r_2' e^{i\theta_2'}$, Eq. (3.1) can be rewritten as:

$$l_2 m_1 r_1 e^{i\theta_1} = l_1 m_2 \tilde{r}_2' e^{i\tilde{\theta}_2'} \tag{3.4}$$

where $\tilde{r}_2' = \sqrt{(r_2' \cos\theta_2' - m_{12} l_2 / m_2)^2 + (r_2' \sin\theta_2')^2}$

$$\tilde{\theta}_2' = \tan^{-1}\left(\frac{r_2' \sin\theta_2'}{r_2' \cos\theta_2' - m_{12} l_2 / m_2}\right)$$

Similarly, Eq. (3.2) can be rewritten as:

$$l_2 m_3 r_3 e^{i\theta_3} + l_3 m_2 \tilde{r}_2 e^{i\tilde{\theta}_2} = 0 \tag{3.5}$$

where $\tilde{r}_2 = \sqrt{(r_2 \cos\theta_2 + m_{23} l_2 / m_2)^2 + (r_2 \sin\theta_2)^2}$

$$\tilde{\theta}_2 = \tan^{-1}\left(\frac{r_2 \sin\theta_2}{r_2 \cos\theta_2 + m_{23} l_2 / m_2}\right)$$

Likewise, Eq. (3.3) can be rewritten as:

$$l_2 m_4 r_4 e^{i\theta_4} + l_4 m_2 \hat{r}_2 e^{i\hat{\theta}_2} = 0 \tag{3.6}$$

where $\hat{r}_2 = \sqrt{(r_2 \cos\theta_2 + (m_3 + m_{23} + m_{34}) l_2 / m_2)^2 + (r_2 \sin\theta_2)^2}$

$$\hat{\theta}_2 = \tan^{-1}\left(\frac{r_2 \sin\theta_2}{r_2 \cos\theta_2 + (m_3 + m_{23} + m_{34}) l_2 / m_2}\right)$$

Eqs. (3.4) to (3.6) are the new force balancing equations and can be rearranged as:

$$l_2 m_1 r_1 = l_1 m_2 \tilde{r}_2' \quad \text{and} \quad \theta_1 = \tilde{\theta}_2' \tag{3.7}$$

$$l_2 m_3 r_3 = l_3 m_2 \tilde{r}_2 \quad \text{and} \quad \theta_3 = \tilde{\theta}_2 + \pi \tag{3.8}$$

$$l_2 m_4 r_4 = l_4 m_2 \hat{r}_2 \quad \text{and} \quad \theta_4 = \hat{\theta}_2 + \pi \tag{3.9}$$

Compared with the original force balancing Eqs. (2.10)-(2.12), it can be seen that the effect due to the sliding blocks is reflected by the augmented parameters, i.e., ($\tilde{r}_2$, $\tilde{r}_2'$, $\hat{r}_2$) and ($\tilde{\theta}_2$, $\tilde{\theta}_2'$, $\hat{\theta}_2$), which are only related to link 2, the masses of the sliding blocks and link 3. The force balancing condition equations, i.e., Eqs. (3.7)-(3.9), imply that the mass distribution of a force balanced mechanism should satisfy Eqs. (3.7)-(3.9). It is noted that the force balancing condition equations above are derived by following principle (i), and therefore, they are applicable to the AKP method.

3.3 The extended AKP method

Examining the original and the new force balancing equations shown in Eqs. (2.10) to (2.12) and Eqs. (3.7) to (3.9), respectively, it is clear that these equations can also be satisfied by changing the kinematic parameters, l_i (i=*1,2,3,4*), whilst maintaining the total mass of a mechanism unchanged. It should be noted when l_i is varied, the parameters r_i and θ_i will be changed accordingly. Both the original and the extended AKP method are developed based on this observation. In particular, the derivation of the extended AKP method based on the new force balancing equations is given as follows. A general design case will be presented first, followed by a special design case.

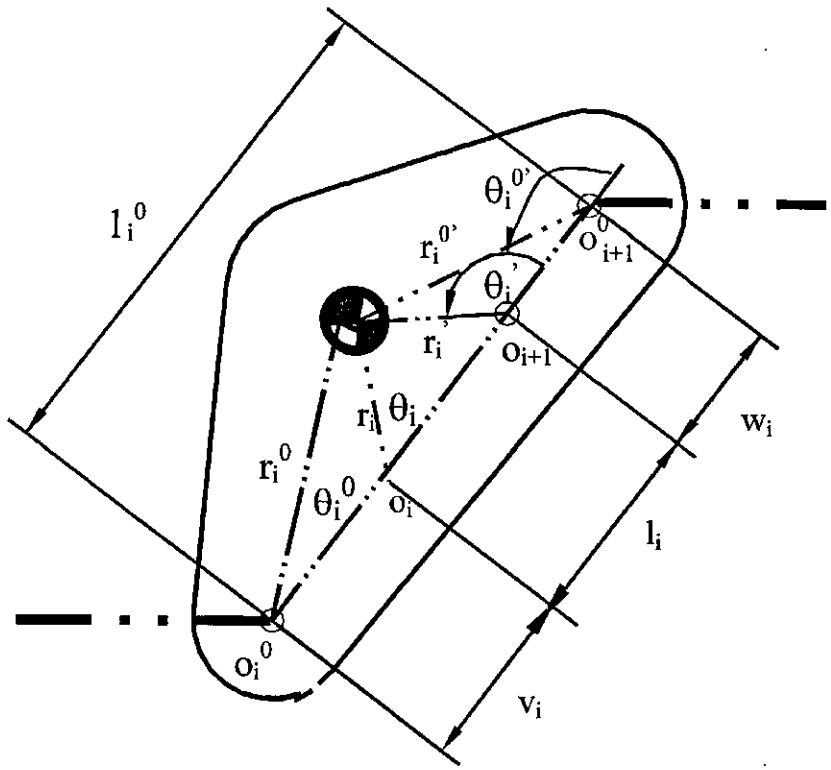

Figure 3.3 Two-step kinematic parameter adjustment in the extended AKP method

In the general design situation, assume the mass centers of the links are arbitrarily distributed, with $\theta_i \neq 0$ for i=1 to 4, as shown in Figure 3.3. Let l_i^0 and (r_i^0, θ_i^0) represent the length and the mass center of link i respectively, where superscript "0" indicates the parameters prior to the adjustment of pivot o_i^0. It is observed that in order to satisfy the force balancing condition equations specified in Eqs. (3.7) to (3.9), adjusting of only one pivot on a link is not sufficient; instead, two pivots must be adjusted. The extended AKP method is thus accomplished in two steps. The first step is to adjust a pivot from o_i^0 to o_i so that the angle relationship between link i and link

$i+1$ can be satisfied. The second step is to adjust o_{i+1}^0 to o_{i+1} so that all Eqs. (3.7) to (3.9) can be satisfied. Now, let l_i and (r_i, θ_i) represent the new length and the new mass center of link *i*, respectively, and let v_i and w_i represent the adjusted amounts of the two pivots o_i and o_{i+1}, respectively. From Figure 3.3, the following equations can be obtained:

$$l_i = l_i^0 - v_i - w_i \tag{3.10}$$

$$r_i^0 \cos\theta_i^0 = v_i + r_i \cos\theta_i \tag{3.11}$$

$$r_i^0 \sin\theta_i^0 = r_i \sin\theta_i \tag{3.12}$$

for i=1, 2, 3, 4.

Eq. (3.12) can be rewritten as:

$$r_i = \frac{r_i^0 \sin\theta_i^0}{\sin\theta_i} \tag{3.13}$$

Substituting Eq. (3.13) into Eq. (3.11) yields:

$$v_i = r_i^0 \sin(\theta_i - \theta_i^0) / \sin\theta_i \tag{3.14}$$

Based on the force balancing condition equations given in Eqs. (3.7) to (3.9) and the results given in Eqs. (3.10) to (3.14), the implementation of the extended AKP method

can be illustrated using the following example. Referring to Figure 3.2, assume that the pivots of link 2 are unchanged, and the force balancing conditions can be achieved by adjusting the pivots of the other three links. The detailed procedure is illustrated below.

For link1:

Pivot O_1 on link 1 is adjusted using the following equation derived from Eq. (3.14) and Eq. (3.7),

$$v_1 = r_1^0 \sin(\tilde{\theta}_2' - \theta_1^0) / \sin\tilde{\theta}_2' \tag{3.15}$$

Pivot O_2 on link 1 is adjusted using Eq. (3.7). To determine the amount of adjustment for pivot O_2 on link 1, i.e., w_1, substituting Eq. (3.15) and Eqs. (3.10) to (3.12) into Eq. (3.7) yields:

$$w_1 = l_1^0 - \frac{r_1^0 (m_2 \tilde{r}_2' \sin(\tilde{\theta}_2' - \theta_1^0) + m_1 l_2 \sin\theta_1^0)}{m_2 \tilde{r}_2' \sin\tilde{\theta}_2'} \tag{3.16}$$

For link 3:

Substituting Eq. (3.8) into Eq. (3.14) yields:

$$v_3 = r_3^0 \sin(\tilde{\theta}_2 - \theta_3^0) / \sin\tilde{\theta}_2 \tag{3.17}$$

Substituting Eq. (3.17) and Eqs. (3.10) to (3.12) into Eq. (3.8) yields:

$$w_3 = l_3^0 - \frac{r_3^0(m_2\tilde{r}_2 \sin(\tilde{\theta}_2 - \theta_3^0) - m_3 l_2 \sin\theta_3^0)}{m_2\tilde{r}_2 \sin\tilde{\theta}_2} \tag{3.18}$$

For link 4:

Substituting Eq. (3.9) into Eq. (3.14) yields:

$$v_4 = r_4^0 \sin(\hat{\theta}_2 - \theta_4^0)/\sin\hat{\theta}_2 \tag{3.19}$$

Substituting Eq. (3.19) and Eqs. (3.10) to (3.12) into Eq. (3.9) yields:

$$w_4 = l_4^0 - \frac{r_4^0(m_2\hat{r}_2 \sin(\hat{\theta}_2 - \theta_4^0) - m_4 l_2 \sin\theta_4^0)}{m_2\hat{r}_2 \sin\hat{\theta}_2} \tag{3.20}$$

For the special design case where mass distributions of all the links are in line with their kinematic axes, adjusting of only one pivot for each link is sufficient. In this case, since conditions $\theta_i^0 = 0$ and $\theta_i = 0$ hold, Eq. (3.12) thus becomes meaningless. Furthermore, if the sliding blocks are not considered in the implementation, the force balancing equations given in Eqs. (3.10) to (3.12) are simplified as the original ones given in Eqs. (2.10) to (2.12). Substituting Eqs. (3.10) and (3.11) into Eqs. (2.10) to (2.12), the adjusting amounts for links 1, 3, and 4, respectively, can be obtained as follows:

$$v_1 = (m_2 r_2' l_1^0 \cos\theta_1 - m_1 r_1^0 l_2 \cos\theta_1^0)/(m_2 r_2' \cos\theta_1 - m_1 l_2) \tag{3.21}$$

$$v_3 = (m_2 r_2 l_3^0 \cos\theta_3 - m_3 r_3^0 l_2 \cos\theta_3^0)/(m_2 r_2 \cos\theta_3 - m_3 l_2) \tag{3.22}$$

$$v_4 = (kl_4^0 \cos\theta_4 - m_4 r_4^0 \cos\theta_4^0)/(k\cos\theta_4 - m_4) \tag{3.23}$$

with $k = \sqrt{(m_2 r_2 / l_2)^2 + m_3^2 + (2m_2 r_2 m_3 \cos\theta_2 / l_2)}$.

Moreover, following the above discussion, if link 3 is selected to be unchanged, the adjusting amounts for other three links can be determined as follows:

$$v_1 = (hl_1^0 \cos\theta_1 - m_1 r_1^0 \cos\theta_1^0)/(h\cos\theta_1 - m_1) \tag{3.24}$$

$$v_2 = (m_3 r_3 l_2^0 \cos\theta_2 - m_2 r_2^0 l_3 \cos\theta_2^0)/(m_3 r_3 \cos\theta_2 - m_2 l_3) \tag{3.25}$$

$$v_4 = (m_3 r_3' l_4^0 \cos\theta_4 - m_4 r_4^0 l_3 \cos\theta_4^0)/(m_3 r_3' \cos\theta_4 - m_4 l_3) \tag{3.26}$$

with $h = \sqrt{(m_3 r_3 / l_3)^2 + m_2^2 + (2m_3 r_3 m_2 \cos\theta_3 / l_3)}$.

When designing an RTC mechanism, for a given task, i.e., a set of trajectory points that the end-effector should follow, through the inverse kinematics, the corresponding joint angles are readily determined. However, if the extended AKP method is adopted for force balancing design, the kinematic parameters of the mechanism will vary. This will in turn change the inverse kinematics of the mechanism. In order to enable the end-effector of the mechanism to follow the same trajectory, the motion profiles of the joints must be adjusted according to the new inverse kinematics. This adjustment is only possible through the implementation of programmable actuators, i.e., RTC actuators.

Therefore, the application of the extended AKP method is only limited to RTC mechanisms.

To verify the extended AKP method, a five-bar mechanism prototype was built using LEGO blocks, as shown in Figure 3.4. Figure 3.4(a) shows the unbalanced system. After applying the extended AKP method, the kinematic parameters were changed and the shaking force of the mechanism was cancelled. Figures 3.4(b) and 3.4(c) illustrate two configurations of the force balanced mechanism. The mechanism was stabilized at these two positions, and in fact, it was stable at any other positions as well. That is, the mechanism is force balanced.

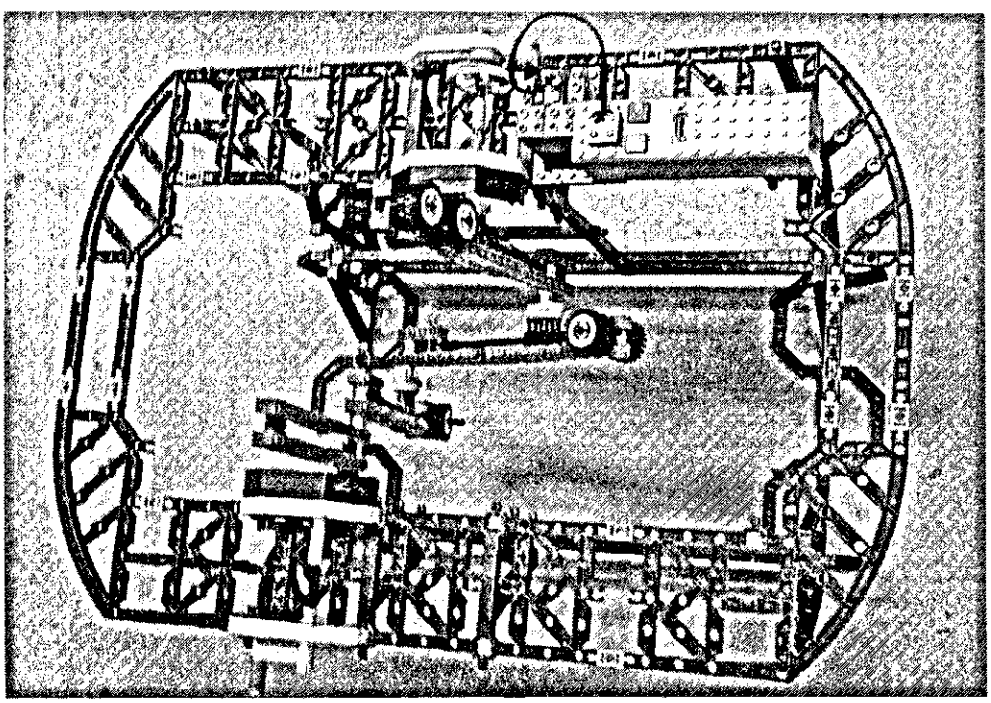

Figure 3.4(a) Unbalanced mechanism

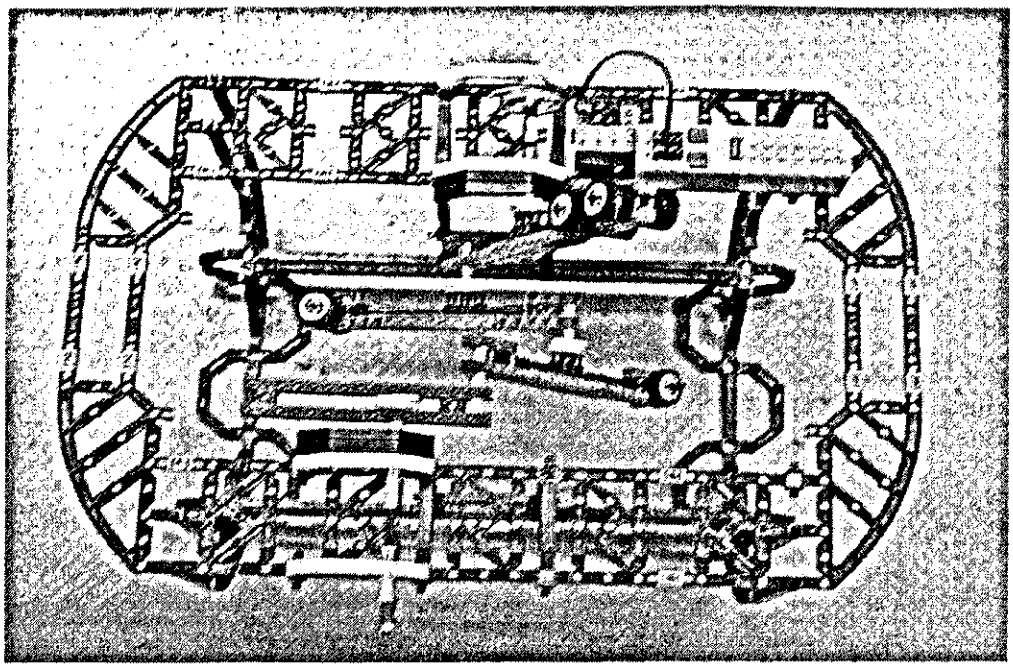

Figure 3.4(b) Balanced mechanism using the extended AKP method (1)

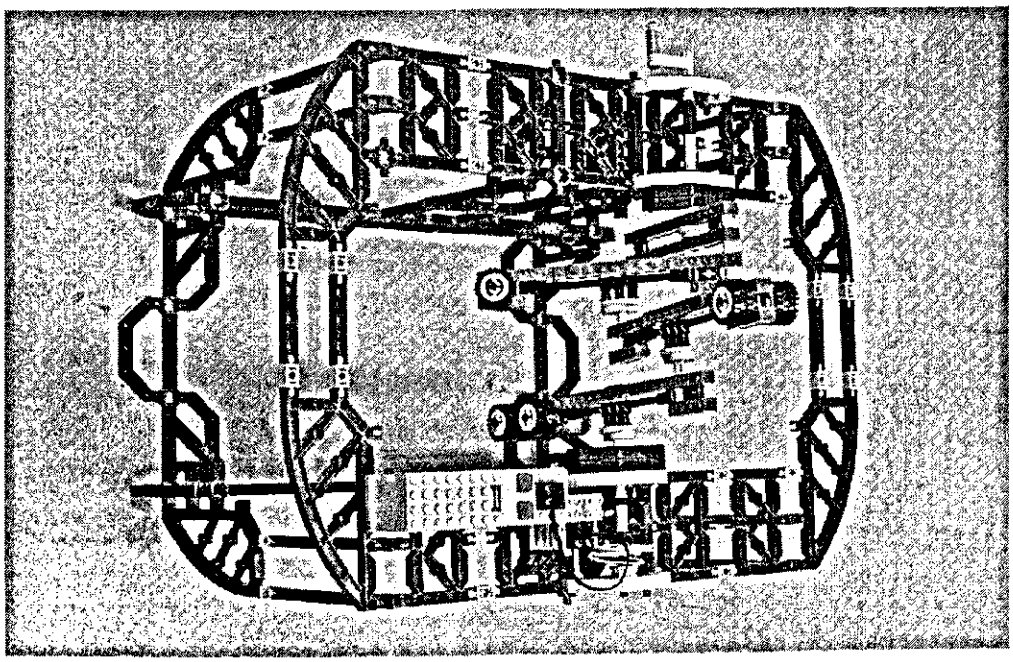

Figure 3.4(c) Balanced mechanism using the extended AKP method (2)

3.4 Comparison of the extended AKP method with the CW Method: Joint reaction force

Two examples are used here to verify the effectiveness of the extended AKP method. Comparison is made between the extended AKP method and the CW method in terms of reduction of the joint forces.

Example 1

The kinematic parameters of the original mechanism without considering force balancing are listed in Table 3.1. Using the CW method and the extended AKP method, the kinematic parameters of the force balanced mechanism are computed and listed in the same table. In the CW case, assume link 3 is unchanged and the other three links are subject to additional masses. In the extended AKP case, assume all the movable links are subject to pivot adjustments.

Table 3.1 Parameters for different mechanisms (in-line case 1)

Parameters	Unbalanced linkage	CW linkage	AKP linkage
l_1 (m)	0.2	0.2	0.0977
l_2 (m)	0.3	0.3	0.28
l_3 (m)	0.4	0.4	0.2445
l_4 (m)	0.3	0.3	0.1009
l_5 (m)	0.3	0.3	0.3
r_1 (m)	0.05	0.1758	0.0523

r_2 (m)	0.15	0.0506	0.13
r_3 (m)	0.08	0.08	0.0756
r_4 (m)	0.1	0.103	0.0991
m_1 (kg)	0.25	0.5912	0.25
m_2 (kg)	0.25	0.4445	0.25
m_3 (kg)	0.375	0.375	0.375
m_4 (kg)	0.5	0.8742	0.5
$I_1(kg \cdot m^2)$	0.004	0.0133	0.004
$I_2(kg \cdot m^2)$	0.01	0.0229	0.01
$I_3(kg \cdot m^2)$	0.02	0.02	0.02
$I_4(kg \cdot m^2)$	0.02	0.0475	0.02
$\theta_1(rad)$	0	π	π
$\theta_2(rad)$	0	π	0
$\theta_3(rad)$	0	0	π
$\theta_4(rad)$	0	π	π

The mechanism is supposed to fulfill the following task: the end-effector is requested to move from point A (0.3, 0.2) to point B (0.2, 0.3) within 1 second, and subsequently to point C (0.1, 0.2) within 2 seconds. The unit of the coordinates is meter for all examples. Furthermore, for each segment of the trajectories, (i) the velocities of the end-effector at these three points are zero, and (ii) the accelerations of the end-effector at the initial and final points are zero. The trajectories at the two actuators can be determined based on the inverse kinematic and the motion planning method that will be described in Chapter 4. In particular, the trajectories at the two actuators for the

unbalanced mechanism and the force balanced mechanism using the CW method are respectively expressed as follows:

For actuator 1:

$$q_1(t) = 90.0 + 187.2701 \times t^3 - 261.4406 \times t^4 + 96.7905 \times t^5 \qquad if \quad t \le 1$$

$$q_1(t) = 112.6199 - 38.9289 \times (t-1)^2 + 109.4122 \times (t-1)^3 - 67.4608 \times (t-1)^4 + 12.5189 \times (t-1)^5 \qquad if \quad 1 < t \le 3$$

For actuator 2:

$$q_4(t) = -13.688 + 657.9647 \times t^3 - 894.1248 \times t^4 + 320.5211 \times t^5 \qquad if \quad t \le 1$$

$$q_4(t) = 27.5324 - 87.5649 \times (t-1)^2 + 157.4044 \times (t-1)^3 - 85.2165 \times (t-1)^4 + 14.8542 \times (t-1)^5 \qquad if \quad 1 < t \le 3$$

As mentioned in Section 3.3, the trajectory of the force balanced mechanism using the extended AKP method must be re-planned due to the change of the kinematic parameters. After re-planning, the expressions of the new trajectories at the two actuators are as follows:

For actuator 1:

$$q_1(t) = 63.4541 + 201.7492 \times t^3 - 290.3993 \times t^4 + 111.27 \times t^5 \qquad if \quad t \le 1$$

$$q_1(t) = 86.0739 - 24.4488 \times (t-1)^2 + 152.8515 \times (t-1)^3 - 105.4703 \times (t-1)^4 + 20.4828 \times (t-1)^5 \qquad if \quad 1 < t \le 3$$

For actuator 2:

$$q_4(t) = -13.688 + 657.9647 \times t^3 - 894.1248 \times t^4 + 320.5211 \times t^5 \qquad if \quad t \le 1$$

$$q_4(t) = 70.6729 - 185.6443 \times (t-1)^2 + 286.676 \times (t-1)^3 - 145.3904 \times (t-1)^4 + 24.437 \times (t-1)^5 \qquad if \quad 1 < t \le 3$$

Using the software called "Working Model 2D" (Knowledge Revolution, 1999), the joint forces in the five pivots can be calculated. Figure 3.5 shows the joint forces in the two actuators.

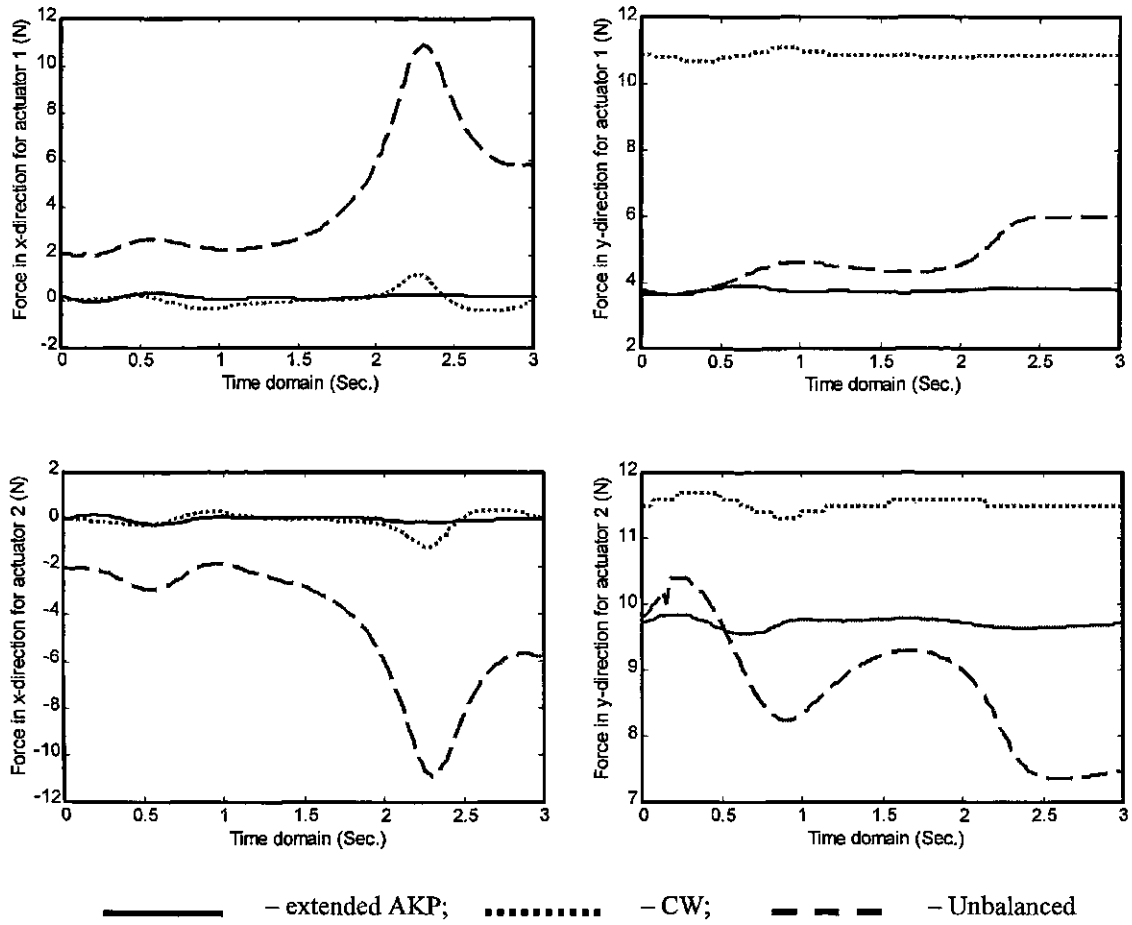

Figure 3.5 Joint forces in the two actuators at low speeds

It can be seen from Figure 3.5 that, when the mechanism runs at low speeds (about 5 rpm), the forces in the two actuators for the force balanced mechanism do not change very much, and the extended AKP method insures smaller forces at both the x-direction and the y-direction than the CW method. Furthermore, the joint forces at the y-direction using the CW method are significantly larger than those of the extended AKP method and the unbalanced mechanism. This phenomenon agrees with one of the weaknesses associated with the CW method, i.e., joint forces will be increased. It is interesting to observe that the variations of joint forces using both the CW and the extended AKP methods are small, while the joint forces of the unbalanced mechanism vary considerably, especially in the x-direction. The reason for this phenomenon can be explained as follows. After the shaking force is balanced, the mass center of the system is stationary during operation. Furthermore, the inertia term is small at low speeds. Therefore, the variation of the forces in the two actuators is small. On the other hand, for the unbalanced mechanism, the mass center of the mechanism changes with the system configurations. Therefore, variation of the forces in the two actuators is large.

It should be noted that, for the force balanced mechanism, the total forces at the two actuators should be zero in the x-direction and should be equal to the total weight of the mechanism in the y-direction. This observation is confirmed with the results shown in Figure 3.5.

Figure 3.6 shows the results when the mechanism runs at high speeds (about 50rpm). Performance totally different from the low speed motion is observed. First, variations of

the forces are very large for all three cases. Second, the CW method generates the worst performance in the x-direction, although the total forces in the two actuators in the x-direction are still maintained at zero, the sharp variation of forces exhibits. Nevertheless, the extended AKP method remains to produce the best performance.

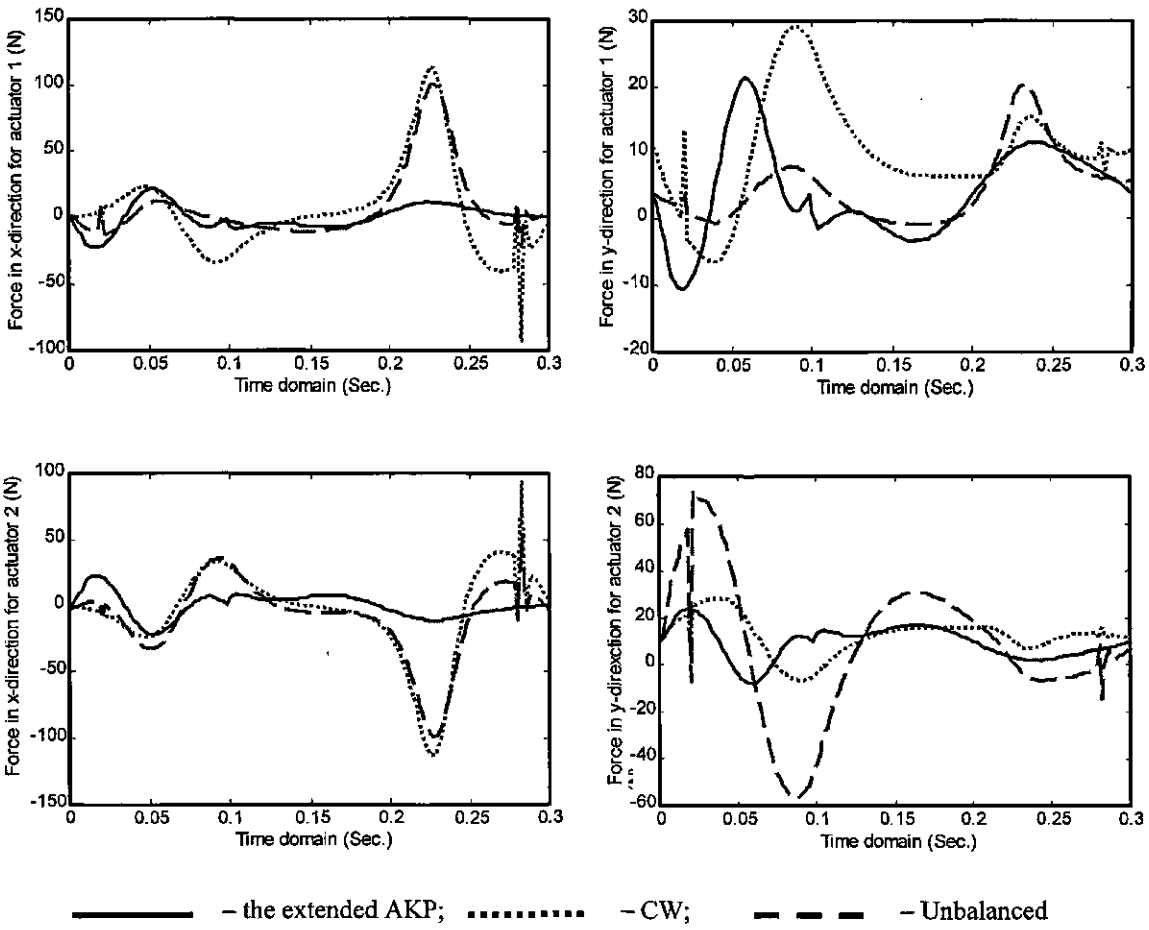

Figure 3.6 Joint forces in the two actuators at high speeds

The results above are expected. When the mechanism runs at high speeds, the inertia forces becomes the dominant term in the dynamics. Since the CW method adopts the adding mass approach for force balancing purpose, its inertia force takes more weight.

While with the extended AKP method, the total mass of the system is unchanged, therefore the inertia force does not differ significantly from the unbalanced mechanism.

To further illustrate the effectiveness of the extended AKP method, Table 3.2 lists the minimum and maximum joint forces in the x-direction and the y-direction for the cases of applying the AKP method and the CW method, respectively. It is observed that the joint forces generated by using the extended AKP method have a smaller variation range than those using the CW method. The reduction of the forces in the x-direction is more remarkable by using the AKP method than by using the CW method.

Table 3.2 Joint forces (min & max) using different force balancing methods

Speeds	Pivot No.	Joint forces in X-direction				Joint forces in Y-direction			
		AKP method		CW method		AKP method		CW method	
		Min	Max	Min	Max	Min	Max	Min	Max
Low Speeds	1	-0.205	0.204	-0.405	1.130	3.640	3.930	10.70	11.10
	2	-0.208	0.228	-1.210	0.338	-1.470	-1.200	-5.350	-4.870
	3	-0.233	0.164	-1.130	0.387	0.930	1.320	-0.869	-0.595
	4	-0.514	0.444	-1.140	0.487	4.320	5.300	2.430	3.420
	5	-0.204	0.205	-1.130	0.405	9.560	9.840	11.30	11.70
High speeds	1	-22.80	21.60	-93.50	113.0	-10.50	21.40	-6.40	29.20
	2	-21.30	25.00	-121.0	81.00	-18.10	11.80	-31.10	17.30
	3	-24.20	18.30	-113.0	89.40	-21.90	22.30	-14.10	13.30
	4	-56.90	42.10	-114.0	110.0	-50.10	60.70	-48.30	51.90
	5	-21.60	22.80	-113.0	93.50	-7.870	23.90	-6.770	28.80

Example 2

In this example, a mechanism with the mass center off line of the kinematic axis is studied. The kinematic parameters of the original mechanism without force balancing and the modified mechanisms using the CW method and the extended AKP method are listed in Table 3.3, respectively. In the redesign of the mechanism, link 2 is assumed to be unchanged.

Table 3.3 Parameters for different mechanisms (off-line)

Parameters	Unbalanced linkage	CW linkage	AKP linkage
l_1 (m)	0.15	0.15	0.0866
l_2 (m)	0.26	0.26	0.26
l_3 (m)	0.26	0.26	0.2078
l_4 (m)	0.14	0.14	0.08838
l_5 (m)	0.30	0.30	0.30
r_1 (m)	0.075	0.0866	0.10
r_2 (m)	0.15	0.15	0.15
r_3 (m)	0.08485	0.10	0.12
r_4 (m)	0.115	0.1415	0.135
m_1 (kg)	1	2	1
m_2 (kg)	2	2	2
m_3 (kg)	2	3	2
m_4 (kg)	2	4	2
$I_1(kg \cdot m^2)$	0.01	0.03	0.01
$I_2(kg \cdot m^2)$	0.05	0.05	0.05

$I_3(kg \cdot m^2)$	0.04	0.06	0.04
$I_4(kg \cdot m^2)$	0.02	0.04	0.02
θ_1(deg.)	90	150	150
θ_2(deg.)	30	30	30
θ_3(deg.)	225	210	210
θ_4(deg.)	192.83	169.11	188.21

In this example, the mechanism is supposed to fulfill the following task: the end-effector is requested to move from point A (0.3, 0.25) to point C (0.1, 0.2) intermediate point B (0.2, 0.2). The time duration between two neighbouring points is 2 seconds at low speeds (about 5rpm) and 0.1 second at high speeds (about 100rpm). Furthermore, for each segment of the trajectories, (i) the velocity of the end-effector at the intermediate point B is determined by the method that will be discussed in Chapter 4, and (ii) the accelerations of the end-effector at the initial and final tracking points are zero.

Figures 3.7 and 3.8 show the total forces in the two actuators for the unbalanced mechanism and the balanced mechanism using the extended AKP method and the CW method at low speeds and high speeds, respectively. From these two Figures, it can be seen that the extended AKP method is the best in terms of the reduction of forces at both low speeds and high speeds, and the CW method is the worst. So it is demonstrated that the extended AKP method is better than the CW method in the reduction of the joint forces for an off-line mechanism.

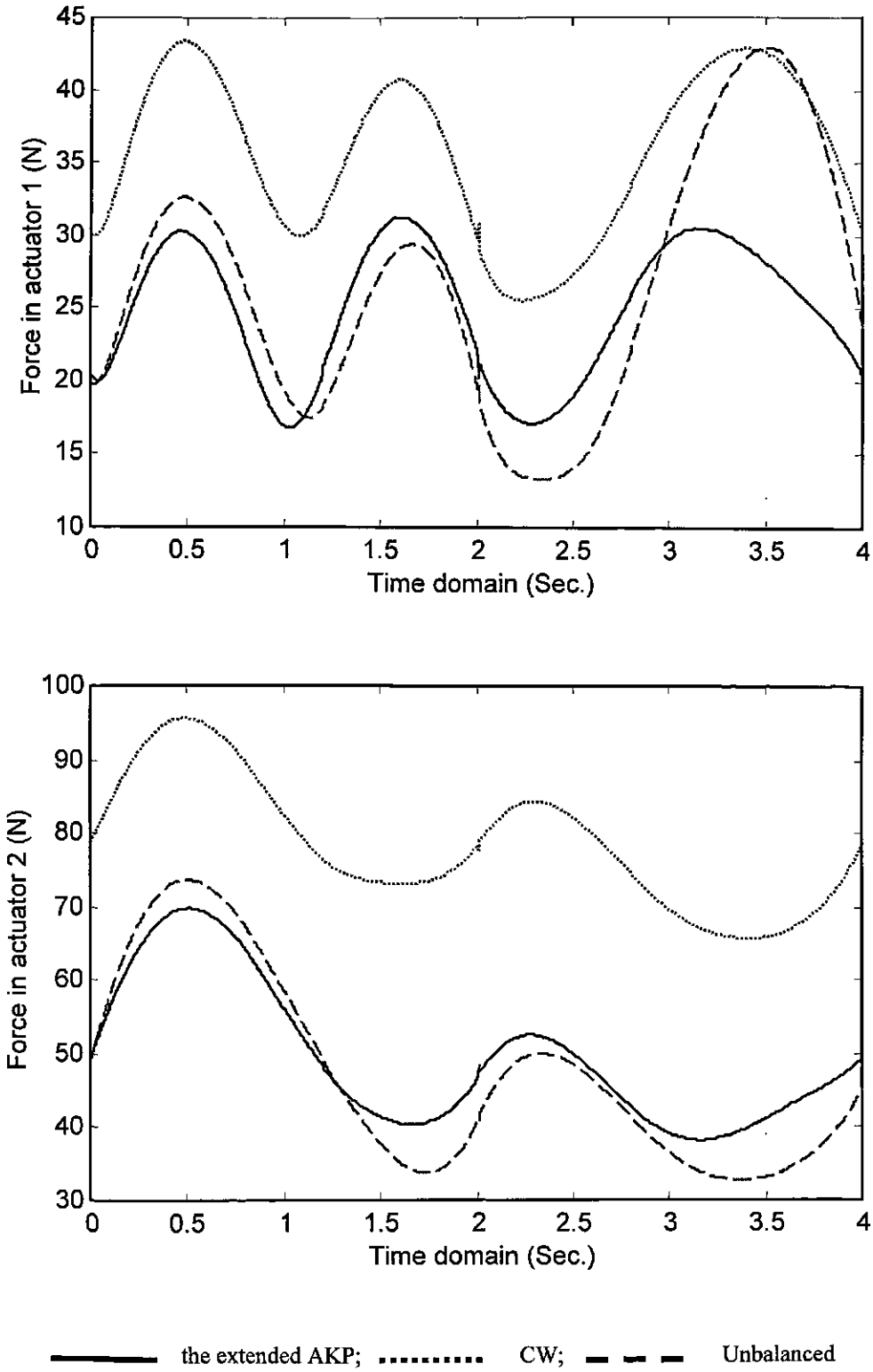

Figure 3.7 Total forces in the two actuators at low speeds

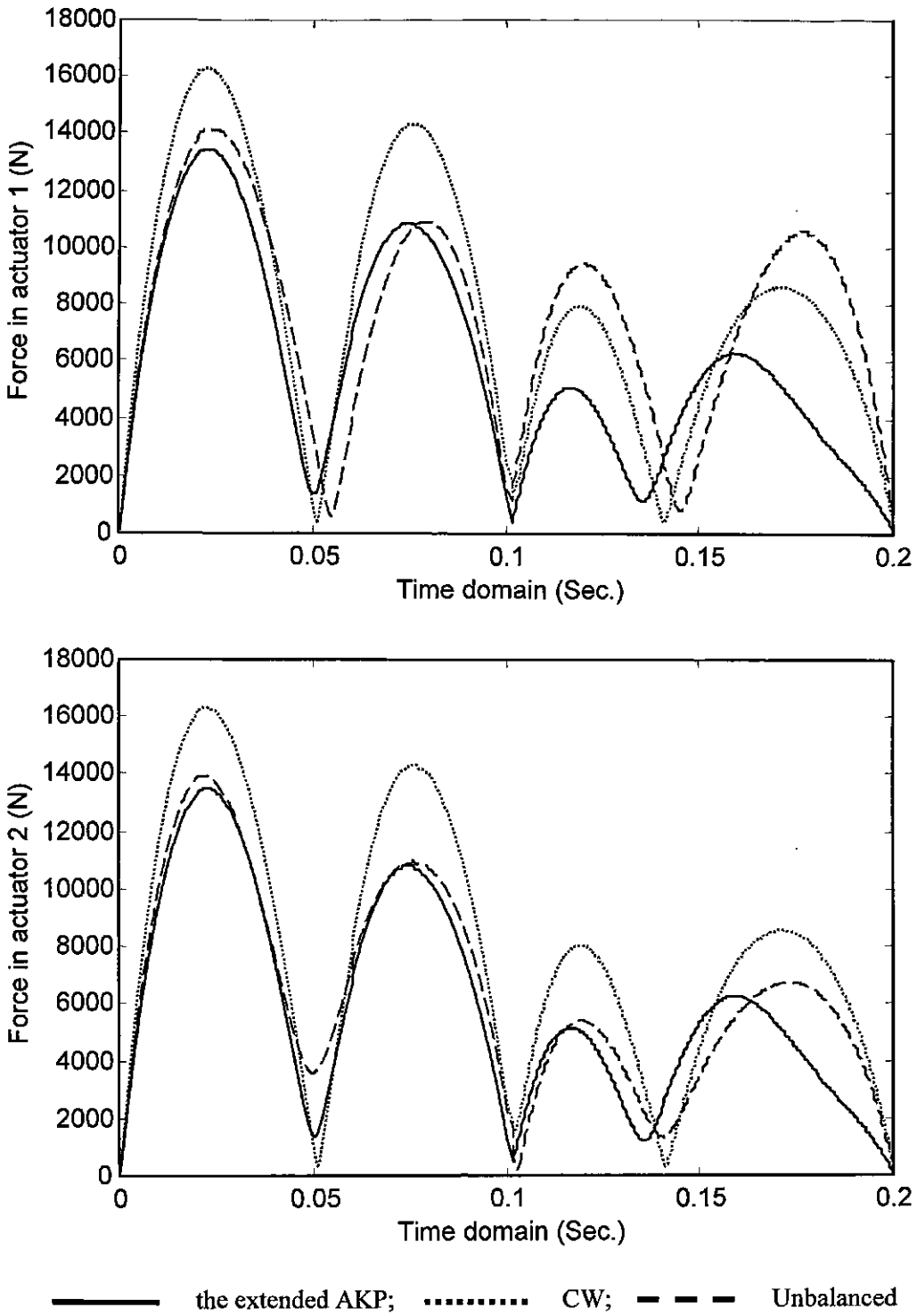

Figure 3.8 Total forces in the two actuators at high speeds

From the force profiles shown in these figures, it can be seen that, in order to accomplish the same motion task, the extended AKP method needs the least amount of forces at both low speeds and high speeds among all the three design cases. The CW method, however, demands the highest forces. The extended AKP method is thus demonstrated to be better than the CW method in terms of the joint force reductions.

3.5 Conclusion

The extended AKP method is developed in this chapter. One of the important contributions of this extension lies in the new idea on the adjustment of two pivots on each link. With this design idea, the original AKP method developed by Wang (2000) can be extended to any planar mechanism with "off-line" mass centers. The derived design equations of the extended method are in the general form, from which the special design case with "in-line" mass centers can be readily derived. Two different configurations for three cases: the force unbalanced mechanism, the force balanced mechanism using the extended AKP method and the CW method, respectively, are studied to demonstrate the effectiveness of the extended AKP method. The joint forces of the individual pivots are calculated at both low speeds and high speeds for these configurations. All the results have shown that the extended AKP method is better than the CW method in terms of the joint force reductions and the variation decrease at high speeds.

CHAPTER 4

KINEMATICS AND TRAJECTORY PLANNING

4.1 Introduction

As pointed out in previous chapters, in order to balance the shaking force of the mechanism using the extended AKP method whilst satisfying the same desired trajectory tracking task, trajectory planning must be performed to adapt to a new setting of kinematic parameters of the mechanism. Since inverse kinematics is the basis of trajectory planning, and kinematics is also the foundation for dynamics and control in an RTC mechanism, the first objective of this chapter is to derive the kinematics of 2 DOF five-bar closed-loop mechanisms. The detailed derivation is presented in Section 4.2. The second objective of this chapter is to develop a new method for trajectory planning, which is presented in Section 4.3. Section 4.4 gives an example to illustrate the effectiveness of the new method, followed by a conclusion in Section 4.5.

4.2 Kinematics of 2 DOF five-bar closed-loop mechanisms

By definition, *kinematics* of a mechanism describes the relationship between the motion of the joints and the motion of the end-effector. Kinematics is classified into forward kinematics and inverse kinematics. In the following discussion, the mechanism used in Chapter 2 will be used here again. For convenience of the readers, the schematic diagram is repeated in Figure 4.1. the methodology for the kinematics of the system shown in Figure 4.1 is straightforward. For the sake of completeness, the kinematic equations are presented in the following.

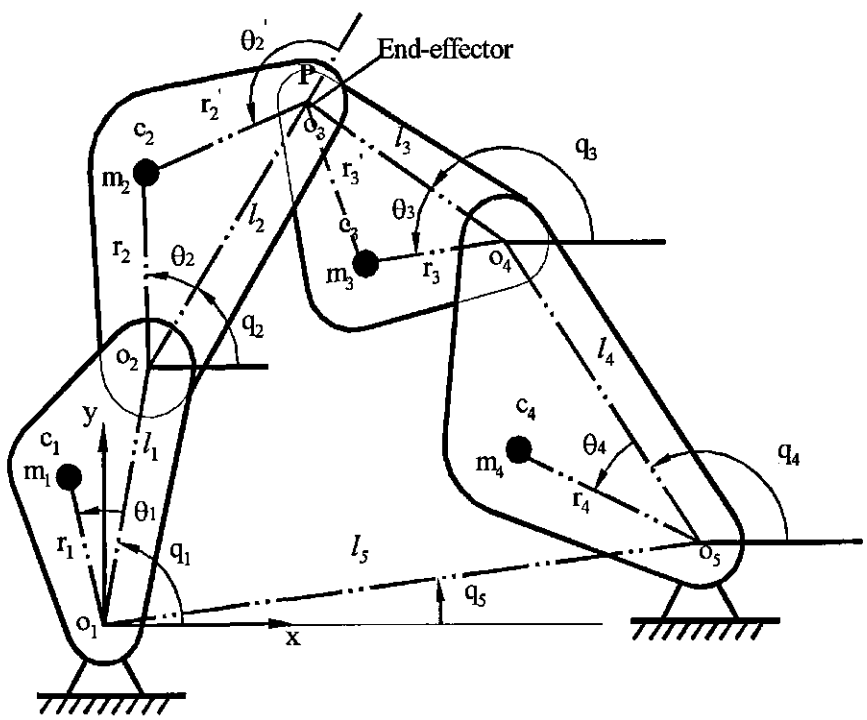

Figure 4.1 Scheme of a 2 DOF closed-loop mechanism

4.2.1 Forward kinematics

Forward kinematics of a mechanism is defined as follows: given a set of joint angles, to compute the position and orientation of the end-effector relative to the base frame. For the 2 DOF closed-loop mechanism shown in Figure 4.1, the end-effect coordinates, x and y, are given as:

$$\begin{cases} x = l_1 \cos q_1 + l_2 \cos q_2 \\ y = l_1 \sin q_1 + l_2 \sin q_2 \end{cases} \tag{4.1a}$$

or

$$\begin{cases} x = l_5 + l_3 \cos q_3 + l_4 \cos q_4 \\ y = l_3 \sin q_3 + l_4 \sin q_4 \end{cases} \tag{4.1b}$$

In Eq. (4.1b), q_5 is assumed to be zero.

In Eq. (4.1), only q_1 and q_4 are independent variables that are the inputs generated by the two actuators. Equating Eq. (4.1a) and Eq. (4.1b) results in the following equations:

$$l_1 \cos q_1 + l_2 \cos q_2 = l_5 + l_3 \cos q_3 + l_4 \cos q_4 \tag{4.2}$$

$$l_1 \sin q_1 + l_2 \sin q_2 = l_3 \sin q_3 + l_4 \sin q_4 \tag{4.3}$$

For any given configuration of the mechanism, the input variables q_1 and q_4, and the kinematic parameters l_1 through l_5 are known. From Eqs. (4.2) and (4.3), the dependent variables q_2 and q_3 can be derived as:

$$q_3 = \tan^{-1}\left[\frac{\pm\sqrt{A^2+B^2-C^2}}{C}\right] + \tan^{-1}\left[\frac{B}{A}\right] \tag{4.4}$$

$$q_2 = \tan^{-1}\left[\frac{\mu + l_4 \sin q_3}{\lambda - l_4 \cos q_3}\right] \tag{4.5}$$

where $\lambda = l_4 \cos q_4 - l_1 \cos q_1 + l_5$, $\mu = l_4 \sin q_4 - l_1 \sin q_1$, $A = 2l_3\lambda$, $B = 2l_3\mu$, and $C = l_2^2 - l_3^2 - \lambda^2 - \mu^2$. The sign "+/-" in Eq. (4.4) corresponds to the two different configurations of the system. For the configuration shown in Figure 4.1, "+" is chosen.

The procedure to compute the forward kinematics can thus be illustrated as follows: given q_1 and q_4, from Eqs. (4.4) and (4.5), q_3 and q_2 can be calculated; from Eqs. (4.1) and (4.2), the coordinates *x*, *y* of the end-effector ***P*** can be determined. Velocities and accelerations of the end-effector can be readily obtained by differentiating the coordinates (*x*, *y*).

4.2.2 Inverse kinematics

Inverse kinematics of a mechanism is defined as follows: given the position and orientation of the end-effector, to calculate all possible sets of joint angles which can make the end-effector attain the given position and orientation. For the 2 DOF closed-loop mechanism shown in Figure 4.1, through the chain formed by link 1 and link 2, the following two equations can be obtained:

$$\begin{cases} l_1 \cos q_1 + l_2 \cos q_2 = x \\ l_1 \sin q_1 + l_2 \sin q_2 = y \end{cases} \tag{4.6}$$

From Eq. (4.6), the following equation can be derived:

$$x^2 + y^2 = l_1^2 + l_2^2 + 2l_1 l_2 \cos(q_1 - q_2) \tag{4.7}$$

Let $\Delta = q_1 - q_2$. From Eq. (4.7), one obtains:

$$\Delta = \cos^{-1}\left(\frac{x^2 + y^2 - l_1^2 - l_2^2}{2l_1 l_2}\right) \tag{4.8}$$

From Eq. (4.8) and Eq. (4.6), one obtains:

$$\begin{cases} x = m_x \cos q_2 - n_x \sin q_2 \\ y = m_y \cos q_2 + n_y \sin q_2 \end{cases} \tag{4.9}$$

From Eq. (4.9), variables q_2 and q_1 can be obtained as:

$$q_2 = \tan^{-1}\left(\frac{ym_x - xm_y}{yn_x + xn_y}\right) \tag{4.10}$$

$$q_1 = q_2 + \Delta \tag{4.11}$$

where $m_x = l_1 \cos\Delta + l_2$, $n_x = l_1 \sin\Delta$, $m_y = n_x$, *and* $n_y = m_x$

With the same procedure as above, the variables q_3 and q_4 can be obtained as:

$$\begin{cases} l_3 \sin q_3 + l_4 \sin q_4 = l_1 \sin q_1 + l_2 \sin q_2 \\ l_3 \cos q_3 + l_4 \cos q_4 = l_1 \cos q_1 + l_2 \cos q_2 - l_5 \end{cases} \tag{4.12}$$

Let $x' = l_1 \cos q_1 + l_2 \cos q_2 - l_5$ and $y' = l_1 \sin q_1 + l_2 \sin q_2$

and

$$\Delta' = \cos^{-1}\left(\frac{x'^2 + y'^2 - l_3^2 - l_4^2}{2 l_3 l_4}\right) \tag{4.13}$$

Substituting Eq. (4.13) into Eq. (4.12), q_3 and q_4 can be derived as:

$$q_3 = \tan^{-1}\left(\frac{y' m_x' - x' m_y'}{y' n_x' + x' n_y'}\right) \tag{4.14}$$

$$q_4 = q_3 + \Delta' \tag{4.15}$$

where $m_x' = l_3 \cos\Delta' + l_4$, $n_x' = l_3 \sin\Delta'$, $m_y' = n_x'$, *and* $n_y' = m_x'$

The angular velocities of all the moving links can be found in the following. Differentiating Eq. (4.6) yields:

$$\begin{cases} l_1 \cos(q_1)\dot{q}_1 + l_2 \cos(q_2)\dot{q}_2 = \dot{y} \\ -l_1 \sin(q_1)\dot{q}_1 - l_2 \sin(q_2)\dot{q}_2 = \dot{x} \end{cases} \tag{4.16}$$

The angular velocities of link 1 and link 2 can be derived from Eq. (4.16) as:

$$\begin{cases} \dot{q}_1 = \dfrac{\dot{y}\sin(q_2) + \dot{x}\cos(q_2)}{l_1 \sin(q_2 - q_1)} \\ \dot{q}_2 = \dfrac{\dot{y}\sin(q_1) + \dot{x}\cos(q_1)}{l_2 \sin(q_1 - q_2)} \end{cases} \tag{4.17}$$

With the same procedure above, the angular velocities of link 3 and link 4 can be derived as:

$$\begin{cases} \dot{q}_3 = \dfrac{\dot{y}\sin(q_4) + \dot{x}\cos(q_4)}{l_3 \sin(q_4 - q_3)} \\ \dot{q}_4 = \dfrac{\dot{y}\sin(q_3) + \dot{x}\cos(q_3)}{l_4 \sin(q_3 - q_4)} \end{cases} \tag{4.18}$$

4.3 A new trajectory planning method

To consider trajectory tracking in the force balanced RTC mechanisms with any method, the CW method or the extended AKP method, the trajectory planning needs to

be performed. The problem of trajectory planning can be stated as follows: given a set of points, see Figure 4.2, where there are five points, i.e., O, A, B, C, and D, the mathematical functions that describe curves between these points are to be determined. In Figure 4.2, points O and D are called *end points*, and points A, B and C called *intermediate points*, and *one segment* is called between any two points.

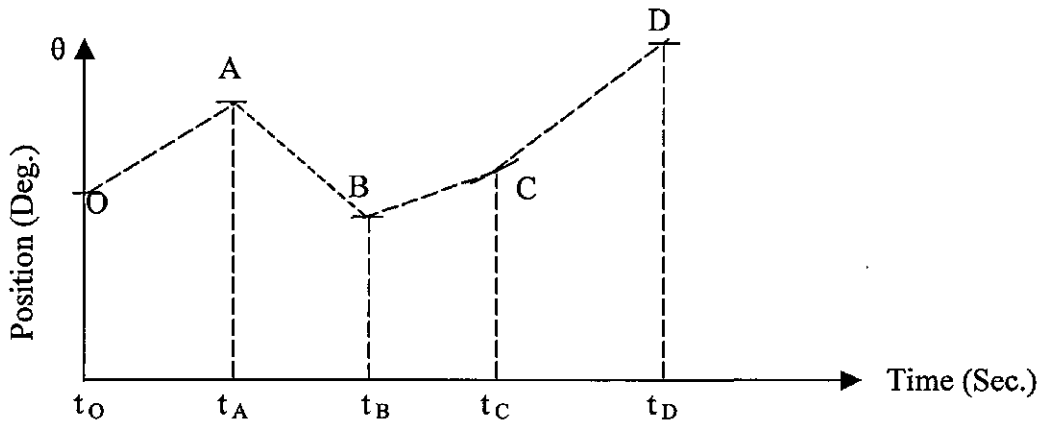

Figure 4.2 Trajectory planning problem definition

It should be noted that though the trajectory planning problem is defined at the end-effector level, the problem can be converted to the one defined at the joint displacement level through inverse kinematics when the flexibility of links is not considered. This thesis does not consider the flexibility of links, and considers trajectory planning at the joint level. The requirement for determining these functions is that the curves expressed by these functions should be of continuity with a certain degree of smoothness at the intermediate points. The smoothness is measured by so-called C^i continuity, which is defined as follows:

Definition 4.1 C^i ***continuity***: If a curve has the *ith* order derivative at an intermediate point, say P, and is continuous, then continuity of the curve at point P is said to be of C^i continuity.

In the applications of RTC mechanisms, C^3 continuity implies that the acceleration is differentiable at the intermediate points, which further implies the derivative of the acceleration (i.e., jerk) at the intermediate points is of continuity. As commented from the literature review discussed in Chapter 2, the studies presented in the literature only achieved at most C^2 continuity. In the following, a method to achieve C^3 continuity is proposed for our applications.

4.3.1 General methodology for determining curves between two points

The general methodology for trajectory planning is to assume a polynomial function to "fit" the desired points, and determine its coefficients. The coefficients are determined based on the prescriptions of the motions at the two end points of a segment. The motions to be prescribed determine the degree of smoothness. For instance, if the position, velocity and acceleration are prescribed at an intermediate point, C^3 continuity can be achieved. Therefore, to achieve C^3 continuity, a quintic polynomial function is assumed and it takes the form as follows:

$$q_{i,i+1}(t) = a_{0i} + a_{1i}t + a_{2i}t^2 + a_{3i}t^3 + a_{4i}t^4 + a_{5i}t^5 \qquad t \in [0, t_i] \tag{4.19}$$

Where $q_{i,i+1}$ is a function defined between point i and point i+1, and its physical meaning is the angular value of a input link. a_{0i} to a_{5i} are the coefficients for the quintic polynomials, and t_i is the time that the input link moves from one end point to the other point within the *i-th* segment. Suppose that positions are prescribed by q_i, q_{i+1} at the two end points of a segment. Their corresponding first derivatives and second derivatives, i.e., velocities and accelerations, are prescribed by $\dot{q}_i$, $\dot{q}_{i+1}$ and $\ddot{q}_i$, $\ddot{q}_{i+1}$, respectively, i.e.:

$$\dot{q}_i = \frac{dq_{i,i+1}(t)}{dt}\Big|t=0, \quad \dot{q}_{i+1} = \frac{dq_{i,i+1}(t)}{dt}\Big|t=t_i$$

$$\ddot{q}_i = \frac{d^2q_{i,i+1}(t)}{dt^2}\Big|t=0, \ \ddot{q}_{i+1} = \frac{d^2q_{i,i+1}(t)}{dt^2}\Big|t=t_i$$

Substituting these prescribed motion conditions (six conditions in total) into Eq. (4.19) will lead to six equations for six coefficients. The coefficients in Eq. (4.19) can be found and expressed as:

$$A_i = LQ \tag{4.20}$$

where $A_i = [a_{5i} \quad a_{4i} \quad a_{3i} \quad a_{2i} \quad a_{1i} \quad a_{0i}]$ and $Q = [q_i \quad q_{i+1} \quad \dot{q}_i \quad \dot{q}_{i+1} \quad \ddot{q}_i \quad \ddot{q}_{i+1}]^T$. The matrix L, which is also called the universal transformation matrix, is represented as:

$$L=\begin{bmatrix} -\frac{6}{t_i^5} & \frac{6}{t_i^5} & -\frac{3}{t_i^4} & -\frac{3}{t_i^4} & -\frac{1}{2t_i^3} & \frac{1}{2t_i^3} \\ \frac{15}{t_i^4} & -\frac{15}{t_i^4} & \frac{8}{t_i^3} & \frac{7}{t_i^3} & \frac{3}{2t_i^2} & -\frac{3}{2t_i^2} \\ -\frac{10}{t_i^3} & \frac{10}{t_i^3} & -\frac{6}{t_i^2} & -\frac{4}{t_i^2} & -\frac{3}{2t_i} & \frac{1}{2t_i} \\ 0 & 0 & 0 & 0 & \frac{1}{2} & 0 \\ 0 & 0 & 1 & 0 & 0 & 0 \\ 1 & 0 & 0 & 0 & 0 & 0 \end{bmatrix} \quad (4.21)$$

The positions, velocities and accelerations at intermediate points may not be provided by applications. In such case, there should be methodologies to determine these quantities.

4.3.2 Determination of velocities at intermediate points

The procedure of determining velocities at intermediate points is as follows. Given an intermediate point, say P_i, examine the average velocities at the left side and the right side of P_i. The average velocity at the left side of P_i is computed by $\vec{V}_{i-1} = \frac{\left|\overrightarrow{P_{i-1}P_i}\right|}{t_{i-1}}$,

where t_{i-1} is the time needed to move from P_{i-1} to P_i. Similarly, the average velocity of the right side of P_i is computed by $\vec{V}_i = \frac{\left|\vec{P_i P_{i+1}}\right|}{t_i}$, where t_i is the time needed to move from P_i to P_{i+1}. After that, if $\vec{V}_{i-1}$ and $\vec{V}_i$ have different signs, the velocity at point P_i is set to zero, i.e., $\vec{V}_i^P$ =0; otherwise $\vec{V}_i^P = (\vec{V}_{i-1} + \vec{V}_i)/2$. For the example shown in Figure 4.2, one can find:

$$\dot{\theta}_x = \dot{\theta}_B = \dot{\theta}_D = 0$$
$$\dot{\theta}_C = \frac{1}{2}\left(\frac{\theta_C - \theta_B}{t_C - t_B} + \frac{\theta_D - \theta_C}{t_D - t_C}\right) \tag{4.22}$$

It should be noted that when the velocity at a particular point is given, the above procedure would not be applied to that point.

4.3.3 Determination of accelerations at intermediate points

The procedure proposed in the following assumes that the accelerations at intermediate points are not prescribed by applications. To make curves be of C^3 continuity, the following conditions should be satisfied:

C^1 : $\dot{q}_{i,i+1}(t_i) = \dot{q}_{i+1,i+2}(0)$ for *i=1, 2, ..., n-1*

C^2: $\ddot{q}_{i,i+1}(t_i) = \ddot{q}_{i+1,i+2}(0)$ for *i=1, 2, ..., n-1*

$$C^3: \quad \ddot{q}_{i,i+1}(t_i) = \ddot{q}_{i+1,i+2}(0) \quad \text{for } i=1, 2, \ldots, n-1$$

where $\dot{q}_{i,i+1}$ means the velocity of the *i-th* segment, $\dot{q}_{i+1,i+2}$ the velocity of the *(i+1)-th* segment. Applying the third condition above to two segments around point $i+1$, one can obtain the following equation from Eqs. (4.19) to (4.21).

$$\begin{aligned} &-\frac{60}{t_i^3}q_i + \frac{60}{t_i^3}q_{i+1} - \frac{24}{t_i^2}\dot{q}_i - \frac{36}{t_i^2}\dot{q}_{i+1} - \frac{3}{t_i}\ddot{q}_i + \frac{9}{t_i}\ddot{q}_{i+1} \\ &= -\frac{60}{t_{i+1}^3}q_{i+1} + \frac{60}{t_{i+1}^3}q_{i+2} - \frac{36}{t_{i+1}^2}\dot{q}_{i+1} - \frac{24}{t_{i+1}^2}\dot{q}_{i+2} - \frac{9}{t_{i+1}}\ddot{q}_{i+1} + \frac{3}{t_{i+1}}\ddot{q}_{i+2} \end{aligned} \tag{4.23}$$

Rearrangement of Eq. (4.23) leads to:

$$\begin{aligned} &t_{i+1}\ddot{q}_i - 3(t_i + t_{i+1})\ddot{q}_{i+1} + t_i\ddot{q}_{i+2} \\ &= -\frac{20t_i}{t_{i+1}^2}(q_{i+2} - q_{i+1}) + \frac{20t_{i+1}}{t_i^2}(q_{i+1} - q_i) + \frac{4t_i}{t_{i+1}}(2\dot{q}_{i+2} + 3\dot{q}_{i+1}) - \frac{4t_{i+1}}{t_i}(2\dot{q}_i + 3\dot{q}_{i+1}) \end{aligned} \tag{4.24}$$

It is usually assumed that the accelerations at two end points of a trajectory (i.e., point 1 and point n), for example, the accelerations of point O and point D (Figure 4.2), are given. From Eq. (4.24), such an equation for every internal point can be derived, and thus linear equations for $\ddot{q}_i$ (i=2 to n-1) can be expressed in Eq. (4.25). From Eq. 4.25), one can compute $\ddot{q}_i$ (i=2 to n-1).

$$
\begin{bmatrix}
-3(t_1+t_2) & t_1 & 0 & 0 & \cdots & \cdots & 0 \\
t_3 & -3(t_2+t_3) & t_2 & 0 & \cdots & \cdots & 0 \\
0 & t_4 & -3(t_3+t_4) & t_3 & & & 0 \\
0 & 0 & \cdots & \cdots & 0 & 0 & 0 \\
0 & \cdots & t_{i+1} & -3(t_i+t_{i+1}) & t_i & \cdots & 0 \\
0 & 0 & \cdots & \cdots & \cdots & & 0 \\
0 & 0 & & & t_{n-1} & & -3(t_{n-1}+t_n)
\end{bmatrix}
\begin{bmatrix}
\ddot{q}_2 \\ \ddot{q}_3 \\ \cdots \\ \\ \ddot{q}_{i+1} \\ \\ \ddot{q}_{n-1}
\end{bmatrix} =
$$

$$
\begin{bmatrix}
-\frac{20t_1}{t_2^2}(q_3-q_2)+\frac{20t_2}{t_1^2}(q_2-q_1)+\frac{4t_1}{t_2}(2\dot{q}_3+3\dot{q}_2)-\frac{4t_2}{t_1}(3\dot{q}_2+2\dot{q}_1)-t_2\ddot{q}_1 \\
-\frac{20t_2}{t_3^2}(q_4-q_3)+\frac{20t_3}{t_2^2}(q_3-q_2)+\frac{4t_2}{t_3}(2\dot{q}_4+3\dot{q}_3)-\frac{4t_3}{t_{21}}(3\dot{q}_3+2\dot{q}_2) \\
-\frac{20t_3}{t_4^2}(q_5-q_4)+\frac{20t_4}{t_3^2}(q_4-q_3)+\frac{4t_3}{t_4}(2\dot{q}_5+3\dot{q}_4)-\frac{4t_4}{t_3}(3\dot{q}_4+2\dot{q}_3) \\
\cdots \\
-\frac{20t_i}{t_{i+1}^2}(q_{i+2}-q_{i+1})+\frac{20t_{i+1}}{t_i^2}(q_{i+1}-q_i)+\frac{4t_i}{t_{i+1}}(2\dot{q}_{i+2}+3\dot{q}_{i+1})-\frac{4t_{i+1}}{t_i}(3\dot{q}_{i+1}+2\dot{q}_i) \\
\cdots \\
-\frac{20t_{n-2}}{t_{n-1}^2}(q_n-q_{n-1})+\frac{20t_{n-1}}{t_{n-2}^2}(q_{n-1}-q_{n-2})+\frac{4t_{n-2}}{t_{n-1}}(2\dot{q}_n+3\dot{q}_{n-1})-\frac{4t_{n-1}}{t_{n-2}}(3\dot{q}_{n-1}+2\dot{q}_{n-2})-t_{n-2}\ddot{q}_n
\end{bmatrix}
\tag{4.25}
$$

4.3.4 Determination of the coefficients of the quintic function

After the velocities and accelerations at the intermediate points on a trajectory are determined, the following equations can be obtained for each segment:

$$\begin{cases} q_i = a_{0i} \\ q_{i+1} = a_{0i} + a_{1i}t_i + a_{2i}t_i^2 + a_{3i}t_i^3 + a_{4i}t_i^4 + a_{5i}t_i^5 \\ \dot{q}_i = a_{1i} \\ \dot{q}_{i+1} = a_{1i} + 2a_{2i}t_i + 3a_{3i}t_i^2 + 4a_{4i}t_i^3 + 5a_{5i}t_i^4 \\ \ddot{q}_i = 2a_{2i} \\ \ddot{q}_{i+1} = 2a_{2i} + 6a_{3i}t_i + 12a_{4i}t_i^2 + 20a_{5i}t_i^3 \end{cases} \tag{4.26}$$

From Eq. (4.26), the coefficients of the quintic polynomials can be found by

$$\begin{cases} a_{0i} = q_i \\ a_{1i} = \dot{q}_i \\ a_{2i} = \dfrac{\ddot{q}_i}{2} \\ a_{3i} = \dfrac{20(q_{i+1} - q_i) - (8\dot{q}_{i+1} + 12\dot{q}_i)t_i - (3\ddot{q}_i - \ddot{q}_{i+1})t_i^2}{2t_i^3} \\ a_{4i} = \dfrac{30(q_i - q_{i+1}) + (14\dot{q}_{i+1} + 16\dot{q}_i)t_i + (3\ddot{q}_i - 2\ddot{q}_{i+1})t_i^2}{2t_i^4} \\ a_{5i} = \dfrac{12(q_{i+1} - q_i) - 6(\dot{q}_{i+1} + \dot{q}_i)t_i - (\ddot{q}_i - \ddot{q}_{i+1})t_i^2}{2t_i^5} \end{cases} \tag{4.27}$$

4.4 Case study

The example is taken from example 1 in Chapter 3. It is assumed that in this example the velocities and accelerations at all the three points of the end-effector are zero. In the following, the methods for trajectory planning, the Cubic polynomials method and the method developed in this chapter, are compared. First of all, the motions at the three points of the end-effector are converted to the motions at the joint level, and this results in:

For point A (0.3, 0.2), q_1 =63.4541, q_4=-13.688, $\dot{q}_1=\dot{q}_4=0$

For point B (0.2, 0.3), q_1 =86.0739, q_4=70.6729, $\dot{q}_1=\dot{q}_4=0$

For point C (0.1, 0.2), q_1 =179.016, q_4=77.2405, $\dot{q}_1=\dot{q}_4=0$

Take actuator 1 for the illustration purpose. Using the new method developed in this chapter, the trajectories for actuator 1 are given as follows:

Angular position for actuator 1:

$$q_1(t) = 63.4541 + 201.7492 \times t^3 - 290.3993 \times t^4 + 111.27 \times t^5 \qquad if \quad t \le 1$$

$$q_1(t) = 86.0739 - 24.4488 \times (t-1)^2 + 152.8515 \times (t-1)^{3^4} - 105.4703 \times (t-1) + 20.4828 \times (t-1)^5 \qquad if \quad 1 < t \le 3$$

Velocity for actuator 1:

$$\dot{q}_1(t) = 605.25 \times t^2 - 1161.60 \times t^3 + 556.35 \times t^4 \qquad if \quad t \le 1$$

$$\dot{q}_1(t) = -48.90 \times (t-1) + 458.55 \times (t-1)^2 - 421.88 \times (t-1)^3 + 102.41 \times (t-1)^4 \qquad if \quad 1 < t \le 3$$

Acceleration for actuator 1:

$$\ddot{q}_1(t) = 1210.50 \times t - 3484.8 \times t^2 + 2225.4 \times t^3 \qquad if \quad t \le 1$$

$$\ddot{q}_1(t) = -48.90 + 917.1 \times (t-1) - 1265.64 \times (t-1)^2 + 409.64 \times (t-1)^3 \qquad if \quad 1 < t \le 3$$

Jerk for actuator 1:

$$\dddot{q}_1(t) = 1210.50 - 6969.6 \times t + 6676.2 \times t^2 \qquad if \quad t \le 1$$

$$\dddot{q}_1(t) = 917.1 - 2531.28 \times (t-1) + 1228.92 \times (t-1)^2 \qquad if \quad 1 < t \le 3$$

Using the Cubic polynomials method, the trajectories for actuator 1 are given as follows:

Angular position for actuator 1:

$$q_1(t) = 63.4541 + 67.8594 \times t^2 - 45.2396 \times t^3 \qquad if \quad t \le 1$$

$$q_1(t) = 86.0739 + 69.707 \times (t-1)^2 - 23.2357 \times (t-1)^3 \qquad if \quad 1 < t \le 3$$

Velocity for actuator 1:

$$\dot{q}_1(t) = 135.7188 \times t - 135.7188 \times t^2 \qquad if \quad t \le 1$$

$$\dot{q}_1(t) = 139.414 \times (t-1) - 69.707 \times (t-1)^2 \qquad if \quad 1 < t \le 3$$

Acceleration for actuator 1:

$$\ddot{q}_1(t) = 135.7188 - 271.4376 \times t \qquad if \quad t \le 1$$

$$\ddot{q}_1(t) = 139.414 - 139.414 \times (t-1) \qquad if \quad 1 < t \le 3$$

Jerk for actuator 1:

$$\dddot{q}_1(t) = -271.4376 \qquad if \quad t \le 1$$

$$\dddot{q}_1(t) = -139.414 \qquad if \quad 1 < t \le 3$$

From the equations above, one can plot the trajectories, which are planned using the two methods above, respectively, see Figure 4.3. From Figure 4.3 it can be seen that using the quintic polynomials the trajectory is smooth at the jerk level, whereas using the cubic polynomials, the acceleration curve is of no continuity at the middle point, which further leads to an infinite jerk at this point.

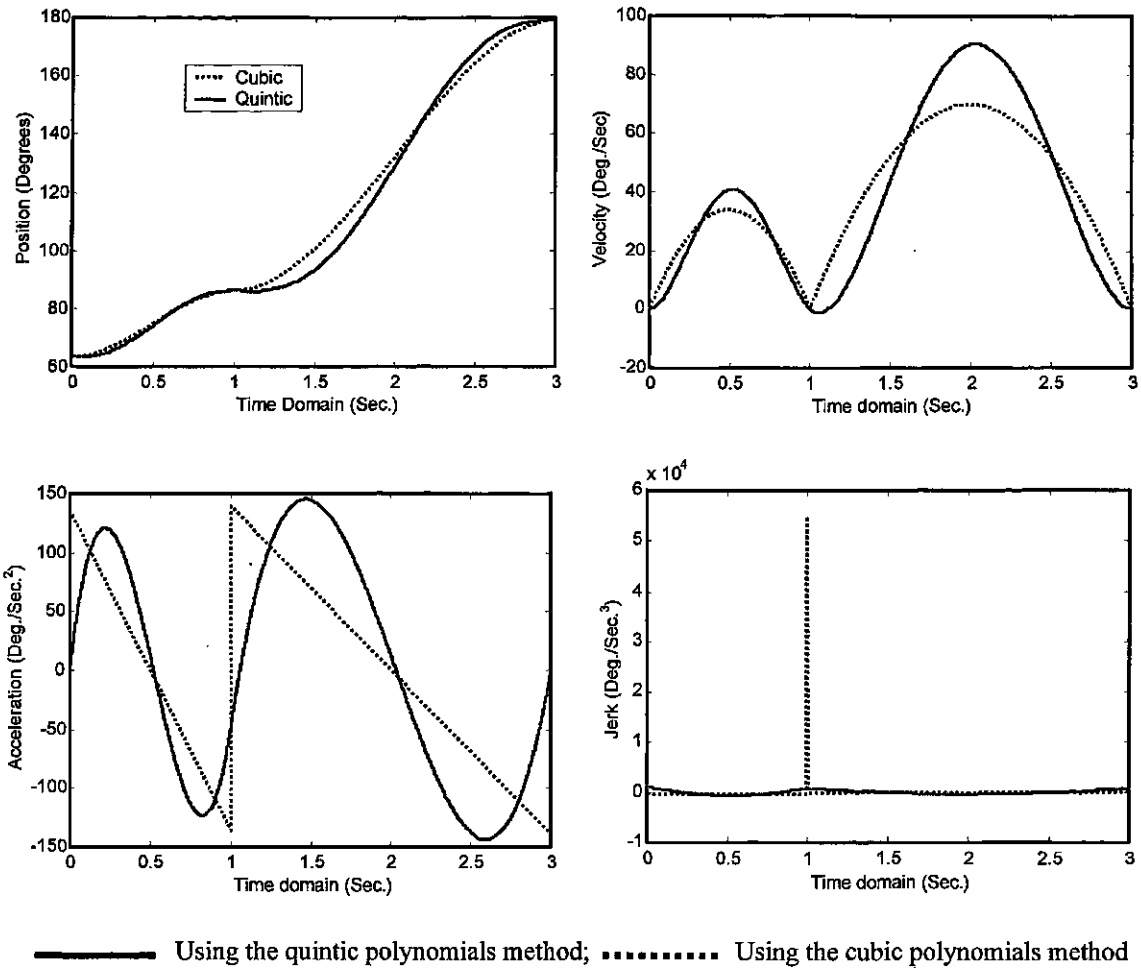

Figure 4.3 Position, velocity, acceleration, and jerk profiles using different tracking planning methods.

4.5 Conclusion

In this chapter, the kinematics of 2 DOF five-bar closed-loop mechanisms is derived, and a new method for trajectory planning is proposed. The new method based on the quintic polynomials for trajectory planning can ensure that the trajectory has a smooth acceleration curve, and therefore there is no infinite jerk on the trajectory, which is the case using quintic polynomials in the AKP method developed by Wang (2000).

CHAPTER 5

DYNAMICS AND CONTROL

5.1 Introduction

The dynamics of RTC mechanisms needs to be thoroughly understood to develop a better controller for achieving optimal trajectory tracking performance. The purpose of this chapter is to develop a dynamic model that describes the dynamical behavior of closed-loop RTC mechanisms. The development of a dynamic model is important in several ways. First, a dynamic model can be used for computer simulation of mechanisms. By examining the dynamic behavior of the model under various operating conditions, it is possible to predict how a mechanism will behave when it is built. Second, it can be used for the development of suitable control strategies. A sophisticated controller requires enough information about a realistic dynamic model to achieve optimal performance. For example, a well-known control method, called *Computed Torque Control* (CTC), requires an accurate dynamic model.

Section 5.2 presents the dynamic model of a 2 DOF closed-loop mechanism using the reduced order method. Section 5.3 discusses PD control law and NPD control law for closed-loop RTC mechanisms, and the stability analysis for PD control. Section 5.4 presents a new control law -- Evolutionary PD (EPD) control law. Section 5.5 is a summary.

5.2 Dynamic model of closed-loop RTC mechanisms

To derive the dynamic model of a 2 DOF closed-loop mechanism, the method called reduced order model (Ghorbel, 1994, 1995) is employed in this thesis. In Ghorbel's studies, the mass center of each link is assumed to be in line with the link axis. In order to deal with a more general situation, i.e., the mass centers of the links are arbitrarily distributed, an extended dynamic model is derived in the following.

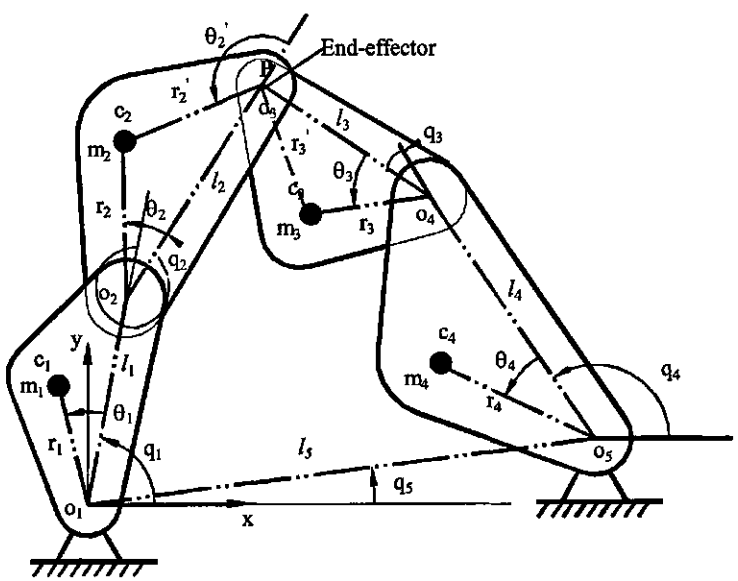

Figure 5.1 A 2 DOF closed-loop mechanism with arbitrary mass distribution

The following discussion is based on Figure 5.1. According to the derivation by Ghorbel (1994, 1995), the dynamic model of the closed-loop mechanism is given as follows:

$$\begin{cases} D(q')\ddot{q} + C(q', \dot{q}')\dot{q} + G(q') = T \\ \dot{q}' = \rho(q')\dot{q} \end{cases} \tag{5.1}$$

where $q = [q_1 \quad q_4]^T$, $q' = [q_1 \quad q_4 \quad q_2 \quad q_3]^T$

$\dot{q} = [\dot{q}_1 \quad \dot{q}_4]^T$, $\dot{q}' = [\dot{q}_1 \quad \dot{q}_4 \quad \dot{q}_2 \quad \dot{q}_3]^T$

$$D(q') = \rho(q')^T D'(q')\rho(q') \tag{5.2}$$

$$C(q', \dot{q}') = \rho(q')^T C'(q', \dot{q}')\rho(q') + \rho(q')^T D'(q')\dot{\rho}(q', \dot{q}') \tag{5.3}$$

$$G(q') = \rho(q')^T G'(q') \tag{5.4}$$

$D'(q')$ represents the inertia matrix of the free system, $C'(q', \dot{q}')$ the Coriolis and centrifugal matrix of the free system, and $G'(q')$ the gravity vector of the free system. According to Appendix A, the expressions for $D'(q')$, $C'(q', \dot{q}')$, and $G'(q')$ can be expressed as follows:

$$D'(q') = \begin{bmatrix} d(1,1) & 0 & d(1,3) & 0 \\ 0 & d(2,2) & 0 & d(2,4) \\ d(3,1) & 0 & d(3,3) & 0 \\ 0 & d(4,2) & 0 & d(4,4) \end{bmatrix} \tag{5.5}$$

where
$$\begin{cases} d(1,1) = m_1 r_1^2 + m_2 (l_1^2 + r_2^2 + 2 l_1 r_2 \cos(q_2 + \theta_2)) + I_1 + I_2 \\ d(1,3) = m_2 (r_2^2 + l_1 r_2 \cos(q_2 + \theta_2)) + I_2 \\ d(2,2) = m_4 r_4^2 + m_3 (l_4^2 + r_3^2 + 2 l_4 r_3 \cos(q_3 + \theta_3)) + I_3 + I_4 \\ d(2,4) = m_3 (r_3^2 + l_4 r_3 \cos(q_3 + \theta_3)) + I_3 \\ d(3,3) = m_2 r_2^2 + I_2 \\ d(4,4) = m_3 r_3^2 + I_3 \\ d(3,1) = d(1,3) \\ d(4,2) = d(2,4) \end{cases}$$

$$C'(q', \dot{q}') = \begin{bmatrix} h_1 \dot{q}_2 & 0 & h_1 (\dot{q}_1 + \dot{q}_2) & 0 \\ 0 & h_2 \dot{q}_3 & 0 & h_2 (\dot{q}_3 + \dot{q}_4) \\ -h_1 \dot{q}_1 & 0 & 0 & 0 \\ 0 & -h_2 \dot{q}_4 & 0 & 0 \end{bmatrix} \tag{5.6}$$

where
$$\begin{cases} h_1 = -m_2 l_1 r_2 \sin(q_2 + \theta_2) \\ h_2 = -m_3 l_4 r_3 \sin(q_3 + \theta_3) \end{cases}$$

$$G'(q') = \begin{bmatrix} m_1 r_1 \cos(q_1 + \theta_1) + m_2 l_1 \cos(q_1) + m_2 r_2 \cos(q_1 + q_2 + \theta_2) \\ m_4 r_4 \cos(q_4 + \theta_4) + m_3 l_4 \cos(q_4) + m_3 r_3 \cos(q_3 + q_4 + \theta_3) \\ m_2 r_2 \cos(q_1 + q_2 + \theta_2) \\ m_3 r_3 \cos(q_3 + q_4 + \theta_3) \end{bmatrix} g \tag{5.7}$$

where g is the gravitational acceleration constant.

The closed-loop mechanism is composed of two open-chains, which introduces two independent scleronomic holomic constraint equations:

$$\phi(q') = \begin{bmatrix} \phi(1) \\ \phi(2) \end{bmatrix} = 0 \tag{5.8}$$

with $$\phi(1) = l_1 \cos q_1 + l_2 \cos(q_1 + q_2) - l_5 - l_3 \cos(q_3 + q_4) - l_4 \cos q_4 \tag{5.9}$$

$$\phi(2) = l_1 \sin q_1 + l_2 \sin(q_1 + q_2) - l_3 \sin(q_3 + q_4) - l_4 \sin q_4 \tag{5.10}$$

Vector q' is the generalized coordinate vector of the free system. Vector q is the generalized coordinate vector of the constrained system. The relationship between q and q' is shown by the following equation:

$$q = \begin{bmatrix} q_1 \\ q_4 \end{bmatrix} = \begin{bmatrix} 1 & 0 & 0 & 0 \\ 0 & 1 & 0 & 0 \end{bmatrix} q' = \alpha(q') \tag{5.11}$$

Define the following quantities:

$$\psi(q') \stackrel{\Delta}{=} \begin{bmatrix} \phi(q') \\ \alpha(q') \end{bmatrix} \text{ and } \psi_{q'}(q') \stackrel{\Delta}{=} \frac{\partial \psi}{\partial q'}$$

From Eqs. (5.9), (5.10) and (5.11), $\psi_{q'}(q')$ can be written as:

$$\psi_{q'}(q') = \begin{bmatrix} \psi(1,1) & \psi(1,2) & \psi(1,3) & \psi(1,4) \\ \psi(2,1) & \psi(2,2) & \psi(2,3) & \psi(2,4) \\ 1 & 0 & 0 & 0 \\ 0 & 1 & 0 & 0 \end{bmatrix} \tag{5.12}$$

Where $\begin{cases} \psi(1,1) = -l_1 \sin(q_1) - l_2 \sin(q_1 + q_2) \\ \psi(1,2) = l_3 \sin(q_3 + q_4) + l_4 \sin(q_4) \\ \psi(1,3) = -l_2 \sin(q_1 + q_2) \\ \psi(1,4) = l_3 \sin(q_3 + q_4) \\ \psi(2,1) = l_1 \cos(q_1) + l_2 \cos(q_1 + q_2) \\ \psi(2,3) = -l_3 \cos(q_3 + q_4) - l_4 \cos(q_4) \\ \psi(2,3) = l_2 \cos(q_1 + q_2) \\ \psi(1,4) = -l_3 \cos(q_3 + q_4) \end{cases}$

From Eq. (5.1), $\rho(q')$ can be expressed as follows:

$$\rho(q') = \psi_{q'}^{-1}(q') \begin{bmatrix} 0_{2\times 2} \\ I_{2\times 2} \end{bmatrix} = \psi_{q'}^{-1}(q') \begin{bmatrix} 0 & 0 \\ 0 & 0 \\ 1 & 0 \\ 0 & 1 \end{bmatrix} \tag{5.13}$$

To find $\rho(q', \dot{q}')$, one needs to differentiate Eq. (5.13), which will involve derivative of an inverse matrix, and this is complex. Pre-multiplying Eq. (5.13) with $\psi_{q'}(q')$ and taking the time derivative, one can obtain:

$$\dot{\rho}(q', \dot{q}') = -\psi_{q'}^{-1}(q') \dot{\psi}_{q'}(q', \dot{q}') \rho(q') \tag{5.14}$$

Where $\dot{\psi}_{q'}(q', \dot{q}')$ is the derivative of $\psi_{q'}(q')$ with respect to time. $\dot{\psi}_{q'}(q', \dot{q}')$ can be written in the following form:

$$\dot{\psi}_{q'}(q',\dot{q}') = \begin{bmatrix} b(1,1) & b(1,2) & b(1,3) & b(1,4) \\ b(2,1) & b(2,2) & b(2,3) & b(2,4) \\ 0 & 0 & 0 & 0 \\ 0 & 0 & 0 & 0 \end{bmatrix} \tag{5.15}$$

where
$$\begin{cases} b(1,1) = -l_1\cos(q_1)\dot{q}_1 - l_2\cos(q_1+q_2)(\dot{q}_1+\dot{q}_2) \\ b(1,2) = l_4\cos(q_4)\dot{q}_4 + l_3\cos(q_3+q_4)(\dot{q}_3+\dot{q}_4) \\ b(1,3) = -l_2\cos(q_1+q_2)(\dot{q}_1+\dot{q}_2) \\ b(1,4) = l_3\cos(q_3+q_4)(\dot{q}_3+\dot{q}_4) \\ b(2,1) = -l_1\sin(q_1)\dot{q}_1 - l_2\sin(q_1+q_2)(\dot{q}_1+\dot{q}_2) \\ b(2,2) = l_4\sin(q_4)\dot{q}_4 + l_3\sin(q_3+q_4)(\dot{q}_3+\dot{q}_4) \\ b(2,3) = -l_2\sin(q_1+q_2)(\dot{q}_1+\dot{q}_2) \\ b(2,4) = l_3\sin(q_3+q_4)(\dot{q}_3+\dot{q}_4) \end{cases}$$

For any given angles of the two input links l_1 and l_4, the angles of the other two links l_2 and l_3 can be obtained as follows:

$$q_3 = \tan^{-1}\left[\frac{\pm\sqrt{A^2+B^2-C^2}}{C}\right] + \tan^{-1}\left[\frac{B}{A}\right] - q_4 \tag{5.16}$$

$$q_2 = \tan^{-1}\left[\frac{\mu + l_3\sin(q_3+q_4)}{\lambda - l_3\cos(q_3+q_4)}\right] - q_1 \tag{5.17}$$

Where
$$\begin{cases} \lambda = l_4\cos(q_4) - l_1\cos(q_1) + l_5 \\ \mu = l_4\sin(q_4) - l_1\sin(q_1) \\ A = 2l_3\lambda \\ B = 2l_3\mu \\ C = l_2^2 - l_3^2 - \lambda^2 - \mu^2 \end{cases}$$

$\dot{q}'$ can be found by the following equation:

$$\dot{q}' = \rho(q')\dot{q} \tag{5.18}$$

But $\dot{q}'$ can also be found by any other way that the velocities of link 2 and link 3 are computed. In the simulation study conducted here, the method presented in Chapter 4 is actually used.

It can be proved that when a closed-loop mechanism is force balanced, one can obtain the following equation:

$$G(q') = \rho^T(q')G'(q') = 0 \tag{5.19}$$

As such, the dynamic model of a force balanced mechanism is represented by

$$D(q')\ddot{q} + C(q', \dot{q}')\dot{q} = T \tag{5.20}$$

It should be noted that the detailed expressions of the items in Eq. (5.20) for the extended AKP method and the CW method are significantly different. This justifies the difference in dynamic performance with these two force balancing methods.

5. 3 PD and NPD control laws

For complex systems like closed-loop mechanisms discussed here, PD or NPD control laws are practically viable. It is important to know the stability of a control law applied to a particular system. In the following, the stability analysis for PD control law for a closed-loop system is presented.

5.3.1 Stability analysis for PD control law for closed-loop mechanisms

For a closed-loop mechanism with n degrees of freedom, the main properties of the dynamics are given as follows (Craig, 1986).

(1) $\dot{D}(q) - 2C(q,\dot{q})$ is a skew-symmetric matrix.

(2) The inertial matrix $D(q)$ is a symmetric positive definite matrix, and there exists positive constants m_1 and m_2 such that

$$m_1 \|x\|^2 \leq x^T D(q) x \leq m_2 \|x\|^2 \tag{5.21}$$

(3) There exists a positive constant k_c such that

$$\|C(x,y)z\| \leq k_c \|y\| \ \|z\| \qquad x,y,z \in R^n \tag{5.22}$$

It can be proved that the closed-loop mechanism considered in this thesis holds the above properties. In the following, a proof is given for property (1) only.

Proof:

Examine the following expression:

$$\begin{aligned}\dot{D}(q')-2C(q',\dot{q}') &= \dot{\rho}^T D'\rho+\rho^T D'\dot{\rho}+\rho^T \dot{D}'\rho-2\rho^T C'\rho-2\rho^T D'\dot{\rho} \\ &= \Delta+\rho^T[\dot{D}'-2C']\rho\end{aligned}$$

where $\Delta=[\dot{\rho}^T D'\rho+\rho^T D'\dot{\rho}-2\rho^T D'\dot{\rho}]$. Because $\Delta^T+\Delta=0$, Δ is skew symmetric.

Note that for a free system that is an open chain, the matrix $\dot{D}'-2C'$ is skew symmetric. This leads that $\rho^T[\dot{D}'-2C']\rho$ is skew symmetric. Therefore, the expression examined, $\dot{D}(q')-2C(q',\dot{q}')$, is skew symmetric since it is the sum of two skew symmetric matrices.

With the help of the properties above, the stability analysis for the mechanism considered in this thesis is presented as follows. First, a lemma is introduced.

Lemma 1 (proof of Lemma 1 was given by Corless, 1990): Consider a dynamic system

$$\dot{x}_1 = f_1(x_1,x_2,t) \tag{5.23}$$

$$\dot{x}_2 = f_2(x_1,x_2,t) \tag{5.24}$$

where $x_1, x_2 \in R^n$. If there exists a Lyapunov function, V, such that

$$\eta_1\|x_1\|^2 + \eta_2\|x_2\|^2 \le V(x_1, x_2) \le \eta_3\|x_1\|^2 + \eta_4\|x_2\|^2 \tag{5.25}$$

$$\dot{V}(x_1, x_2) \le -\eta_5\|x_1\|^2 - \eta_6\|x_2\|^2 + \varepsilon \tag{5.26}$$

where ε and η_i $(i = 1,2,\ldots,6)$ are positive constants.

Define $\delta = \max(\eta_3/\eta_5, \eta_4/\eta_6)$, $r_i = (\delta\varepsilon/\eta_i)^{(1/2)} (i = 1,2)$. For arbitrary initial states $x_1(t_0)$ and $x_2(t_0)$, one can obtain:

$$\|x_1\| \le r_1 + \gamma \exp\left(-\frac{1}{2\delta}(t - t_0)\right) \tag{5.27}$$

$$\|x_2\| \le r_2 + \gamma \exp\left(-\frac{1}{2\delta}(t - t_0)\right) \tag{5.28}$$

where γ is a constant greater than 0, $t \ge t_0$; i.e., $x_1(t)$ and $x_2(t)$ are exponentially convergent to the closed spheres B_{r1} and B_{r2}. r_1 and r_2 are the radiuses of the spheres, respectively.

Theorem. For the closed-loop mechanism studied in this thesis, consider the following PD control scheme:

$$T = K_p e + K_d \dot{e} \tag{5.29}$$

where: $e = q_d - q$, $\dot{e} = \dot{q}_d - \dot{q}$, $e, \dot{e} \in R^2$. If the expected trajectory tracking speed $\dot{q}_d$ and acceleration $\ddot{q}_d$ are bounded, it is guaranteed that e and $\dot{e}$ can be exponentially convergent to the closed spheres with radius r_i (i=1,2). The radius of the spheres can be arbitrarily small when increasing K_p and K_d.

$$K_p = diag(k_{p1}, k_{p2})^T, \quad k_{pi} > 0$$

$$K_d = diag(k_{d1}, k_{d2})^T, \quad k_{di} > 0$$

Proof:

From Eqs. (5.1) and (5.29), the error equation of the system can be written as:

$$D(q')\ddot{e} + C(q', \dot{q}')\dot{e} + K_p e + K_d \dot{e} = D(q')\ddot{q}_d + C(q', \dot{q}')\dot{q}_d + G(q') \tag{5.30}$$

Let $\sigma = D(q')\ddot{q}_d + C(q', \dot{q}')\dot{q}_d + G(q')$. Define a Lyapunov function, V, as

$$V(e, \dot{e}) = \frac{1}{2} e^T K_p e + \frac{1}{2} \dot{e}^T D \dot{e} + \dot{e}^T D f(e) \tag{5.31}$$

where: $f(e) = \dfrac{e}{\alpha + \|e\|} = \beta e, \quad \alpha > 1$

One can proof that $V(e, \dot{e}) > 0$ and satisfies Lemma 1.

Differentiating Eq. (5.31) yields:

$$\begin{aligned}\dot{V}(e,\dot{e}) = &-\dot{e}^T K_d \dot{e} - f(e)^T K_P e - f(e)^T K_d \dot{e} \\ &+ \dot{e}^T D\dot{f}(e) + \dot{e}^T C(q', \dot{q}') f(e) + [\dot{e}^T + f(e)^T]\sigma\end{aligned} \tag{5.32}$$

Because: $\dot{f}(e) = \dfrac{\dot{e}}{\alpha + \|e\|} - \dfrac{e^T \dot{e} e}{(\alpha + \|e\|^2)\ \|e\|}$

Therefore, $\dot{e}^T D\dot{f}(e) \le 2\beta\lambda_{\max}(D)\ \|\dot{e}\|^2$

Where $\lambda_{\max}(\bullet)$ and $\lambda_{\min}(\bullet)$ for the largest and the smallest eigenvalues of a matrix.

Notice the following equation:

$$\sigma = D(q')\ddot{q}_d + C(q', \dot{q}')\dot{q}_d + G(q') \tag{5.33}$$

One can have:

$$\begin{aligned}\|\sigma\| &= \|D(q')\ddot{q}_d + C(q', \dot{q}')\dot{q}_d + G(q')\| \\ &\le \|D(q')\|\ \|\ddot{q}_d\| + \|C(q', \dot{q}')\|\ \|\dot{q}_d\| + \|G(q')\| \\ &\le \|D(q')\|\ \|\ddot{q}_d\| + k_c\|\dot{q}'\|\ \|\dot{q}_d\| + \|G(q')\| \\ &\le \gamma_1 + \gamma_2\|\dot{e}\|\end{aligned} \tag{5.34}$$

where: $\gamma_1 = \sup[\ \|D(q')\|\ \|\ddot{q}_d\| + k_c\|\dot{q}_d\|^2 + \|G(q')\|\ ]$

$$\gamma_2 = \sup(\ k_c\|\dot{q}_d\|\ )$$

Using Eq. (5.22), one can obtain:

$$\begin{aligned}\dot{e}^T C(q',\dot{q}')f(e) &= \dot{e}^T C(q',\dot{e}-\dot{q}_d)f(e) \\ &\le \beta \sup(\ k_{c1}\|\dot{q}_d\|\ )\ \|e\|\ \|\dot{e}\| + k_{c2}\|\dot{e}\|^2 \\ &= \beta\gamma_3\|e\|\ \|\dot{e}\| + \gamma_4\|\dot{e}\|^2\end{aligned} \tag{5.35}$$

Hence,

$$\begin{aligned}\dot{V}(e,\dot{e}) = &-[\lambda_{\min}(K_d) - 2\beta\lambda_{\max}(D) - \gamma_2 - \gamma_4]\ \|\dot{e}\|^2 + \gamma_1\|\dot{e}\|^2 \\ &- \beta\lambda_{\min}(K_p)\ \|e\|^2 + \beta\gamma_1\|e\| + \beta[\lambda_{\max}(K_d) + \gamma_2 + \gamma_3]\ \|e\|\ \|\dot{e}\|\end{aligned} \tag{5.36}$$

Define:

$$\gamma_5 = 2\beta\lambda_{\max}(D) + \gamma_2 + \gamma_4 \tag{5.37}$$

$$\gamma_6 = 2\beta\lambda_{\max}(K_d) + \gamma_2 + \gamma_3 \tag{5.38}$$

If K_d is sufficiently large such that $\lambda_{\min}(K_d) - \gamma_5 > 0$, and since

$$\|e\|\ \|\dot{e}\| \le \frac{1}{2}(\ \|e\|^2 + \|\dot{e}\|^2\ ) \tag{5.39}$$

Therefore,

$$\begin{aligned}\dot{V}(e,\dot{e}) = &-[\lambda_{\min}(K_d) - \gamma_5 - \frac{1}{2}\beta\gamma_6]\ \|\dot{e}\|^2 \\ &- \beta[\lambda_{\min}(K_p) - \frac{1}{2}\gamma_6]\ \|e\|^2 + \gamma_1\|\dot{e}\| + \beta\gamma_1\|e\|\end{aligned} \tag{5.40}$$

If K_p and K_d are sufficiently large, we have

$$\lambda_{\min}(K_d) - \gamma_5 - \frac{1}{2}\beta\gamma_6 > 0 \tag{5.41}$$

$$\lambda_{\min}(K_p) - \frac{1}{2}\gamma_6 > 0 \tag{5.42}$$

Also, due to the following inequalities,

$$\begin{aligned} &\gamma_1\|\dot{e}\| - [\lambda_{\min}(K_d) - \gamma_5 - \frac{1}{2}\beta\gamma_6]\ \|\dot{e}\|^2 \\ &\le \frac{\gamma_1^2}{\lambda_{\min}(K_d) - \gamma_5 - \frac{1}{2}\beta\gamma_6} - \frac{1}{4}[\lambda_{\min}(K_d) - \gamma_5 - \frac{1}{2}\beta\gamma_6]\ \|\dot{e}\|^2 \end{aligned} \tag{5.43}$$

and

$$\begin{aligned} &\gamma_1\|e\| - [\lambda_{\min}(K_p) - \frac{1}{2}\gamma_6]\ \|e\|^2 \\ &\le \frac{\gamma_1^2}{\lambda_{\min}(K_p) - \frac{1}{2}\gamma_6} - \frac{1}{4}[\lambda_{\min}(K_d) - \frac{1}{2}\gamma_6]\ \|e\|^2 \end{aligned} \tag{5.44}$$

Finally, one can obtain:

$$\begin{aligned} \dot{V}(e,\dot{e}) \le &-\frac{1}{4}[\lambda_{\min}(K_d) - \gamma_5 - \frac{1}{2}\beta\gamma_6]\ \|\dot{e}\|^2 - \frac{1}{4}[\lambda_{\min}(K_d) - \frac{1}{2}\gamma_6]\ \|e\|^2 \\ &+ \frac{\gamma_1^2}{\lambda_{\min}(K_d) - \gamma_5 - \frac{1}{2}\beta\gamma_6} + \frac{\gamma_1^2}{\lambda_{\min}(K_p) - \frac{1}{2}\gamma_6} \end{aligned} \tag{5.45}$$

Due to Lemma 1, it can be assured that e and $\dot{e}$ are exponentially convergent to the closed spheres with radius r_i (i=1,2), respectively, i.e.,

$$\lim_{t\to\infty}|e_j| < r_1 \text{ and } \lim_{t\to\infty}|\dot{e}_j| < r_2 \text{ for } j = 1,2$$

The radius of the sphere, r_1 and r_2, are arbitrarily small when increasing K_p and K_d.

5.3.2 NPD control law

A NPD controller can result in superior point-set tracking and disturbance rejection performances compared to the linear fixed-gain PD controller. Past and recent studies have shown that the NPD control can provide increased damping, reduced rise time for step or rapid inputs, improved tracking accuracy, and friction compensation.

A NPD control law may be any control structure of the form:

$$\mathbf{T}(t) = \mathbf{K}_p(\cdot)\mathbf{e}(t) + \mathbf{K}_d(\cdot)\dot{\mathbf{e}}(t) \tag{5.46}$$

where $\mathbf{T}(t)$ is the driving torque vector generated by the controller; $\mathbf{K}_p(\cdot)$ and $\mathbf{K}_d(\cdot)$ are the time-varying proportional and derivative gain matrices.

The NPD control enables the controller to adapt to its response by changing the gains. When the error between the desired and actual values of the controlled variables is large, the gain amplifies the error substantially to generate a large corrective action to rapidly drive the system to its goal. As the error diminishes, the gain is automatically

reduced to avoid excessive oscillations and large overshoots in the response. The NPD control enjoys advantages over the fixed-gain PD control in terms of disturbance rejection. Another merit with the NPD control is its less sensitive to delays than fixed-gain PD control.

The nonlinear gain function for the NPD control in Eq. (5.46) is not unique. In our study, the following functions of the nonlinear gains are used

$$\begin{aligned} \mathbf{K}_p &= \mathbf{K}_{p0} * \mathbf{K}(t) \\ \mathbf{K}_d &= \mathbf{K}_{d0} * \mathbf{K}(t) \end{aligned} \tag{5.47}$$

where $K(t) = K_{\max} - K_{\min} sech(alf * e(t))$. $K_{\max}$, $K_{\min}$, and alf are user-defined positive constants.

5.4 Evolutionary PD control law

Although the previous discussion in Section 5.3.1 proved that the PD controller can assure the global stability for the closed-loop mechanism. There are the following problems with the fixed-gain PD control method. First, it is not easy to find a suitable control gain. Second, the increase of the control gain may cause the oscillation of the required torques in actuators, which is harmful to the actuators. A novel PD-oriented control method called the Evolutionary PD (EPD) controller is proposed.

The main idea of the EPD control is to answer the questions of how to incorporate the information of plant dynamics into a PD-based control law. This leads to the formulation of a PD-based control law as follows:

$$T = K_p e + K_d \dot{e} + \tilde{T} \tag{5.48}$$

where $\tilde{T}$ is a function of plant dynamics.

In order to incorporate our idea (i.e., incorporating plant dynamics into a PD-based control law), either K_p, K_d or $\tilde{T}$ should be related to plant dynamics. It is easy to see here that the NPD control method can be viewed as incorporating plant dynamics with the gains K_p and K_d. In the following, a scheme that makes $\tilde{T}$ incorporating plant dynamics is proposed. The scheme can be generally expressed by the following equation:

$$T_i^j = K_p e_i + K_d \dot{e}_i + T_i^{j-1} \tag{5.49}$$

where j means the $j-th$ generation, $j = 1,2,\ldots,m$; i means the $i-th$ time step, $i = 1,2,\ldots,n$. Eq. (5.49) implies: $\tilde{T} = T^{j-1}$, which means the torque profile in the actuators for the previous run or generation.

The scheme will start with $j = 1$, in this case, T_i^0 is set to zero, which means at the first run, the control method is just the fixed-gain PD method. The scheme will end when the

improvement of system performance is not significant, which can numerically be controlled by a prescribed small positive number, say ε. The verification of the EPD is given in Chapter 6 based on simulation.

5.5 Summary and discussion

The dynamic analysis of a 2 DOF closed-loop mechanism is addressed in this chapter. The analysis of the position, velocity, and dynamic model based on the reduced order model is performed. Stability analysis for the fixed-gain control law applied to the closed-loop mechanism system is discussed, which shows that the PD controller can guarantee the global stability for trajectory tracking.

The NPD control method is introduced. The NPD control method can be viewed as incorporating plant dynamics in a control law because the gains are adjusted based on the error of the trajectory tracking which reflects plant dynamics. Along this line of thinking and also inspired by the CTC approach, a new PD-based control method called Evolutionary PD control method is developed, which shows promising at this point. Simulation will be performed to verify this new control method in next chapter.

CHAPTER 6

RESULTS AND DISCUSSION

6.1 Introduction

In this chapter, several case studies for closed-loop RTC mechanisms are presented to demonstrate the validity and effectiveness of the AKP method in terms of trajectory tracking performance. Furthermore, different control laws (i.e., PD control, NPD control, and EPD control) are applied to these cases in order to see the effects on different force balancing methods. It should be noted that in Chapter 3, the benefit of the extended AKP method over the CW method was demonstrated in terms of joint reaction forces. The results and discussion in this chapter will therefore provide a complete picture of the benefits of the extended AKP method over the CW method. In Section 6.2, trajectory tracking performances between the extended AKP method and the CW method are compared using conventional PD control law and NPD control law. Section 6.3 presents the comparison results based on EPD control law for the extended AKP method and the CW method. Section 6.4 gives a conclusion.

6.2 PD and NPD control laws: results and discussion

The closed-loop RTC mechanism shown in Figure 2.1 is used as an example. The parameters of the mechanism under different situations are listed in Table 6.1, while the unbalanced case describes the original mechanism that is unbalanced, the CW case shows the parameters of the force balanced mechanism using the CW method, and the AKP case shows the parameters of the force balanced mechanism using the extended AKP method. From Table 6.1, one can see that both the kinematic parameters and the inertias of the mechanism of the AKP case are significantly different from those of the CW case.

Table 6.1 Parameters for different mechanisms (in-line case 2)

Parameters	Unbalanced Case	CW Case	AKP Case
l_1 (m)	0.2	0.2	0.1
l_2 (m)	0.3	0.3	0.3
l_3 (m)	0.4	0.4	0.24
l_4 (m)	0.3	0.3	0.1
l_5 (m)	0.3	0.3	0.3
r_1 (m)	0.05	0.05	0.05
r_2 (m)	0.15	0.15	0.15
r_3 (m)	0.08	0.1	0.08
r_4 (m)	0.1	0.1875	0.1
m_1 (kg)	0.25	0.5	0.25
m_2 (kg)	0.25	0.25	0.25

m_3(kg)	0.375	0.5	0.375
m_4(kg)	0.5	1.0	0.5
$I_1(kg \cdot m^2)$	0.004	0.01	0.004
$I_2(kg \cdot m^2)$	0.01	0.01	0.01
$I_3(kg \cdot m^2)$	0.02	0.035	0.02
$I_4(kg \cdot m^2)$	0.02	0.038	0.02
$\theta_1(rad)$	0	π	π
$\theta_2(rad)$	0	0	0
$\theta_3(rad)$	0	π	π
$\theta_4(rad)$	0	π	π

A desired set of points that the end-effector is requested to pass is given in Table 6.2, where the initial conditions at these points are as follows: (i) velocities and accelerations at points A and E are zero, (ii) the velocities at B, C, and D are not prescribed, and (iii) the accelerations at B, C, and D are not prescribed.

Table 6.2 The coordinates of the via points of the end-effector

Coordinate value	A	B	C	D	E
X axis (m)	0.35	0.30	0.25	0.15	0.04
Y axis (m)	0.15	0.20	0.25	0.20	0.20

Using the inverse kinematics of the mechanism, one can find the five angular positions corresponding to actuators 1 and 2, respectively. The trajectories can be then planned

over these five positions using the trajectory planning method described in Chapter 4, and the results are shown in Figure 6.1.

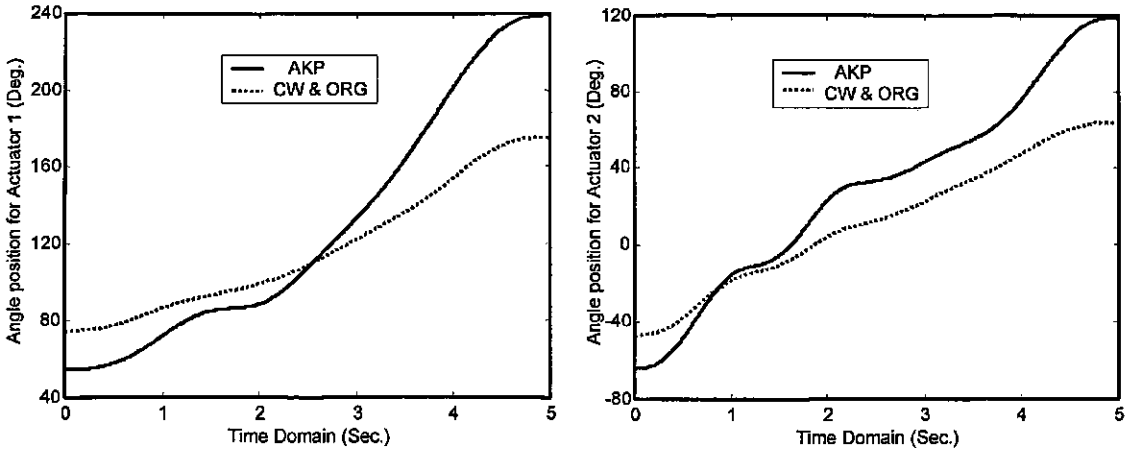

Note: The trajectories of the two actuators at high speeds have the same shape except the time domain changed to the range of [0 0.2].

Figure 6.1 The planned trajectories of two actuators at low speeds

From Figure 6.1, it can be seen that the trajectories are not the same for the mechanism using the extended AKP method and the CW method. It should be noted that the motion range using the extended AKP method is larger than that using the CW method, which means that the average velocity of the AKP case is bigger than that of the CW case, and that of the unbalanced case. In the following, the trajectory tracking performances under two operating conditions, i.e., low speeds and high speeds, are compared using the extended AKP method and using the CW method. On a general note, a particular scheme for implementing the CW method on the mechanism system concerned is obtained through a manual selection procedure for optimal performance, while an arbitrary selection of schemes for the extended AKP method is made.

6.2.1 Case 1: Trajectory tracking performance at low speeds

In this case, the time spans between any two neighboring points are, respectively, 1.25 Sec., 1.0 Sec., 1.25 Sec., and 1.5 Sec. The average angular velocities of both actuators are lower than 6 rpm.

Via trail and error, matrix $\mathbf{K}_P$ is selected to be diagonal with the first element 600 and the second 750. Matrix $\mathbf{K}_D$ is also selected to be diagonal with the first element 78 and the second 96. The simulation results are illustrated in Figure 6.2, where the solid lines indicate the results of the AKP case, the dotted lines indicate the results of the CW case, and the dashed lines represent the results of the unbalanced case.

From Figure 6.2, it can be seen that when the mechanism runs at low speeds, the force balanced mechanism, using either the CW method or the extended AKP method, have better trajectory tracking performance. The improvement in trajectory tracking performance includes: (i) reduced trajectory tracking error, (ii) reduced torques in actuators, and (iii) smaller fluctuations of torques in actuators. It should also be noted that in all aspects of trajectory tracking performances, the results using the extended AKP method is better than those using the CW method.

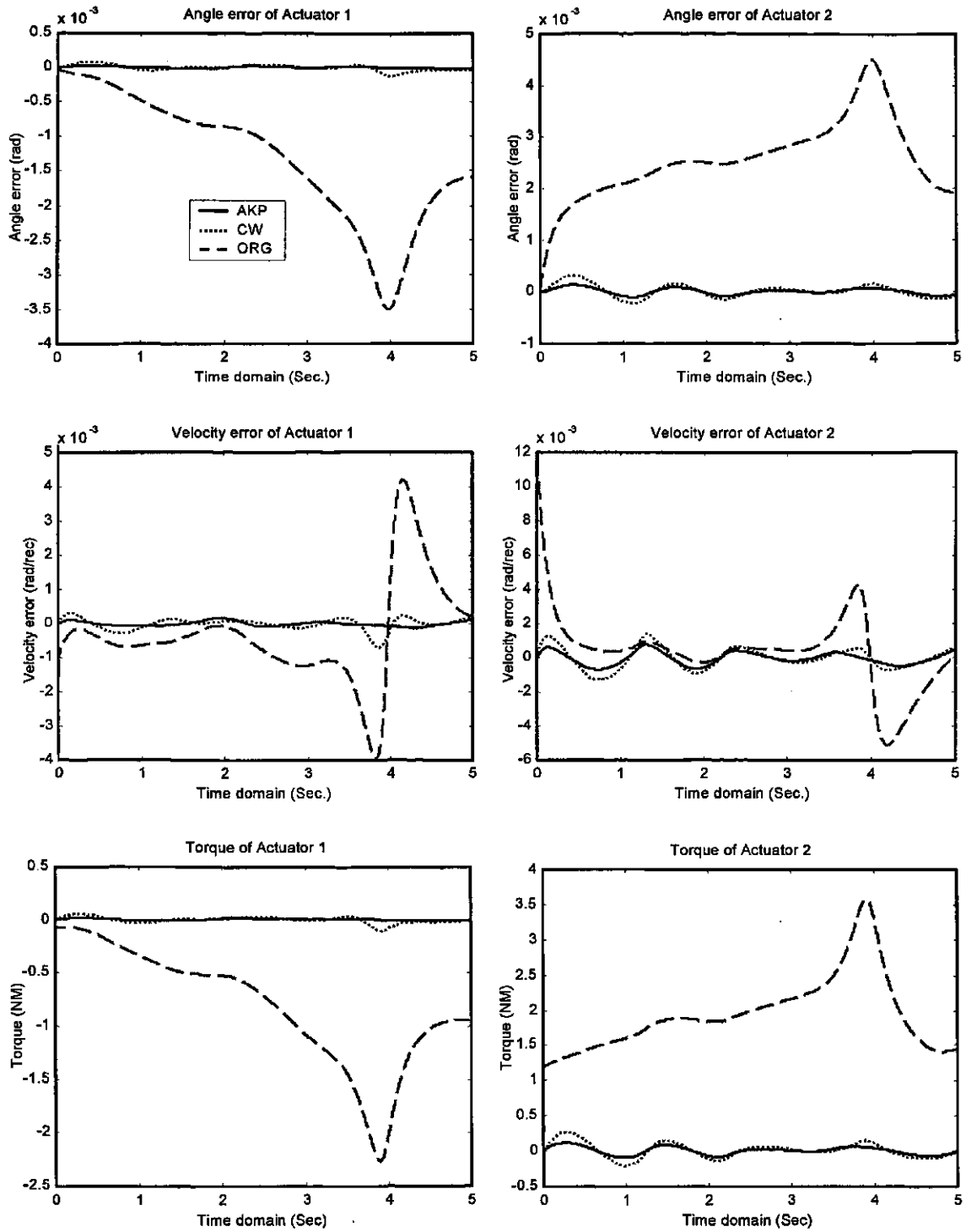

Note: In all the diagrams, the solid lines represent the AKP case; the dotted lines represent the CW case; and the dashed lines represent the original case (ORG).

Figure 6.2 Trajectory tracking performances at low speeds

6.2.2 Case 2: Trajectory tracking performance at high speeds

In this case, the time spans between any two neighboring points are, respectively, 0.05 Sec., 0.04 Sec., 0.05 Sec., and 0.06 Sec. The average angular velocities of both actuators are about 100 rpm.

Via trail and error, matrix $\mathbf{K}_P$ is selected to be diagonal with the first element 2000 and the second one 2500. Matrix $\mathbf{K}_D$ is also selected to be diagonal with the first element 500 and the second one 700. The simulation results are illustrated in Figure 6.3.

From Figure 6.3, it can be seen that the performance of the AKP method is the best among the three cases. The position errors and velocity errors of two actuators using the extended AKP method are the smallest. Moreover, the position control using the extended AKP method is the best at each desired via point. It should be noticed that the performance using the CW method is poorer than that of the unbalanced case. This means that when the mechanism runs at high speeds, the force balanced mechanism using the CW method would degrade the trajectory tracking performance of the mechanism. This phenomenon may be explained as follows: When the CW method is used, both the mass and the inertia of the system are increased. The increase of mass and inertia means the increase of the inertia forces of the links. The higher the velocity and the acceleration of the mechanism, the bigger the inertia forces, and thus the more likely the errors occur in the tracking.

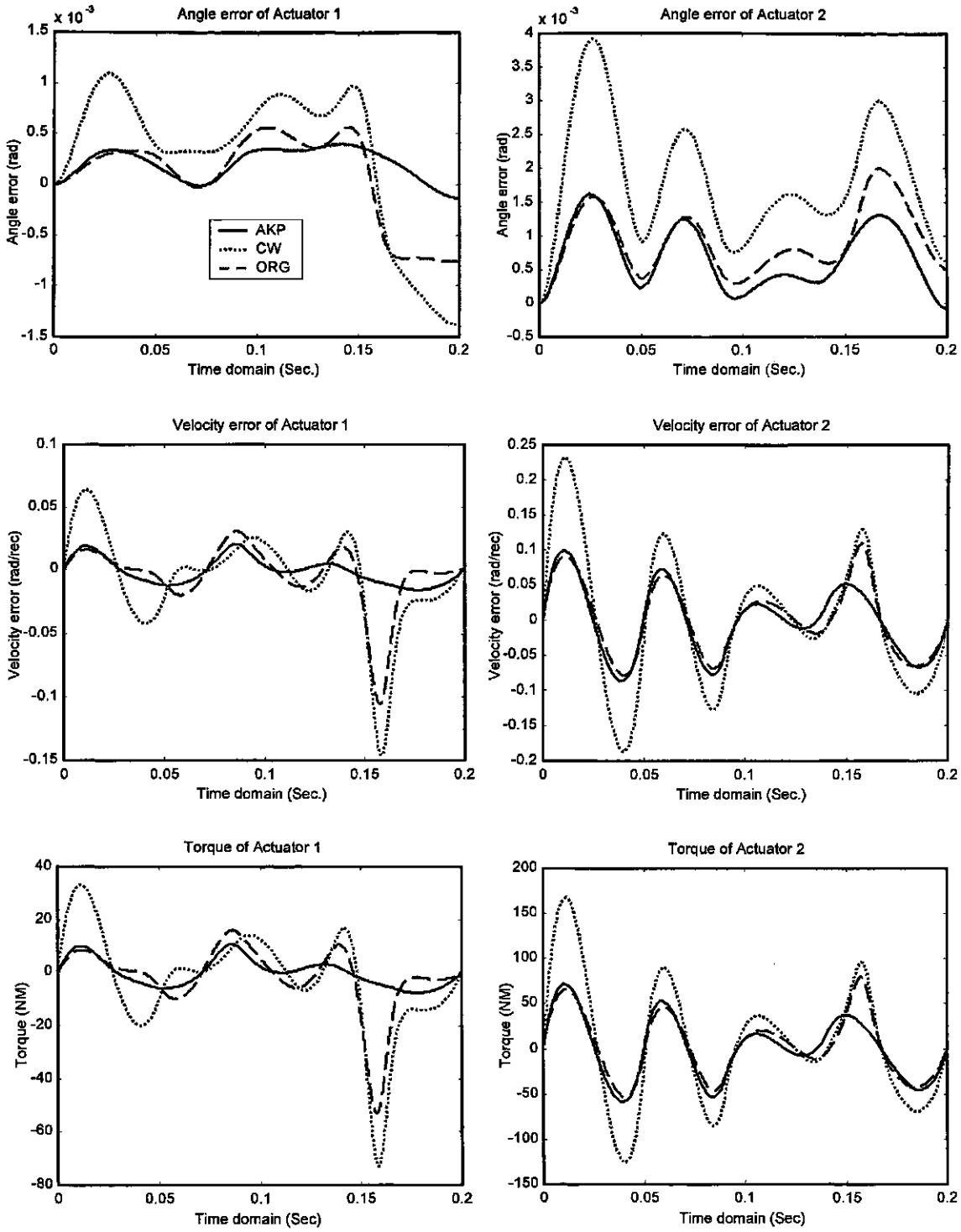

Note: In all the diagrams, the solid lines represent the AKP case; the dotted lines represent the CW case; and the dashed lines represent the original case (ORG).

Figure 6.3 Trajectory tracking performances at high speeds

It is interesting to compare Figure 6.2 with Figure 6.3, which leads to the observation that with the increase of the velocities in the actuators, the tracking position errors will increase for all three cases, but the increase of the tracking position errors using the CW method is the most considerable among the three cases.

6.2.3 Effects using NPD control law

The nonlinear gains of the NPD controller are selected as follows:

$$\begin{aligned} K_1(t) &= 3 - 2sech(alf_1 e_1(t)) \\ K_2(t) &= 3 - 2sech(alf_2 e_2(t)) \end{aligned} \tag{6.2}$$

where alf_1 and alf_2 are user-defined positive constants.

From the above equations, one can see that K_1 and K_2 may vary from *1* through *3*. It can also be seen that when alf_1 and alf_2 are set to zero, K_1 and K_2 will be 1, and an NPD controller will reduce to a PD controller. To examine how the NPD controller works, a simulation study on the same mechanism as used before (Its parameters are listed in Table 6.1) is performed. The user-defined positive constants are selected as follows:

For low speeds:

alf_1=5000, alf_2=2000

For high speeds:

alf_1=50000, alf_2=20000

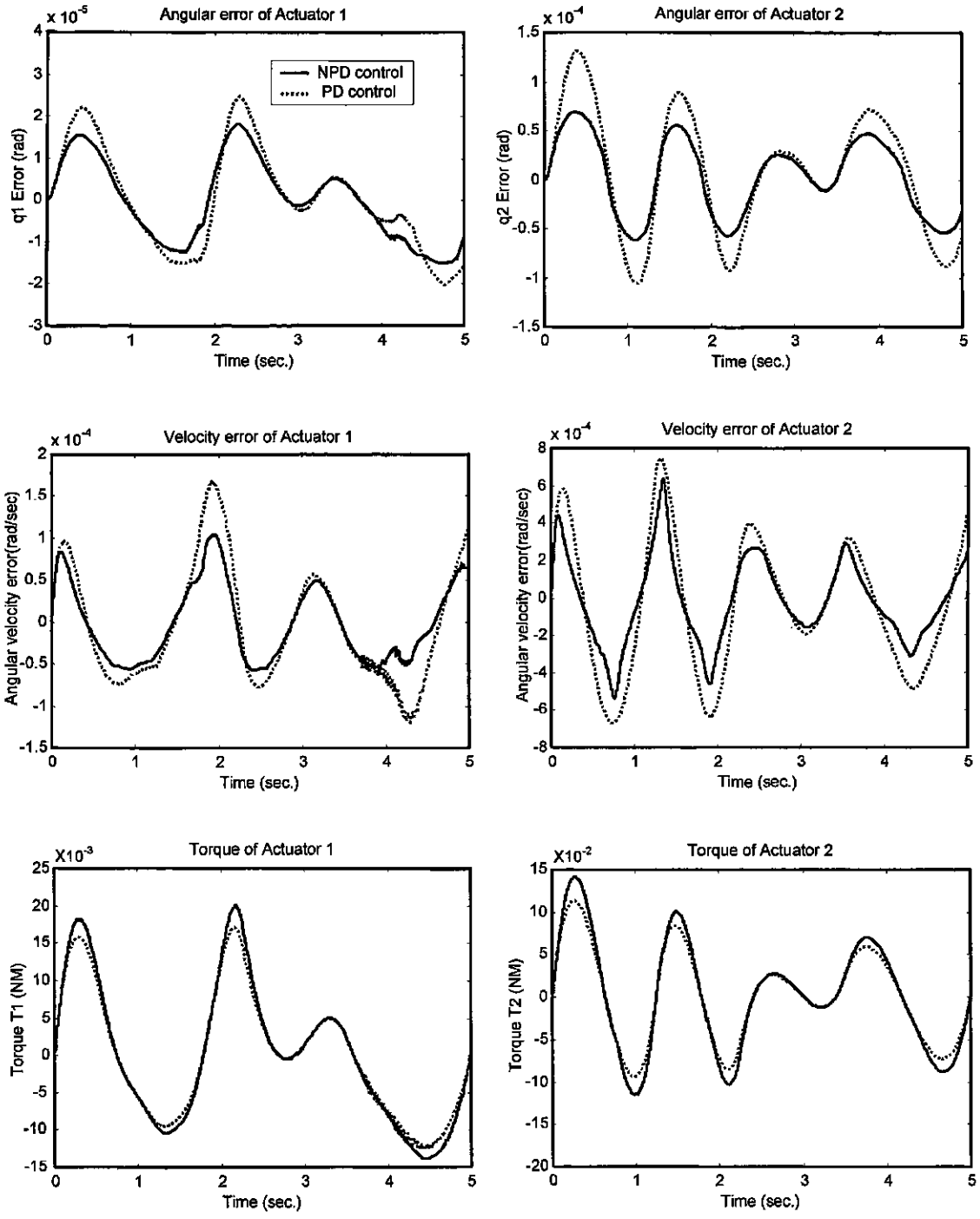

Note: Solid lines: NPD control law; Dotted line: PD control law.

Figure 6.4 Comparison of performance under PD/NPD controllers using the extended AKP method at low speeds

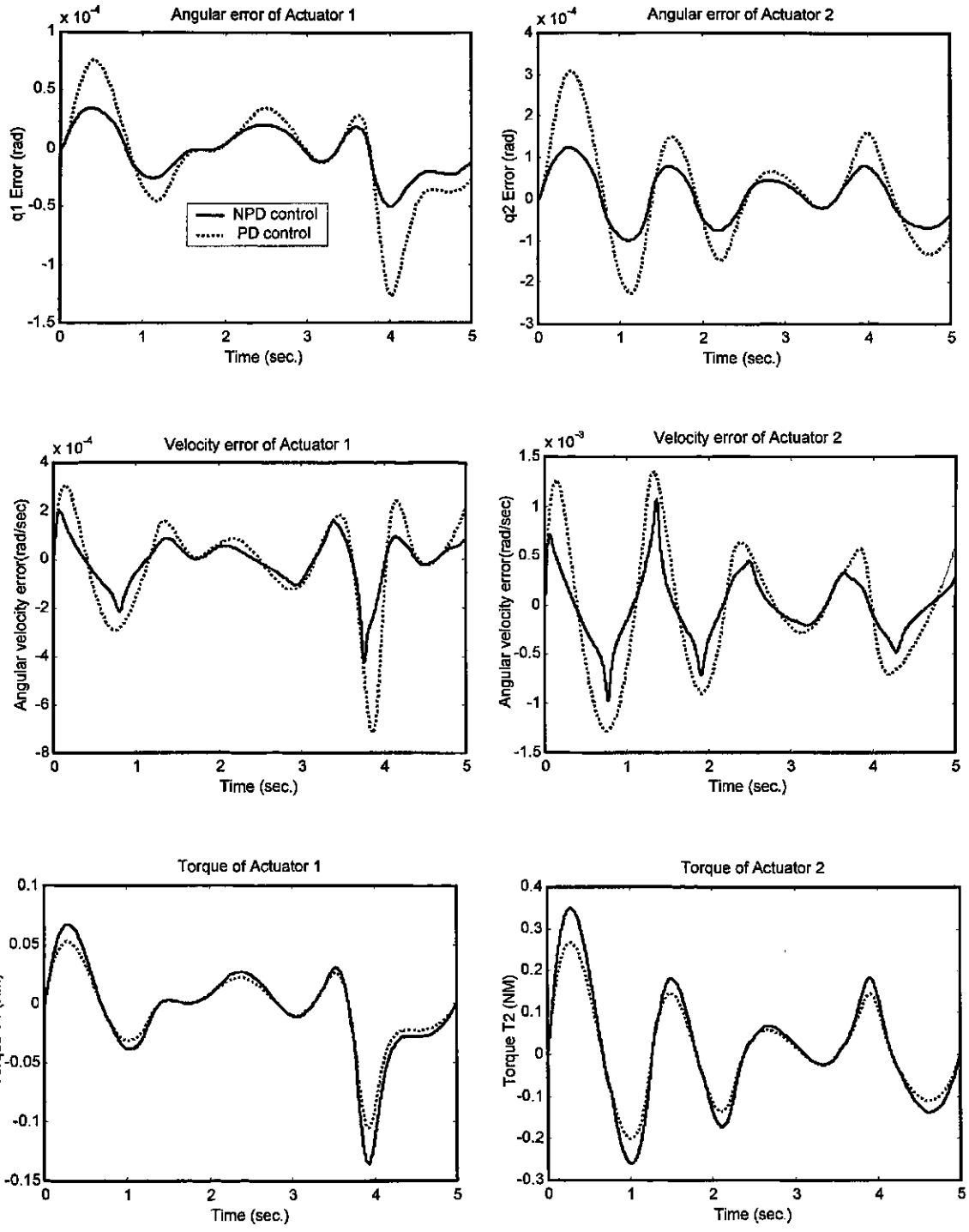

Note: Solid lines: NPD control law; Dotted line: PD control law.

Figure 6.5 Comparison of performance under PD/NPD controllers using the CW method at low speeds

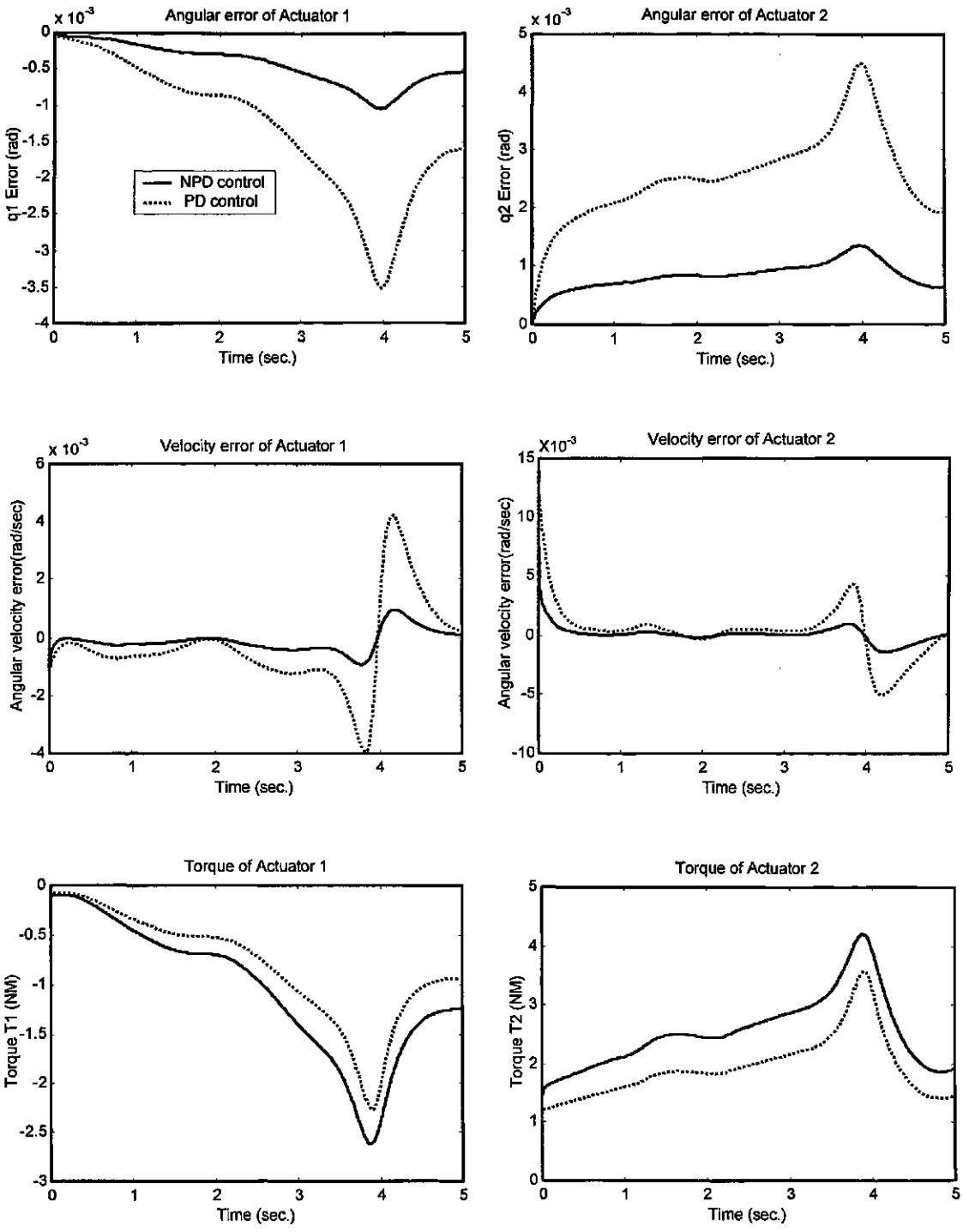

Note: Solid lines: NPD control law; Dotted line: PD control law.

Figure 6.6 Comparison of performance for the unbalanced mechanism under PD/NPD controllers at low speeds

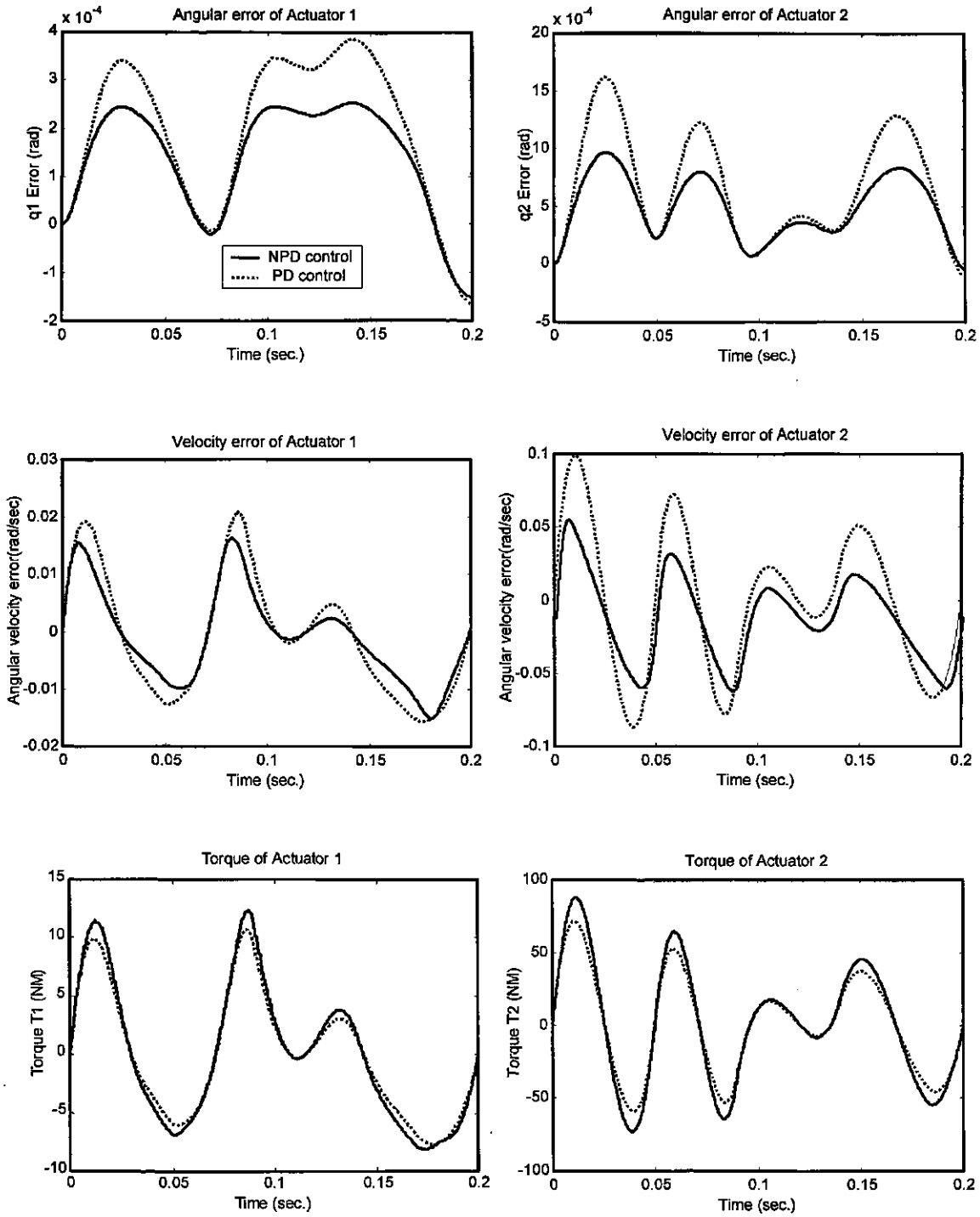

Note: Solid lines: NPD control law; Dotted line: PD control law.

Figure 6.7 Comparison of performance under PD/NPD controllers using the extended AKP method at high speeds

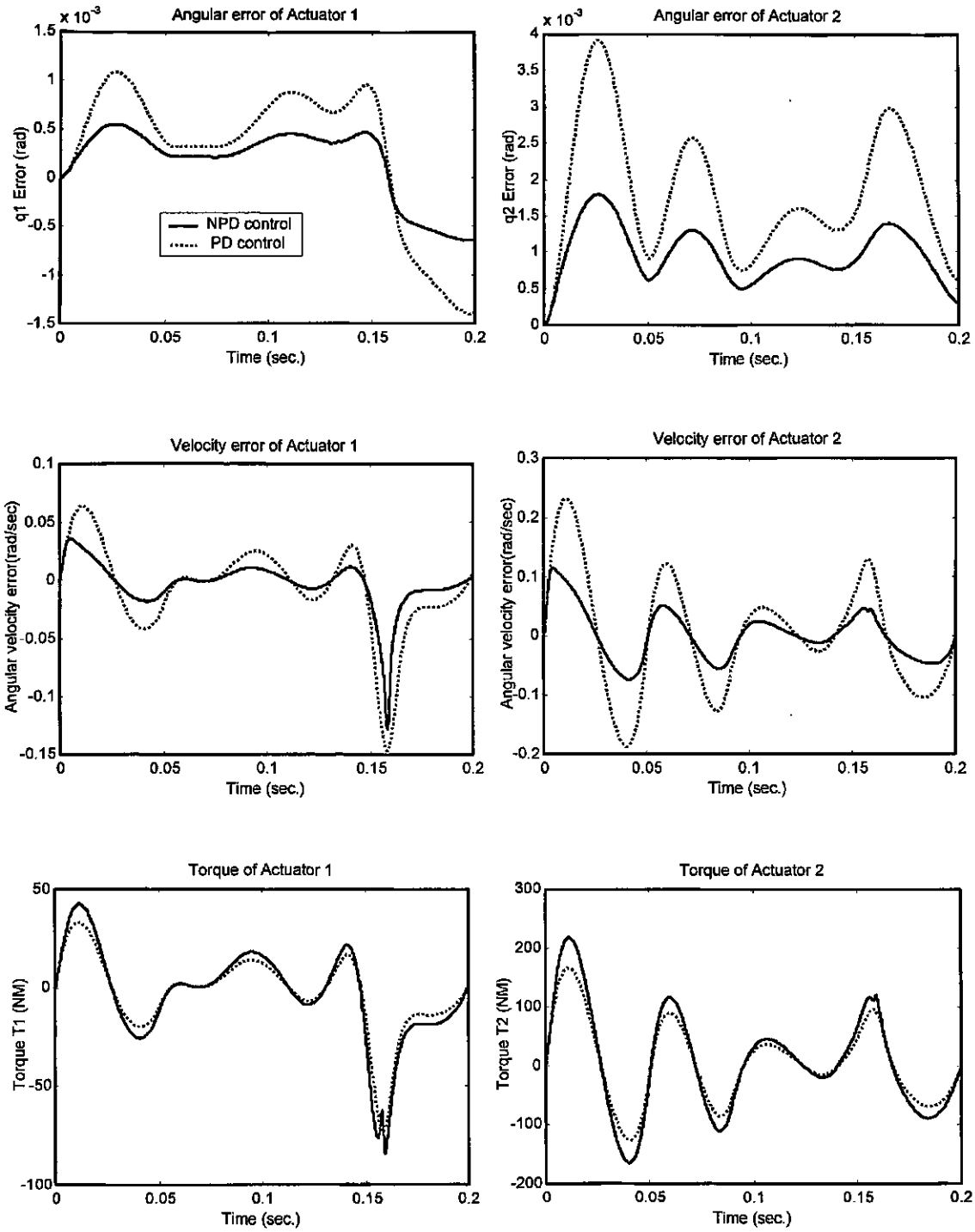

Note: Solid lines: NPD control law; Dotted line: PD control law.

Figure 6.8 Comparison of performance under PD/NPD controllers using the CW method at high speeds

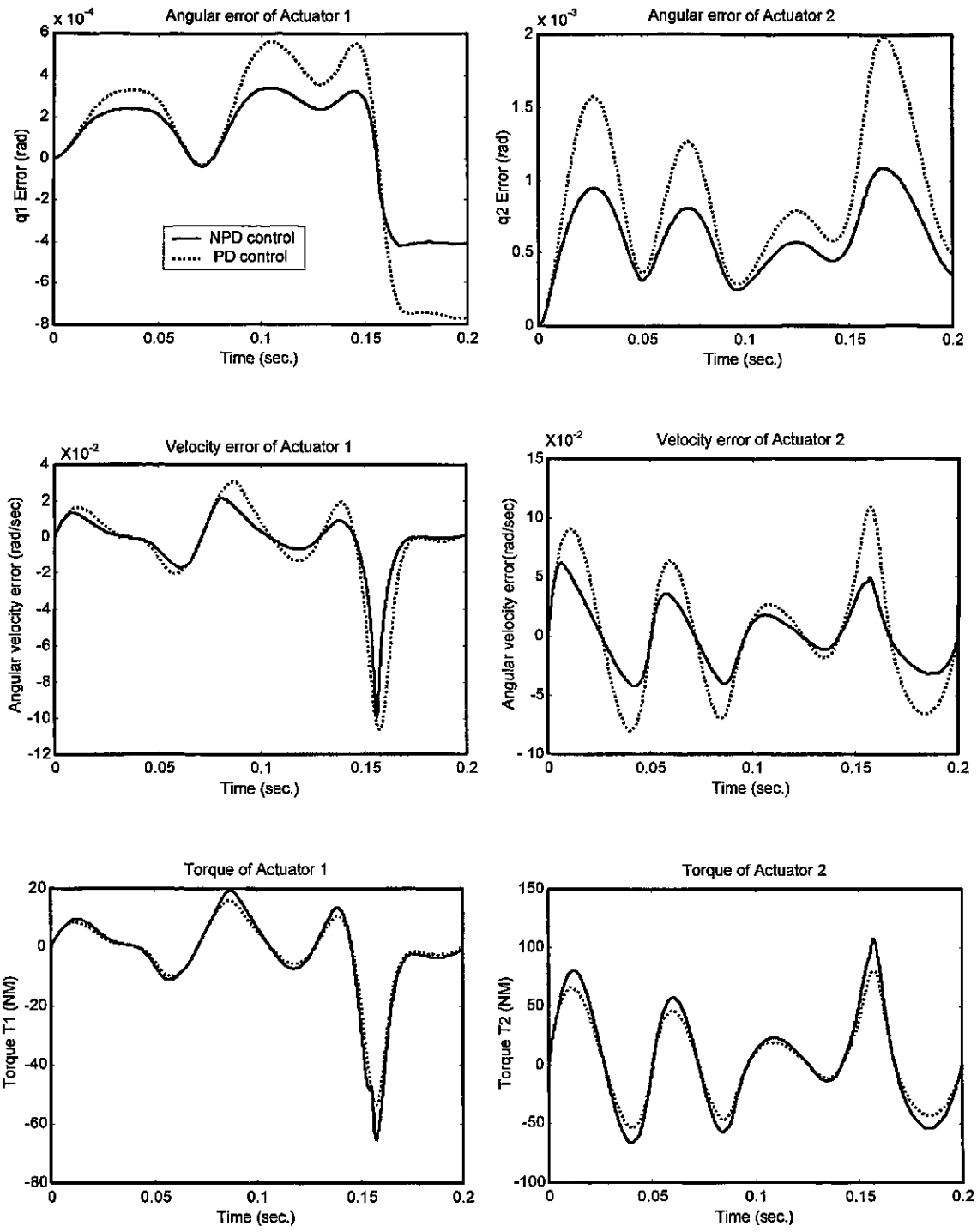

Note: Solid lines: NPD control law; Dotted line: PD control law.

Figure 6.9 Comparison of performance for the unbalanced mechanism under PD/NPD controllers at high speeds

Figures 6.4 to 6.6 show the comparative results using PD control law and NPD control law, respectively, at low speeds, while Figures 6.7 to 6.9 show the results at high speeds. From these figures, it can be seen that the NPD controller generally improves the performances in terms of the reduction of trajectory tracking errors both at low speeds and high speeds, and further, the best improvement in performance is achieved with the extended AKP method.

To understand how alf_1 and alf_2 affect trajectory tracking performance, the following simulation is performed. The control parameters are selected as follows:

$$\mathbf{K}_{p0} = diag\{1650,\ \ 2400\} \text{ and } \mathbf{K}_{d0} = diag\{600,\ \ 800\}$$

The user-defined constants for NPD control law are chosen as:

For Case 1: alf_1=1500 and alf_2 =3000; For Case 2: alf_1=3000 and alf_2 =6000

For Case 3: alf_1=5000 and alf_2 =9000; For Case 4: alf_1=8000 and alf_2 =12000

Simulation results produced at high speeds are documented in Table 6.3 and Table 6.4, respectively. It should be noted that the units of the performance indexes in all the tables are as follows:

Position error (e_i): *rad*; velocity error ($\dot{e}_i$): *rad/sec.*; Torque (T_i): $N \cdot m$.

Table 6.3 Simulation results for different controllers using the extended AKP method

Cases	Limits	$e_1(10^{-4})$	$e_2(10^{-4})$	$\dot{e}_1(10^{-3})$	$\dot{e}_2(10^{-3})$	T_1	T_2
NPD	Min	-0.141	-3.030	-4.2	-29.2	-2.284	-24.95
Case	Max	2.224	9.026	4.1	25.5	2.529	23.34
NPD	Min	-0.083	-2.114	-4.0	-22.6	-2.339	30.02
Case 1	Max	2.201	5.877	4.1	18.3	2.536	28.11
NPD	Min	-0.016	-1.682	-3.7	-19.4	-2.477	-31.89
Case 2	Max	2.079	4.816	4.0	14.7	2.556	29.75
NPD	Min	0	-1.303	-3.3	-16.7	-2.644	-32.64
Case 3	Max	1.892	4.429	3.9	12.7	2.603	30.37
NPD	Min	0	-1.137	-2.9	-15.7	-2.829	-32.92
Case 4	Max	1.694	4.189	3.7	11.3	2.699	30.67

Table 6.4 Simulation results for different controllers using the CW method

Cases	Limits	$e_1(10^{-4})$	$e_2(10^{-4})$	$\dot{e}_1(10^{-3})$	$\dot{e}_2(10^{-3})$	T_1	T_2
PD	Min	-4.421	-5.999	-32.1	-50.1	-19.07	-43.19
Case	Max	6.126	13.998	15.1	37.6	9.37	34.57
NPD	Min	-3.924	-4.142	-30.9	-44.6	-19.06	-52.36
Case 1	Max	5.158	7.639	14.1	23.6	9.75	43.42
NPD	Min	-3.327	-3.225	-29.8	-43.2	-20.02	-55.33
Case 2	Max	4.313	6.356	12.7	18.5	10.45	45.10

NPD	Min	-2.789	-2.798	-28.8	-42.5	-21.42	-56.41
Case 3	Max	3.699	5.841	11.2	16.3	11.11	45.63
NPD	Min	-2.388	-2.562	-28.2	-42.2	-22.61	-56.91
Case 4	Max	3.228	5.574	9.7	16.3	11.62	45.86

From these two tables, it can be seen that with the increase of alf_1 and alf_2, i.e., the increase of the nonlinear gains, the trajectory tracking errors, including both the positions and the velocities, are reduced. It is shown that the reduction of the trajectory tracking errors is paid for the increase of the torques in the actuators. This result is in agreement with the theoretical predications in Chen et al. (2001), and Shahruz and Schwartz (1997).

6.3 EPD control law: results and discussion

In EPD control law, as proposed in Chapter 5, the PD gains in each generation are selected to be the same, i.e.,

$$K_p = diag\{165,\ \ 240\} \text{ and } K_d = diag\{60,\ \ 88\}.$$

Example 1 of Chapter 3 is used for simulation study here, and information on the geometric and dynamic properties of the mechanism was given in Table 3.1. Using the EPD control method, trajectory tracking performance for each generation can be

simulated, and the results are documented in Tables 6.5 and 6.6 (only the minimum and maximum values of each performance index are given).

Table 6.5 Performance improvement with the EPD control using the extended AKP method

Generation	Limits	$e_1(10^{-4})$	$e_2(10^{-4})$	$\dot{e}_1(10^{-3})$	$\dot{e}_2(10^{-3})$	T_1	T_2
First	Min	-6.862	-3.726	-40.44	-289.7	-2.286	-24.96
Gen.	Max	21.19	86.43	40.9	255.0	2.537	23.37
Second	Min	-0.048	-0.072	-1.048	-4.421	-2.278	-24.95
Gen.	Max	0.603	0.823	0.980	7.582	2.528	23.34
Third	Min	-0.004	-0.016	-0.406	-1.258	-2.279	-24.95
Gen.	Max	0.553	0.707	0.295	1.965	2.528	23.33

Table 6.6 Performance improvement with the EPD control using the CW method

Generation	Limits	$e_1(10^{-4})$	$e_2(10^{-4})$	$\dot{e}_1(10^{-3})$	$\dot{e}_2(10^{-3})$	T_1	T_2
First	Min	-63.82	-64.58	-339.1	-498.5	-20.56	-43.12
Gen.	Max	59.48	134.6	152.6	375.3	9.499	34.49
Second	Min	-16.30	-17.95	-69.16	-180.1	-21.99	-43.41
Gen.	Max	13.94	14.19	170.1	58.03	9.38	34.66
Third	Min	-3.151	-1.171	-54.07	-105.6	-21.22	-43.19
Gen.	Max	12.14	3.667	103.3	63.65	9.35	34.57
Fourth	Min	-0.588	-0.546	-50.92	-54.12	-20.37	-43.18
Gen.	Max	6.420	1.579	53.72	58.17	9.35	34.57

To show the effectiveness of the EPD control method, Figures 6.10 and 6.11 illustrate the performance improvement using the extended AKP method, one generation by one generation in an evolutionary process.

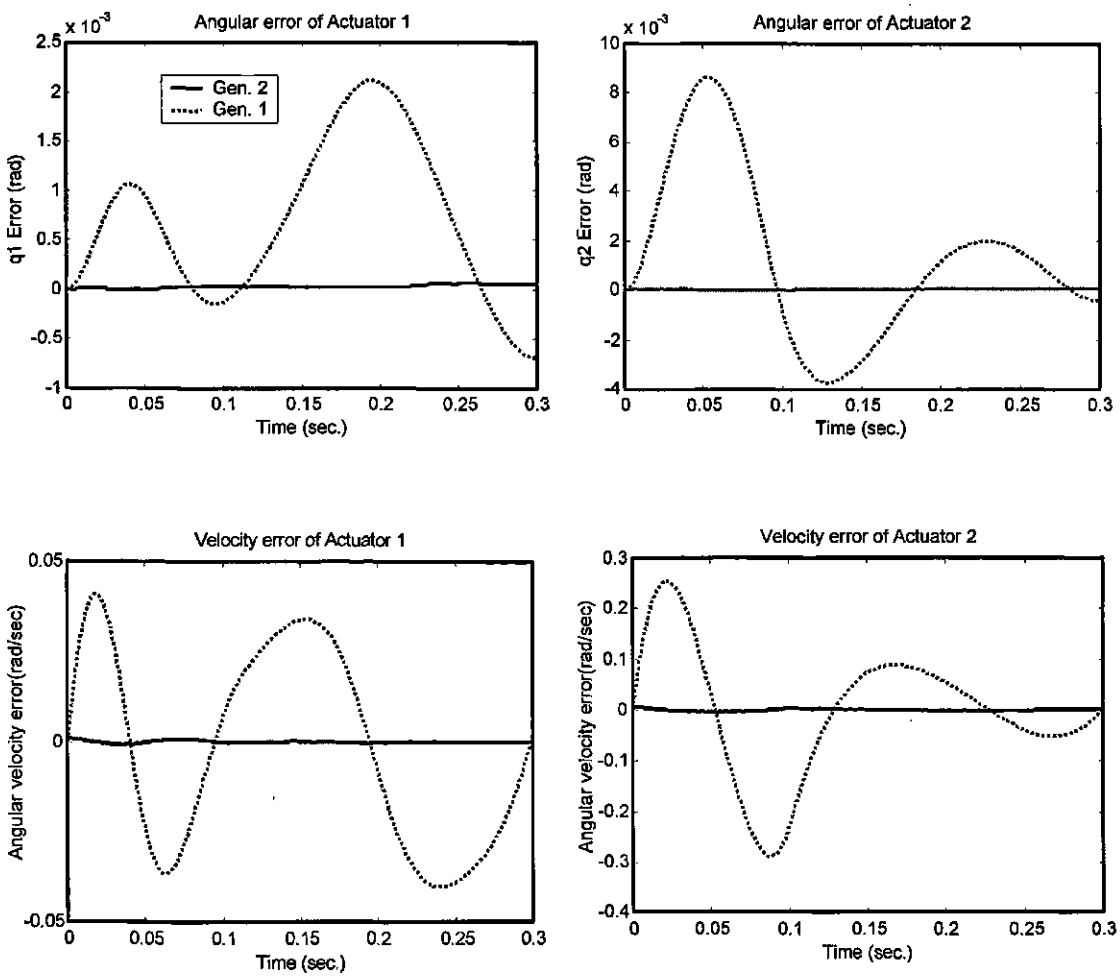

Note: Solid line: Generation 2; Dotted line: Generation 1

Figure 6.10 Trajectory tracking performance from generation 1 to generation 2 using the extended AKP method

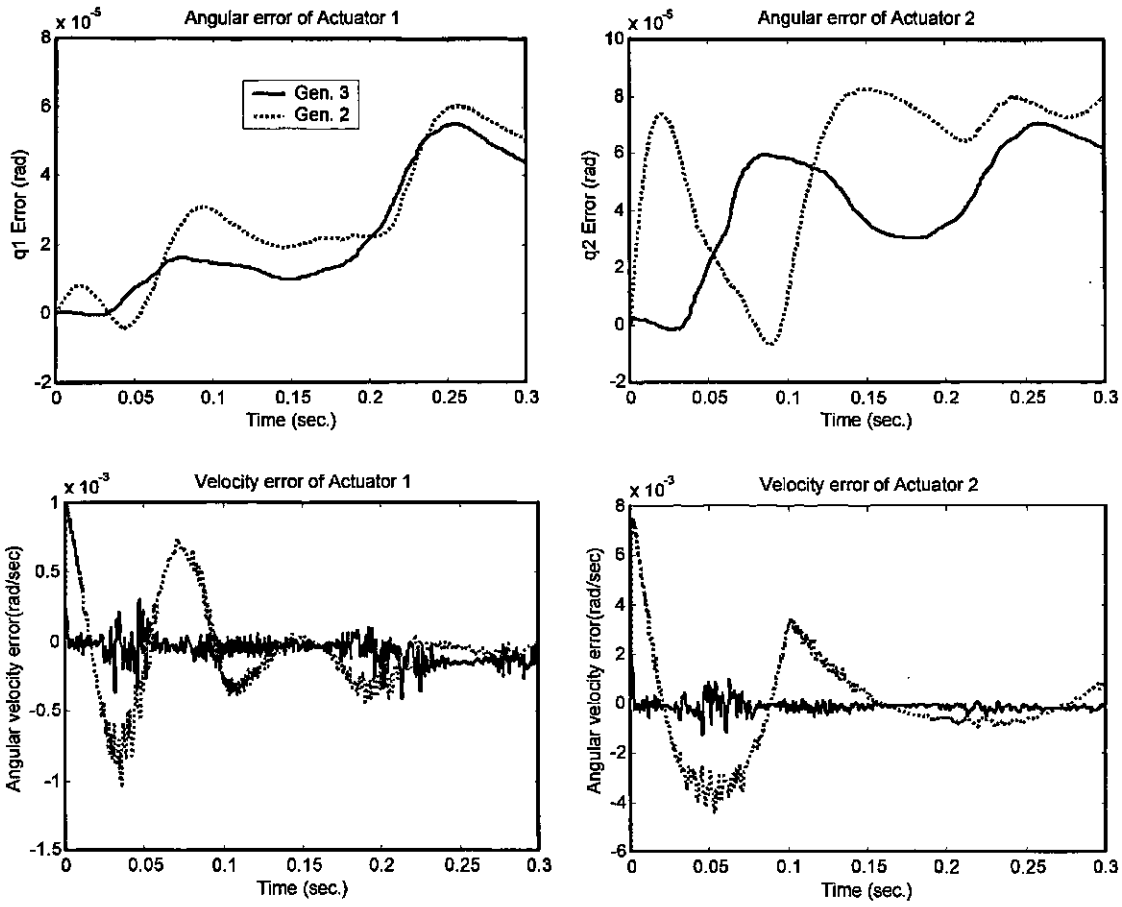

Note: Solid line: Generation 3; Dotted line: Generation 2

Figure 6.11 Trajectory tracking performance from generation 2 to generation 3 using the extended AKP method

Trajectory tracking performance using the EPD control method is compared with that using a high gain PD control method. In the PD control method, the control gains are selected to be 100 times the gains used in the EPD control method, i.e., $K_p = diag\{16500,\ 2400\}$ and $K_d = diag\{6000,\ 8800\}$. Figures 6.12 and 6.13 show the trajectory tracking performance with the EPD control method and PD control method, and using the extended AKP method and the CW method, respectively.

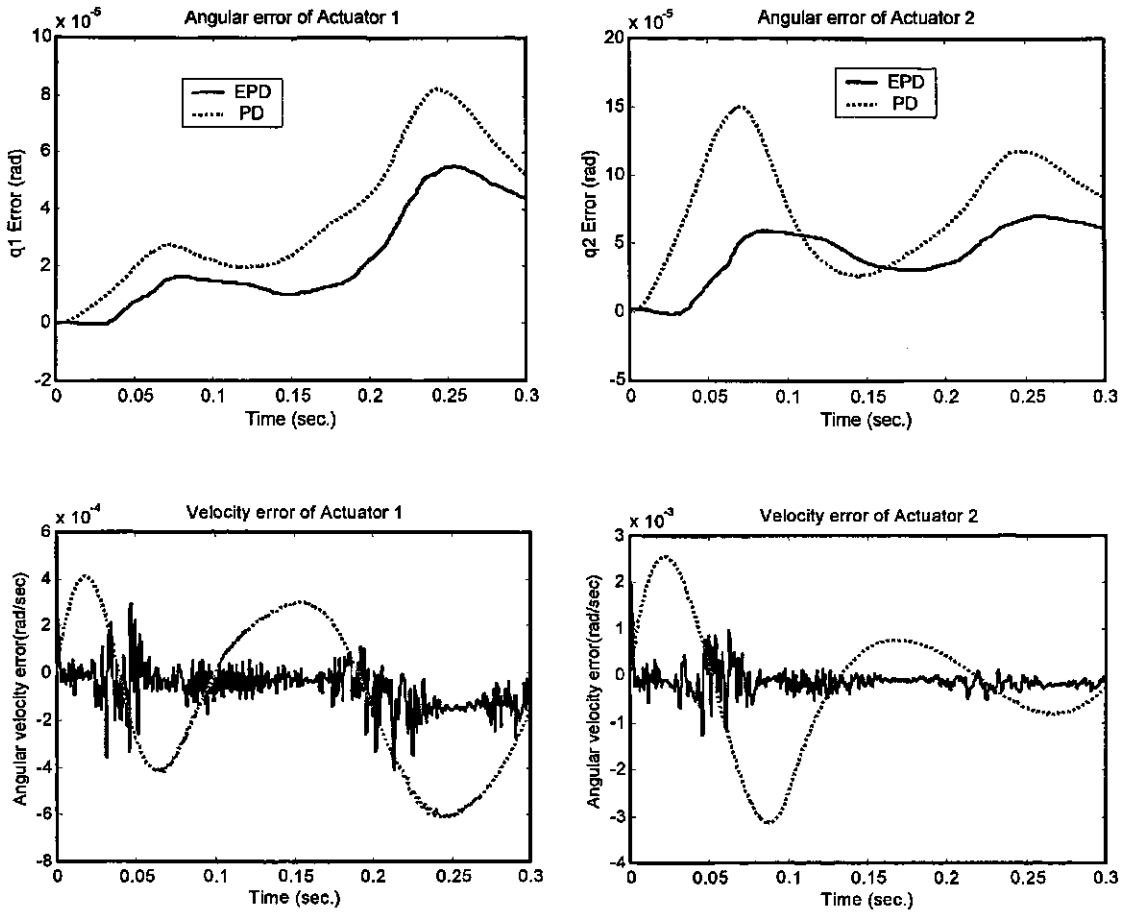

Note: Solid line: EPD control; Dotted line: PD control

Figure 6.12 Comparison of the EPD control with the high-gain PD control using the extended AKP method

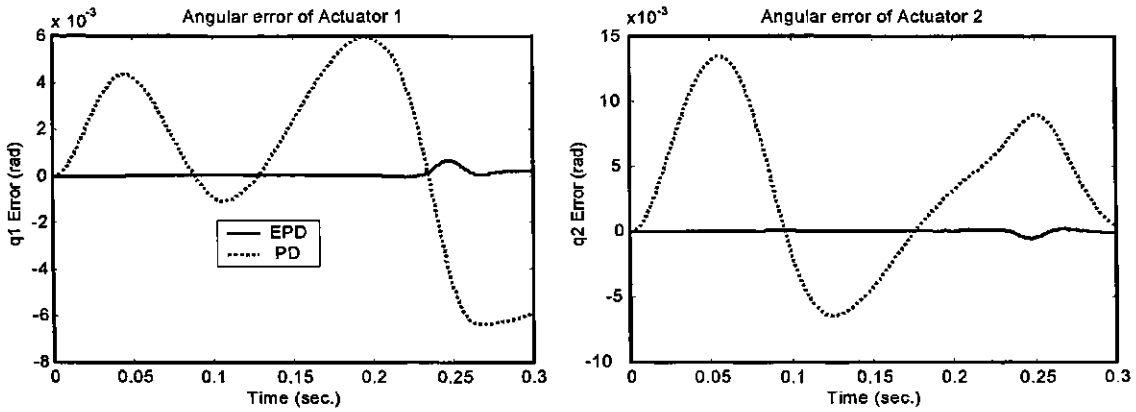

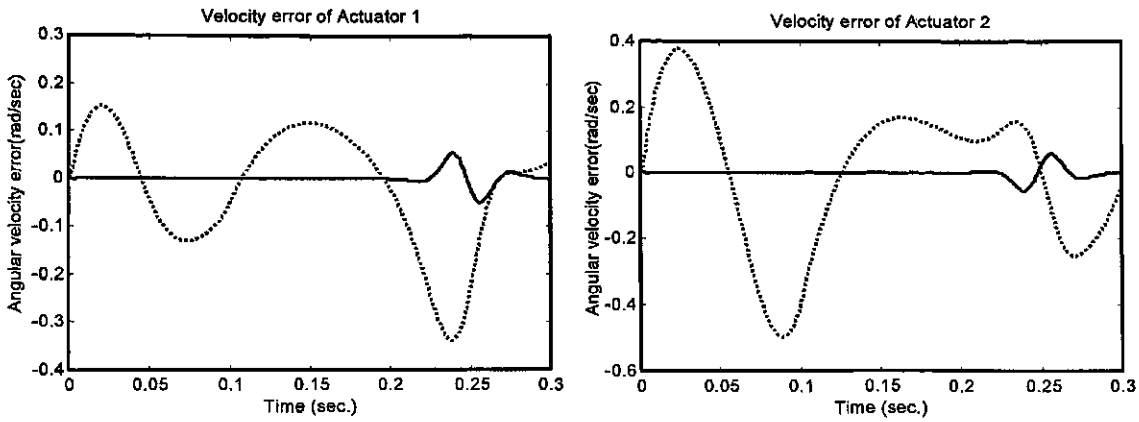

Note: Solid line: EPD control; Dotted line: PD control

Figure 6.13 Comparison of the EPD control with the high-gain PD control using the CW method

Figure 6.14 shows the torque in actuator 1 using the EPD control, and Figure 6.15 shows the torque in actuator 1 using the high gain PD control. From these two figures, it can be seen that the EPD control can reduce the fluctuation of the torque.

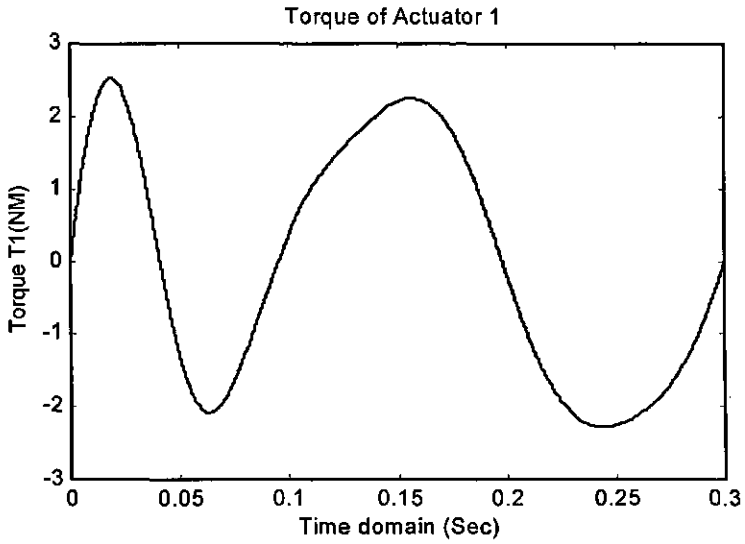

Figure 6.14 Torque in actuator 1 using the EPD control

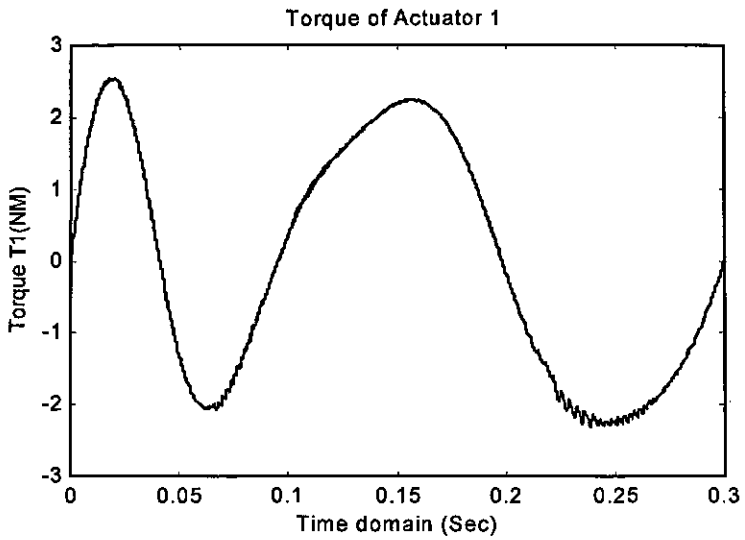

Figure 6.15 Torque in actuator 1 using the PD control with high gain.

Trajectory tracking performance using the EPD control method is also compared with that using the NPD control method. In the NPD control method, the control gains are selected to be 10 times the control gains used in the EPD control method, and the user-defined constants are set as alf_1=5000 and alf_2 =9000. Figures 6.16 and 6.17 show the trajectory tracking performances with the EPD control method and NPD control method, using the extended AKP method and the CW method, respectively.

From Figures 6.16 and 6.17, it can be seen that the EPD control is also better than the NPD control in terms of the reduction of the trajectory tracking errors.

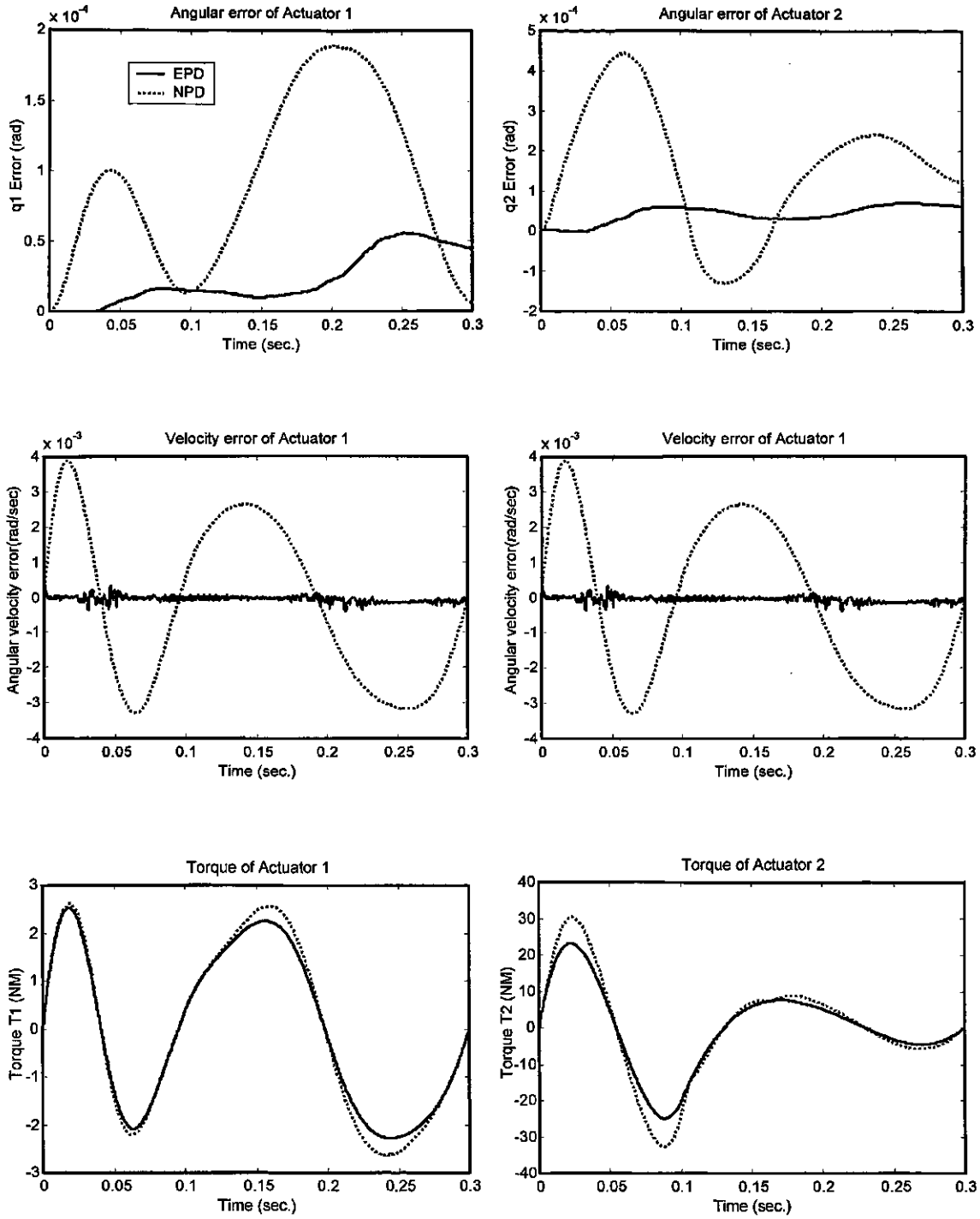

Note: Solid line: EPD control; Dotted line: NPD control

Figure 6.16 Comparison of the EPD control with the NPD control using the extended AKP method

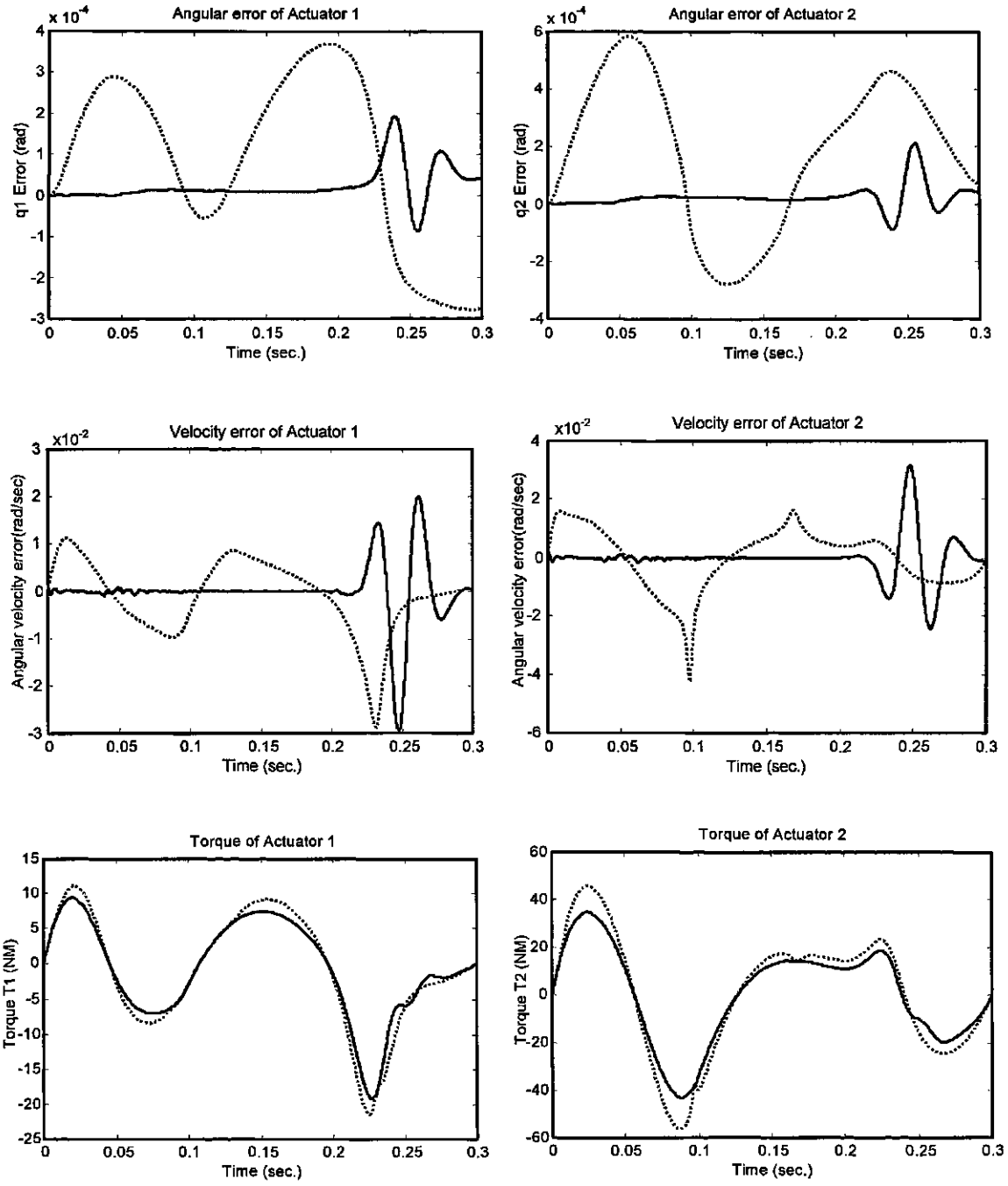

Note: Solid line: EPD control; Dotted line: NPD control

Figure 6.17 Comparison of the EPD control with the NPD control using the CW method

6.4 Conclusions

In this chapter, the force balanced mechanisms using the extended AKP method and the CW method, and the unbalanced mechanism are compared in terms of trajectory tracking performance. Three control laws, i.e., PD control, NPD control, and EPD control, perform the feedback control for several cases. All the simulation results show that the extended AKP method is better than the CW method for trajectory tracking performance in the operating conditions of both low speeds and high speeds. The reduction of the trajectory tracking error and torque fluctuation using the extended AKP method is the most significant among the three cases. Simulation results also show that the EPD control method is a promising control method compared with the PD and NPD control methods in terms of the selection of control gains, high trajectory tracking performance, and small fluctuation of the torques in actuators.

CHAPTER 7

CONCLUSION AND RECOMMENDATIONS

7.1 Overview of the thesis

There are many benefits to an RTC mechanism that is force balanced, in particular in the application areas such as machine tools and flight or drive simulators. The generic task of an RTC mechanism is trajectory tracking. Previous studies have shown that design of mechanical structures of an RTC mechanism for force balancing and design of a controller for RTC actuators are two coupled activities that need to proceed concurrently. A novel method called the AKP method for force balancing of RTC mechanisms was developed at the AEDL of the University of Saskatchewan. The AKP method is promising as it avoids those problems associated with other force balancing methods (i.e., the CW method and the Add-spring method), e.g., degradation of trajectory tracking performance. However, the AKP method when it was first presented had several problems. First of all, the problems with the present version of the AKP method were identified (in Chapter 1). These include: (i) no possibility of dealing with the off-line mass center, (ii) no consideration of the masses of sliding blocks for adjusting the ki-

nematic parameters, (iii) trajectory with an infinite jerk at the via point, and (iv) insufficient understanding of how the control laws affect trajectory tracking performance with respect to different force balancing methods. The motivation of the research described in this thesis is to overcome these problems with the present AKP method and further extend it to be more general and robust.

General force balancing condition equations are developed, which takes the masses of adjusting or sliding blocks into consideration. The AKP method is extended so that the method can work for the situation where the mass center of the link is off its kinematic axis connecting its two end pivots. Furthermore, the design equations are developed for the extended AKP method where the two pivots on a link are adjustable.

Trajectory planning is needed for the purpose of trajectory tracking. A new method for generating a smooth jerk curve for trajectory planning is developed. The control laws are then more thoroughly studied for the closed-loop RTC mechanism, which include the stability analysis of the PD control method, and development of a new PD-based control method in which plant dynamics is incorporated to a certain degree. This new control method is structurally based on the superposition of several runs of a controlled plant system.

The verification of the concepts and methodologies developed in this thesis is as follows. A prototype system was developed to verify the extended AKP method. Simulations were developed for comparative studies of the CW method and the extended AKP

method using different control methods. The simulation consistently showed the benefit of the extended AKP method over the CW method using the control methods such as the PD control method, non-linear PD control method, and the evolutionary PD control method. The simulation study also showed a better result with the evolutionary PD control method over other PD-based control methods.

7.2 Major research contributions

7.2.1 The extended AKP method

The extended AKP method has overcome many problems of the AKP method developed by Wang (2000); in particular the extended method can work for any general mass distribution of a closed-loop mechanism. Along with the development of the extended AKP method, the force balancing condition equations are also extended to incorporate the masses of sliding blocks. The extended force balancing condition equations should also be useful to the CW method in the case where the implementation of the CW method is to adjust some of the point masses on pivots, instead of adding new point masses into the system. The extended AKP method has been verified to be consistently better than the CW method for closed-loop RTC mechanisms.

7.2.2 A novel trajectory planning method

A method for trajectory planning which can achieve C^3 continuity is developed. This method is especially suitable for such problems where a set of points are prescribed, and

the curve fitting to these points needs to be found. In the literature, the trajectory planning for C^2 continuity was achieved only.

7.2.3 A novel PD-based control method: the evolutionary PD method

Based on the analysis of the existing non-linear PD control methods and the Computed Torque Control (CTC) method, a novel PD-based control method is developed. This method incorporates plant dynamics into the control law in such a way that the control law is the result of the superposition of a series of runs of a controlled plant system. As such, this new method is called the evolutionary PD control method.

7.3 Future Work

For best performance, the extended AKP method should be optimized; the question here is what is the best scheme for adjusting the pivots. The optimization may also cover the trajectory planning where there are many options in the existing methods. Other possible future work is the potential to apply the extended AKP method for moment balancing in addition to force balancing. In order to accomplish both the force balancing and the moment balancing, one might consider a hybrid strategy in which both the CW method and the extended AKP method are applied. Furthermore, the stability of the evolutionary PD control method needs to be studied.

REFERENCES

Arakelian, V. H. and Smith, M. R., 1999, Complete shaking force and shaking moment balancing of linkages, Mechanism and Machine Theory, Vol. 34, pp. 1141-1153.

Arakelian, V. and Dahan, M., 2000, Dynamic balancing of mechanisms, Mechanics Research Communications, Vol. 27, No. 1, pp. 1-6.

Armstrong, B., and Wade, B. A., 2000, Nonlinear PID control with partial state knowledge: Damping without derivatives, The International Journal of Robotics Research, Vol.19, No. 8, pp. 715-731.

Asada, H. and Youcef-Toumi, H., 1987, Direct-Drive Robots: Theory and Practice, Cambridge, Mass. MIT Press.

Bagci, C., 1979, Shaking force balancing of planar linkages with force transmission irregularities using balancing idler loops, Mechanism and Machine Theory, Vol. 14, No. 4, pp. 267-284.

Bagci, C., 1982, Complete shaking force and shaking moment balancing of link mechanisms using balancing idler loops, Trans. ASME Journal of Mechanical Design, Vol. 104, No. 2, pp. 482-493.

Bagci, C., 1983, Complete balancing of space mechanisms – shaking force balancing, Trans, ASME, Journal of Mechanisms, Transmissions, and Automation in Design, Vol. 105, No. 3, pp. 609-616.

Berkof, R. S. and Lowen, G. G., 1969, A new method for completely force balancing simple linkages, Trans. ASME, Journal of Engineering for Industry, Vol. 91B, No. 1, pp. 21-26.

Berkof, R.S., 1973, Complete force and moment balancing of inline four-bar linkage, Mechanism and Machine Theory, Vol. 8, No. 3, pp. 397-410.

Chen, Q. J, Chen H. T., Wang, Y. J., and Woo, P. Y, 2001, Robust adaptive trajectory tracking independent of models for robotic manipulators, Journal of Robotic Systems, Vol.18, No. 9, pp. 545-551.

Chen, Q. J, Chen H. T., Wang, Y. J., and Woo, P. Y, 2001, Global stability analysis for some trajectory tracking control schemes of robotic manipulators, Journal of Robotic Systems, Vol. 18, No. 2, pp. 69-75.

Chen, W. H., Ballance, D. J., Gawthrop, P. J., Gribble, J. J., and O'Reilly, J., 1999, Nonlinear PID predictive controller, IEE Proc.—Control Theory Applications, Vol. 146, No. 6, pp. 603-611.

Codourey, A., 1998, dynamic modeling of parallel robots for computed-torque control implementation", The International Journal of Robot Research, Vol. 17, No. 12, pp. 1325-1336.

Colbaugh, R., Seraji, H., and Glass, K., 1994, A new class of adaptive controllers for robot trajectory tracking, Journal of Robotic Systems, Vol. 11, No. 8, pp. 761-772.

Constantinescu, D. and Croft, E. A., 2000, Smooth and time-optimal trajectory planning for industrial manipulators along specified paths, Journal of Robotic Systems, Vol. 17, No. 5, pp. 233-249.

Corless, M., 1990, Guaranteed rates of exponential convergence for uncertain systems, Journal of Optimal Theory Applications, Vol. 64, No. 3, pp. 481-494.

Craig, J. J., 1988, Adaptive Control of Mechanical Manipulators, Addison-Wesley, New York, NY.

Craig, J. J., 1986, Introduction to Robotics: Mechanics and Control, Reading, Addison-Wesley, MA.

Davies, T. H., 1968, The kinematics and design of linkages, balancing mechanisms and machines, Machine Design Engineering, Vol. 6, No. 3, pp. 40-51.

Diken, H., 1997, Trajectory control of mass balanced manipulator, Mechanism and Machine Theory, Vol. 32, No. 3, pp. 313-322.

Ebert-Uphoff, E., Gosselin, C. M. and Laliberte, T., 2000, Static balancing of spatial parallel platform mechanisms-revisited, Trans. ASME, Journal of Mechanical Design, Vol. 122, No. 1, pp. 43-51.

Egerstedt, M. and Martin, C.F., 2001, Optimal trajectory planning and smoothing splines, Automatica, Vol. 37, No. 7, pp. 1057-1064.

Elliott, J. L. and Tesar, D., 1977, The theory of torque, shaking force, and shaking moment balancing of four link mechanisms, Trans. ASME, Journal of Engineering for Industry, Vol. 99 (B), No. 3, pp. 715-722.

Esat, I. and Bahai, H., 1999. A theory of complete force and moment balancing of planer linkage mechanisms, Mechanism and Machine Theory, Vol. 34, No. 6, pp. 903-922.

Feng, B., Morita, N., Torii, T., and Yoshida, S., 2000, Optimum balancing of shaking force and shaking moment for spatial RSSR mechanism using genetic algorithm, JSME international Journal, Series C, Vol. 43, No. 3, pp. 691-696.

Feng, G., 1991, Complete shaking force and shaking moment balancing of 17 types of eight-bar linkages only with revolute pairs, Mechanism and Machine Theory, Vol. 26, No. 2, pp. 197-206.

Ge, S. S., Hang, C. C., and Zhang, T., 1999, Adaptive neural network control of nonlinear systems by state and output feedback, IEEE Trans. On Systems, Man, and Cybernetics – Part C, Vol. 29, No. 6, pp. 818-828.

Ghorbel, F., Chetelat, O., and Longchamp, R., 1994, A reduced model for constrained rigid bodies with application to parallel mechanical system, Proceeding of the 4th IFAC Symposium on Robot Control, Capri, Italy, pp. 45-50.

Ghorbel, F., 1995, Modeling and PD control of a closed-chain mechanical system, Proceeding of the 34th Conference on Decision & Control, New Orleans, LA, USA, pp. 540-542.

Gosselin, C. M., 1999, Static balancing of spherical 3-DoF parallel mechanism and manipulators, The International Journal of Robotics Research, Vol. 18, No. 8, pp. 819-829.

Homaifar, A., Bikdash, M., and Gopalan, V., 1997, Design using genetic algorithms of hierarchical hybrid fuzzy-PID controllers of two-link robotic arms, Journal of Robotic Systems, vol. 14, No. 6, pp. 449-463.

IFToMM, 1991, Terminology for the theory of machines and mechanisms, Mechanism and Machine Theory, Vol. 26, No. 5, pp. 435-439.

Kang, B. S., Kim, S. H., and Smith, C. C., 1999, Robust tracking control of a direct drive robot, Trans. ASME, Journal of Dynamic Systems, Measurement, and Control, Vol. 121, No. 2, pp. 261-269.

Kelly, R. and Salgado, R., 1994, PD control with computed feedforward of robot manipulators: a design procedure, IEEE Trans. On Robotics and Automation, Vol. 10, No. 4, pp. 566-571.

Kelly, R., 1997, PD control with desired gravity compensation of robotic manipulators: a Review, The international Journal of Robotics Research, Vol. 16, No. 5, pp. 660-672.

Kelly, R., 1998, Global positioning of robot manipulators via PD control plus a class of nonlinear integral actions, IEEE Trans. On Automatic Control, Vol. 43, No. 7, pp. 934-938.

Klein, B. A. J., 1987, Kinematic optimization of mechanisms, a finite element approach, Dissertation, Delft University of Technology, The Netherlands.

Knowledge Revolution, 1999, Working model 2D user's manual, San Mateo, California, USA.

Lewis, F. L., and Liu, K., 1996, Multilayer neural-net robot controller with guaranteed tracking performance, IEEE trans. On Neural Networks, Vol. 7, No. 2, pp. 388-399.

Li, Q., Tso, S. K., Guo, L. S., and Zhang, W. J., 2000, Improving motion tracking of servomotor-driven closed-loop mechanisms using mass-redistribution, Mechanism and Machine Theory, Vol. 35, No. 7, pp. 1033-1045.

Li, Q., Zhang, W. J., and Chen L., 2001, Design for control - A concurrent engineering approach for mechatronic systems design, IEEE/ASME Transactions on Mechatronics, Vol. 6, No. 2, pp. 161-169

Lin, C.S., Chang, P.R, and Luh, J.Y.S., 1983, formulation and optimization of cubic polynomial joint trajectories for industrial robots, IEEE Trans. On Automatic Control, Vol. AC-28, No. 12, pp. 1066-1074.

Liu, M., 1997, Decentralized Pd and robust nonlinear control for robot manipulators, Journal of Intelligent Robotic System, Vol. 20, No. 2, pp. 319-332.

Liu, M., 1999, Decentralized control of robot manipulators: Nonlinear and adaptive approaches, IEEE Trans. On Automatic Control, Vol. 44, No. 2, pp. 357-363.

Lowen, G. G. and Berkof, R. S., 1971, Determination of force-balanced four-bar linkages with optimum shaking moment characteristics, Trans. ASME, Journal of Engineering for Industry, Vol. 93(B), No. 1, pp. 39-46.

Lowen, G. G., Tepper, F. R. and Berkof, R. S., 1983, Balancing of linkages – an update, Mechanism and Machine Theory, Vol. 18, No. 3, pp. 213-220.

Macfarlane, S. and Croft, E. A., 2001, Design of jerk bounded trajectories for on-line industrial robot applications, Proceedings of the 2001 IEEE International Conference on Robotics and Automation, Seoul, Korea, pp. 979-984.

Murray, R. M., Li, Z. X., and Sastry, S. S., 1994, A Mathematical Introduction to Robotic Manipulation, CRC Press, Boca Raton, New York.

Nguyen, P. P. and Cipra, R. J., 1999, Dynamic analysis of five-bar mechanism with torsional springs using Lagrange's equation and kinematic coefficients, 1999 ASME Design Engineering Technical Conferences, DAC-8621, Las Vegas, Nevada, USA.

Ouyang, P. R., Zhang, W. J., and Wu, F. X., 2001, Nonlinear PD control for a parallel manipulator with consideration of the design for control strategies, Submitted to IEEE IRAC 2002.

Paul, R. P., 1979, Manipulator Cartesian path control, IEEE Trans. System, Man, Cybern., Vol. SMC-9, Nov., pp. 702-711.

Piazzi, A and Visioli, A., 2000, Global minimum-jerk trajectory planning of robot manipulators, IEEE Trans. On Industrial Electronics, Vol. 47, No. 1, pp. 140-149.

Pil, A. C. and Asada, H., 1996, Integrated structure/control design of mechatronic systems using a recursive experimental optimization method, IEEE/ASME Transactions on Mechatronics, Vol. 1, No. 3, pp. 191-203.

Qu, Z. H., 1994, Global stability of trajectory tracking of robot under PD control, Dynamics and Control, Vol. 5, No. 1, pp. 59-71.

Seraji, H., 1998, Nonlinear and adaptive control of force and compliance in manipulators, The International Journal of Robotics and Research, Vol. 17, No. 5, pp. 467-484.

Shinskey, F. G., 1988, Process Control Systems: Application, Design and Adjustment, 3rd Edition, McGraw-Hill, New York, NY.

Shshruz, S. M., and Schwartz, A. L., 1994, Design and optimal tuning of nonlinear PI compensators, Journal of Optimization Theory and Applications, Vol. 83, No. 1, pp. 181-198.

Simionescu, I. and Ciupitu, L., 2000, The static balancing of the industrial robot arms: Part I: discrete balancing, Mechanism and Machine Theory, Vol. 35, No. 9, pp. 1287-1298.

Simionescu, I. and Ciupitu, L., 2000, The static balancing of the industrial robot arms: Part II: continuous balancing, Mechanism and Machine Theory, Vol. 35, No. 9, pp. 1299-1311.

Streit, D. A. and Shin, E., 1990, Equilibrators for planar linkages, Proceedings of the ASME Mechanisms Conference, Chicago, September, pp.16-19.

Sun, F. C., Sun, Z. Q., and Woo, P. Y., 2001, Neural network-based adaptive controller design of robotic manipulators with an observer, IEEE Trans. On Neural Networks, Vol. 12, No. 1, pp. 54-67.

Sun, D., and Mills, J. K., 1999, Performance improvement of industrial robot trajectory tracking using adaptive-learning scheme, Trans. ASME, Journal of Dynamic Systems, Measurement, and Control, Vol. 121, No. 2, pp. 285-292.

Tao, C. W. and Taur, J. S., 2000, Flexible complexity reduced PID-like fuzzy controllers, IEEE Trans. On Systems, Man, and Cybernetics – Part B, Vol. 30, No. 4, pp. 510-516.

Tarokh, M., 1999, Decoupled nonlinear three-term controllers for robot trajectory tracking, IEEE Trans. On Robotics and Automation, Vol. 15, No. 2, pp. 369-380.

Tomei, P., 1991, Adaptive PD controller for robot manipulators, IEEE Trans. On Robotics and Automation, Vol. 7, No. 4, pp. 565-570.

Tondu, B. and Bazaz S. A., 1999, The three-cubic method: an optimal online robot joint trajectory generator under velocity, acceleration, and wandering constraints, The International Journal of Robotics Research, Vol. 18, No. 9, pp. 893-901.

Tsai, L. W., 1999, Robot Analysis, John Wiley & Sons, Inc., New York.

Visioli, A., 2001, Tuning of PID controllers with fuzzy logic, IEE Proc.—Control Theory Applications, Vol. 148, No. 1, pp. 1-8.

Visioli, A., 2001, Optimal tuning of PID controllers for integral and unstable processes, IEE Proc.—Control Theory Applications, Vol. 148, No. 2, pp. 180-184.

Wang, F. C., Wright, P. K., Barsky, B. A., and Yang, D. C. H., 1999, Approximately arc-length parameterized C^3 quintic interpolatory splines, Trans. ASME, Journal of Mechanical Design, Vol. 121, No. 3, pp. 430-439.

Wang, J. G., and Gosselin, C. M., 2000, Static balancing of spatial four-degree-of-freedom parallel mechanisms, Mechanism and Machine Theory, Vol. 35, No. 4, pp. 563-592.

Wang, Z. H., 2000, "Mechatronic design to real-time controllable mechanical systems: force balancing and trajectory tracking", M.Sc. thesis, University of Saskatchewan.

Wit, C.C. D., Fixot, N., and Astrom, K. J., 1992, Trajectory tracking in robot manipulators via nonlinear estimated state feedback, IEEE Trans. On Robotics and Automation, Vol. 8, No. 1, pp. 138-144.

Wu, F. X., Li, Q., Zhang, W. J., and Ouyang, P. R., 2001, Integrated design of mechanical structure and control algorithm for closed-chain five-bar mechanism, Submitted to ASME Trans. Journal of Mechanical Design.

Xi, F. F. and Sinatra, R., 1997, Effect of dynamic balancing on four-bar linkage vibrations, Mechanism and Machine Theory, Vol. 32, No. 6, pp. 715-728.

Xu, Y. M., Hollerbach, J. M., and Ma, D. H., 1994, Force and contact transient control using nonlinear PD control, Proc. IEEE Int. Conf. Robotics and Automation, San Diego, May, 1994, pp. 924-930.

Xu, Y. M., Hollerbach, J. M., and Ma, D. H., 1995, A nonlinear PD controller for force and contact transient control, IEEE Control Systems Magazine, Vol. 15, No. 1, pp. 15-21.

Yang, L. F., Chew, M. S. and Juang, J. N., 1994, Concurrent mechanism and control design for the slewing of flexible space structures, Trans. ASME, Journal of Mechanical Design, Vol. 116, No. 3, pp. 944-951.

Yang T. L. and Zhang, M., 1994, A general theory for complete balancing of shaking force and shaking moment of spatial linkages using counterweights and inertia-counterweights, ASME, Machine Elements and Machine Dynamics, DE-Vol. 71, pp. 383-390.

Yang, T. L., Zhang, M. and Xu, Z., 2000, A comparative study on some different methods for complete balancing of shaking force and moment of linkages using for counterweights and inertia counterweights, Proceeding of DETC'00 ASME Design Engineering Technical Conferences.

Ye, Z. and Smith, M. R., 1994, Complete balancing of planar linkages by an equivalence method, Mechanism and Machine Theory, Vol. 29, No. 5, pp. 701-712.

Zhang, S. M., Morita, N. and Torii, T., 2000, Reduction of vibration by optimum balancing of shaking force/moment in linkage, JSME International Journal, Series C, Vol. 43, No. 3, pp. 748-754.

Zhang, W. J., Li, Q. and Guo, L. S., 1999, Integrated design of mechanical structure and control algorithm for a programmable four-bar linkage, IEEE/ASME Trans. On Mechatronics, Vol. 4, No. 4, pp. 354-362.

Zhang, W.J., Zou, J., Watson, G., Zhao, W., Zhong, G.H., and Bi, S.S., 2000, Constant-Jacobian Method for Kinematics of a 3-DOF Planar Micro-Motion Stage, Journal of Robotic Systems (accepted in October 2001).

Appendix A

Dynamic model of a 2 DOF serial chain mechanism with arbitrary mass distribution

Let us derive the closed-form dynamic equations for the 2 DOF series chain mechanism, shown in Figure A-1, using the Lagrange's equations of motion.

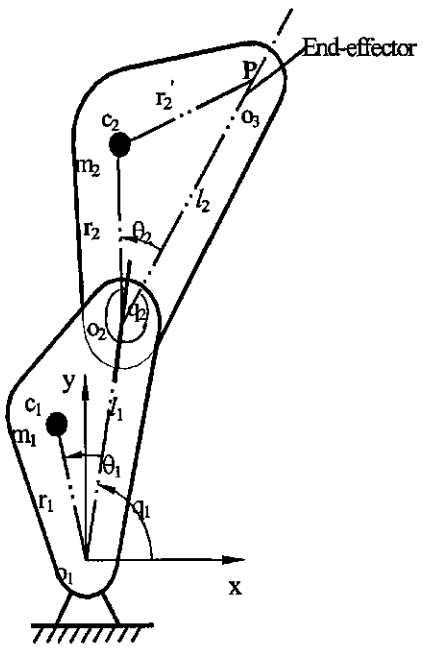

Figure A-1 The scheme of a general 2 DOF serial chain mechanism

For the mechanism shown in Figure A-1, the dynamic model can be expressed as:

$$D(q)\ddot{q} + C(q,\dot{q})\dot{q} + G(q) = T \tag{A-1}$$

The coefficients of the dynamic model can be derived as follows.

1. The determination of the inertia matrix

First, the velocities of the links can be expressed as:

$$V_{c1} = \begin{bmatrix} -r_1 \sin(q_1 + \theta_1) & 0 \\ r_1 \cos(q_1 + \theta_1) & 0 \end{bmatrix} \dot{q} \tag{A-2}$$

$$V_{c2} = \begin{bmatrix} -l_1 \sin q_1 - r_2 \sin(q_1 + q_2 + \theta_2) & -r_2 \sin(q_1 + q_2 + \theta_2) \\ l_1 \cos q_1 + r_2 \cos(q_1 + q_2 + \theta_2) & r_2 \cos(q_1 + q_2 + \theta_2) \end{bmatrix} \dot{q} \tag{A-3}$$

$$\omega_1 = \begin{bmatrix} 1 & 0 \end{bmatrix} \dot{q} \quad \text{and} \quad \omega_2 = \begin{bmatrix} 1 & 1 \end{bmatrix} \dot{q} \tag{A-4}$$

Then, one obtains:

$$J_L^{\ 1} = \begin{bmatrix} -r_1 \sin(q_1 + \theta_1) & 0 \\ r_1 \cos(q_1 + \theta_1) & 0 \end{bmatrix} \tag{A-5}$$

$$J_l^2 = \begin{bmatrix} -l_1 \sin q_1 - r_2 \sin(q_1 + q_2 + \theta_2) & -r_2 \sin(q_1 + q_2 + \theta_2) \\ l_1 \cos q_1 + r_2 \cos(q_1 + q_2 + \theta_2) & r_2 \cos(q_1 + q_2 + \theta_2) \end{bmatrix} \tag{A-6}$$

$$J_A^1 = \begin{bmatrix} 1 & 0 \end{bmatrix} \tag{A-7}$$

$$J_A^2 = [1 \quad 1] \tag{A-8}$$

It is known that the inertia matrix is in the following form:

$$D = \sum_{i=1}^{2} (m_i J_L^{i\,T} J_L^i + J_A^{i\,T} I_i J_A^i) \tag{A-9}$$

Substituting Eqs. (A-5) to (A-8) into (A-9) yields:

$$D = \begin{bmatrix} m_1 r_1^2 + I_1 + m_2(l_1^2 + r_2^2 + 2l_1 r_2 \cos(q_2 + \theta_2)) + I_2 & m_2 l_1 r_2 \cos(q_2 + \theta_2) + m_2 r_2^2 + I_2 \\ m_2 l_1 r_2 \cos(q_2 + \theta_2) + m_2 r_2^2 + I_2 & m_2 r_2^2 + I_2 \end{bmatrix} \tag{A-10}$$

2. Coriolis and centrifugal matrix

From Eq. (A-10), the Coriolis and centrifugal matrix can be derived as:

$$C = \begin{bmatrix} -m_2 l_1 r_2 \sin(q_2 + \theta_2)\dot{q}_2 & -m_2 l_1 r_2 \sin(q_2 + \theta_2)(\dot{q}_1 + \dot{q}_2) \\ m_2 l_1 r_2 \sin(q_2 + \theta_2)\dot{q}_1 & 0 \end{bmatrix} \tag{A-11}$$

3. Gravity torque

The gravity of the system can be derived as follows:

$$u = m_1 g r_1 \sin(q_1 + \theta_1) + m_2 g(l_1 \sin q_1 + r_2 \sin(q_1 + q_2 + \theta_2)) \quad \text{(A-12)}$$

Therefore, the gravity torque can be expressed as:

$$G = \begin{bmatrix} \frac{\partial u}{\partial q_1} \\ \frac{\partial u}{\partial q_2} \end{bmatrix} = \begin{bmatrix} m_1 r_1 \cos(q_1 + \theta_1) + m_2(l_1 \cos q_1 + r_2 \cos(q_1 + q_2 + \theta_2)) \\ m_2 r_2 \cos(q_1 + q_2 + \theta_2)) \end{bmatrix} g \quad \text{(A-13)}$$